Biomass Electrochemistry : from cellulose to sorbitol

Kwon, Y.

Biomass Electrochemistry:
from cellulose to sorbitol

Proefschrift

ter verkrijging van
de graad van Doctor aan de Universiteit Leiden,
op gezag van Rector Magnificus prof.mr. C.J.J.M. Stolker,
volgens besluit van het College voor Promoties
te verdedigen op donderdag 5 september 2013
klokke 13.45 uur

door

Youngkook Kwon

Geboren te Gimcheon in 1979

Promotiecommissie:

Promoter:	Prof. Dr. M. T. M. Koper
Overige Leden:	Prof. Dr. J. Brouwer Prof. Dr. B. E. Nieuwenhuys Prof. Dr. E. Bouwman Prof. Dr. B. M. Weckhuysen (Univ. Utrecht) Prof. Dr. J. Lee (GIST) Prof. Dr. P. Strasser (TU Berlin) Dr. E. De Jong (Avantium)

This research has been performed within the framework of the CatchBio program. The author gratefully acknowledges the support of the Smart Mix Program of the Netherlands Ministry of Economic Affairs and the Netherlands Ministry of Education, Culture, and Science.

For God so loved the world that he gave his one and only Son,
that whoever believes in him shall not perish but have eternal life.

John 3:16

Contents

1

1.1 Biomass

Fossil fuels such as coal, oil, and natural gas provide more than three quarters of the world's energy. Unfortunately, the growing demand for fossil fuel resources comes at a time of diminishing reserves of these nonrenewable resources, such that the worldwide reserves of oil are sufficient to supply energy and chemicals for only about another 40 years, causing widening concerns about rising oil prices.[1]

Biomass, biological material from living, or recently living organisms, most often referring to plants or plant-derived materials, can serve as a renewable source for both energy and carbon. Plant remains the largest biomass energy and chemical source today including forest residues. Biomass energy is derived mainly from several distinct sources i.e. wood, plants, waste, landfill gases, and alcohol fuels.

Biomass-derived energy products have been utilized since the time when people began burning wood to make fire either to generate electricity via steam turbines (or gasifiers) or to produce heat via direct combustion. There are a number of technological options available to make use of a wide variety of biomass types as a renewable energy source. First, thermal conversion processes (i.e. combustion, pyrolysis, and gasification) use heat as the dominant force to convert biomass into another chemical form i.e. syngas. Second, chemical processes (i.e. Fisher-Tropsch synthesis, methanol production) are used to

produce a fuel that is more conveniently used, transported or stored. Third, biochemical processes have been developed in nature by using enzymes of bacteria, micro-organisms to break down the molecules of biomass.

There are many important advantages of producing hydrocarbon fuels and chemicals from biomass. First of all, biomass-derived energy reduces green house gas emissions since biomass does not release "new carbon" into the atmosphere compared to fossil fuels. Second, "green" hydrocarbons are the same as those currently derived from petroleum. Therefore, it will not be necessary to modify existing infrastructure. Third, biomass-based hydrocarbon fuels are produced at high temperatures, which allows for faster conversion reactions in smaller reactors. Thus, processing units can be placed close to the biomass source.[2] Current advances in agriculture and biotechnology have made it possible to produce inexpensive biomass. In this respect, the "Roadmap for Biomass Technologies", a report authored by 26 leading experts, has predicted that 20% of transportation fuel and 25% of chemicals will be produced from biomass by 2030.[3]

As the most important skeletal component in plants, the polysaccharide cellulose is an almost inexhaustible polymeric raw material with fascinating structure and properties formed by the repeated connection of d-glucose building blocks, the highly functionalized, linear stiff-chain homopolymer.[4] Since cellulose cannot be digested by human beings, its use, unlike corn and starch, will not impose a negative impact on food supplies.[5] The most attractive routes for cellulose utilization are its conversion into energy and useful organic compounds by catalysis. The key bottleneck for cellulosic-derived fuels and chemicals is the lack of technology for the efficient conversion of biomass into desired products. Therefore, there's no doubt that chemistry, chemical catalysis, thermal processing, and engineering have to play an essential role in the conversion of cellulosic biomass into green fuels and chemicals.

1.2 Catalysis

Catalysis is the change in rate of a chemical reaction due to the participation of a substance called a catalyst, which is not consumed by the chemical reaction. Catalysis is one of the most important and widely-spread concepts of chemistry and it has been estimated that 85-90% of all chemicals and materials are produced in catalytic processes.[6] Nature is also full of catalysts in the form of enzymes, which are vital to all chemical reactions taking place in organisms.

Catalysts work by providing an (alternative) mechanism involving different transition states and lower activation energy. Consequently, more molecular collisions have the energy needed to reach the transition state. Hence, catalysts can enable reactions that would otherwise be blocked or slowed down by a kinetic barrier. The catalyst may increase both reaction rate and the selectivity.

Catalysis can be either heterogeneous or homogeneous, depending on whether a catalyst exists in the same phase as the substrate or not. Biocatalysis (such as enzymes) are often seen as a separate group.

- Heterogeneous catalysis: catalysis where the phase of the catalyst differs from that of the reactants. The great majority of practical heterogeneous catalysts are solids and the great majority of reactants are gases or liquids. Heterogeneous catalysis is of paramount importance in many areas of the chemical and energy industries.

- Homogeneous catalysis: the catalyst exists in the same phase as the reactants. Most commonly, a homogeneous catalyst is a molecule co-dissolved in a solvent with the reactants.

- Biocatalysis: the use of natural catalysts, such as proteins and enzymes, to perform chemical transformations on organic compounds.

Electrochemistry is the branch of chemistry concerned with the interrelation of electrical and chemical effects.[7] Electrocatalysis is the variation of rate of an electrochemical reaction with change in electrode material. An electrocatalyst is thus a heterogeneous catalyst at which charge transfer occurs between electrode and solution, the region where the charge distribution differs from that of the bulk phases.[8]

1.3 Biomass electrocatalysis

Biomass has the potential to be a valuable energy and chemical resource, but the complexity of biomass limits the access of electrocatalysis to produce feedstock (i.e. from cellulose to glucose). However, biomass derived alcohols have low volatility and high reactivity due to the high level of functionality (i.e. –OH, -C=O, -COOH groups), thus these feeds can be processed in liquid-phase catalysis. Therefore, recent application of electrocatalysis in biomass conversion is to generate hydrogen in direct alcohol fuel cell or electrolyzer from potential fuels (i.e. ethanol, ethylene glycol, and glycerol).[9-13] However, there are challenges of these approaches to develop a suitable catalyst for complete oxidation of biomass-derived alcohols to CO_2 and a resistant system for reactions up to 200°C.[14] Recently, co-generation of hydrogen and valuable chemicals from the partial oxidation of poly-ols has attracted immense research interests.[10,11,14] For instance, the selective oxidation of glycerol can be achievable to glyceraldehyde, glyceric acid, dihydroxyacetone, and formic acid (Chapters 2~4) with careful selection of catalysts, pH, and applied potential.

The real challenge in biomass electrocatalysis is to produce platform chemicals (i.e. glucose, sorbitol) from raw materials (i.e. cellulose) using electrochemistry. Although an extensive

number of works has been devoted to the hydrolysis of cellulose using enzymes, mineral acids, supercritical water, and heterogeneous catalysts,[15-20] the application of electrochemical methods for cellulose conversion to generate feedstock has been limited mainly by the low solubility of cellulose in aqueous media.[21] Many years ago, Baizer and Nobe[22] introduced the acid-catalyzed cellulose hydrolysis by electrochemically generated acid (H^+) at the platinum anode in an electrochemical cell. However, in this research, there's no direct interaction between cellulose and electrocatalyst, thus it provides very limited information of electrocatalysis. Recently, Li[23] reported the effect of hydroxyl radical (OH•) generated on a Pb/PbO_2 anode for depolymerization of cotton cellulose. In these cases, the electrode provides the active homogeneous catalysts or promoters (i.e. H^+, OH•) for the reaction. However, more detailed studies of reaction kinetics, intermediate species, and the effect of heterogeneous reactions between reactants and electrode have not been reported.

As a coupled reaction of cellulose hydrolysis to glucose, the hydrogenation of glucose to sorbitol is a very important reaction from synthetic and hydrogen storage points of view. Sorbitol is a promising platform polyol used as additives in foods, drugs, cosmetics, and various chemicals including vitamin C.[24] Using electrochemical approaches, sorbitol has been produced from aqueous glucose solution by applying certain current or potential on large-surface-area catalysts such as Raney-Ni[25,26] or poor (main group) metals at moderate pH (3~11)[25,27-29] and temperature (<60°C)[25-29] in a flow reactor.[25-27,30] In addition to Raney-Ni[19,20], the most applied catalysts for the electrocatalytic hydrogenation of glucose are poor metals such as Pb,[27-30] Hg,[31] Pb(Hg),[27,31] and Zn(Hg)[25,31] since they suppress the hydrogen evolution reaction (HER).

Although electrocatalytic synthesis of sorbitol from glucose was once applied on an industrial scale,[32] unfortunately, a fundamental understanding of the reactions linking catalysts and voltammetry has not been reported mainly due to existing technical limitations regarding the online analysis of products. Since 1950 sorbitol has been produced

by catalytic hydrogenation of glucose on Raney-Ni or noble metals such as Ru[33-35] under hydrogen pressure (1~350 atm) at various temperatures (ambient to 400°C).[36]

1.4 Scope of this thesis

The primary aim and objective of this thesis is to study and develop an electrochemical route for the conversion of cellulosic material into sorbitol in aqueous-phase solutions, within the framework of the CatchBio program, titled "Biomass Electrochemistry: from Cellulose to Sorbitol". In order to assess the potential of electrochemistry in biomass conversion, we were in need of an analysis method that is consistent with the time scale of the electrochemist's favorite technique, i.e. voltammetry. However, the combination of voltammetry especially with high-performance liquid chromatography (HPLC) has been limited due to the long analysis times in the column. To overcome the different time scale of voltammetry and chromatographic techniques, especially an HPLC system, we developed an online analysis system by using a fraction collector with a micrometer-sized sampling tip placed close to the working electrode. Figure 1 gives an overview of the electrochemical conversions described in this thesis by a combination of voltammetry and HPLC.

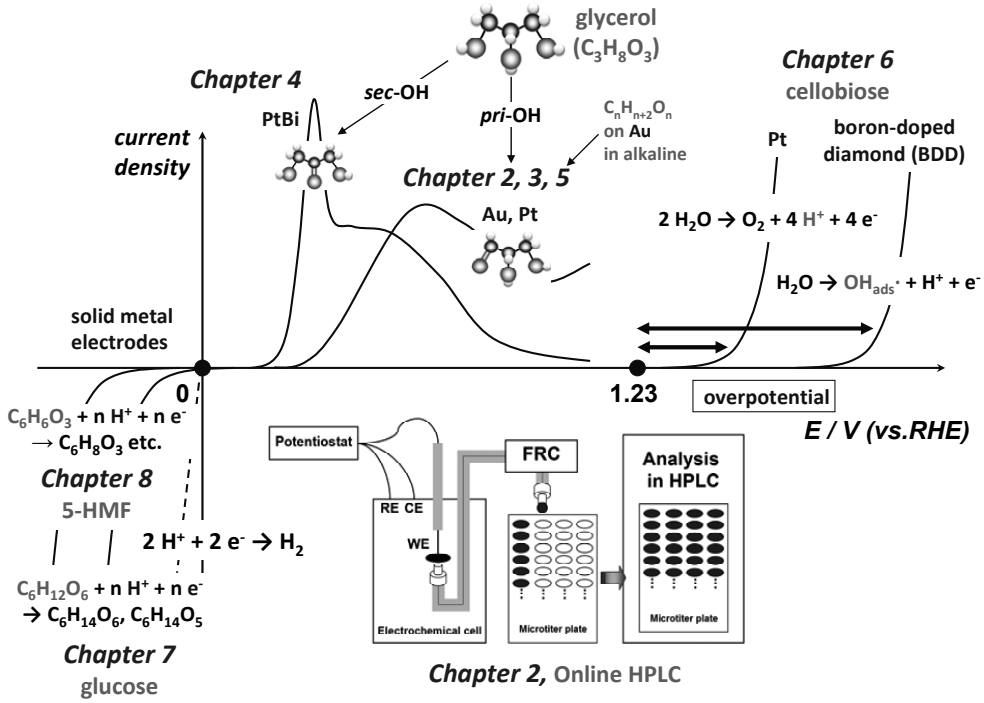

Figure 1. Current-potential representation of the reactions described in the thesis.

The motivation, details of operating conditions, and applications of an online HPLC system are discussed in Chapter 2. In this chapter, glycerol ($C_3H_8O_3$) is used as a model molecule to study its oxidation activity and reaction products on Au and Pt electrodes in alkaline conditions.

Building on Chapter 2, the effect of pH on glycerol oxidation has been investigated on Au and Pt electrodes in Chapter 3 to study the detailed mechanism. Especially, glyceraldehyde and dihydroxyacetone, which are not stable in alkaline condition, are shown in product spectra by continuous injection of 'stabilizing agent' through a modified sample collecting tip during sample collection. From this study, we conclude that gold only catalyzes glycerol oxidation under alkaline conditions, in contrast to platinum, which catalyzes glycerol oxidation over the entire pH range.

In order to alter the reaction pathway towards secondary alcohol oxidation, we study glycerol oxidation on Pt electrode in the presence of bismuth in Chapter 4. In a Bi-saturated acidic solution, Pt/C catalyst lowers the onset potential and enhances the turn-over frequency of glycerol oxidation with almost 100% selectivity to dihydroxyacetone (sec-OH oxidation product).

In Chapter 5, we describe why Au shows such as a high activity towards alcohol oxidation in alkaline solution. Based on a comparison of the oxidation activity of a series of similar alcohols with varying pK_a on gold electrodes in alkaline solution, we find that the first deprotonation is base catalyzed, and the second deprotonation is fast but gold catalyzed.

In Chapters 6 and 7, we extend our interest to cellobiose conversion to sorbitol based on the successful combination of voltammetry with online HPLC. Electrochemistry-assisted cellobiose hydrolysis to glucose is investigated in Chapter 6. Platinum and boron-doped diamond (BDD) electrodes were employed to generate acid (H^+) and hydroxyl radicals ($OH^{\cdot}$), respectively, in order to induce the hydrolysis of cellobiose. The results were compared with the hydrolysis promoted by conventional acid (H_2SO_4) and $OH^{\cdot}$ from Fenton's reaction.

In Chapter 7, glucose hydrogenation to sorbitol in neutral solution is described on solid metal cathodes. Three groups of catalysts in the Periodic Table with regard to reaction products are investigated i.e. hydrogen (early transition metals, platinum group metals), sorbitol (late transition metals), and sorbitol and 2-deoxysorbitol (post-transition metals).

In Chapter 8, the hydrogenation of 5-hydroxymethylfurfural (HMF), a derivative of glucose during acid-hydrolysis of cellulose, is described on solid metals in the presence and absence of glucose. The hydrogenation of 5-HMF is a non-catalytic reaction with lower overpotential than that of glucose, although the reaction pathway is determined by the catalyst. Therefore, the glucose hydrogenation is mostly suppressed by the presence of 5-HMF.

1.5 References

[1] J. N. Chheda, G. W. Huber, and J. A. Dumesic, *Angew. Chem. Int. Ed*. **2007**, 46, 7164-7183.

[2] Roadmap 2007, *Breaking the Chemical and Engineering Barriers to Lignocellulosic Biofuels*, Washington, D.C.

[3] *The Roadmap for Biomass Technologies in the U.S*., Biomass R&D Technical Advisory Committee, US Department of Energy, Accession No. ADA 436527, 2002.

[4] D. Klemm, B. Heublein, H.-P. Fink, and A. Bohn, *Angew. Chem. Int. Ed.* **2005**, 44, 3358-3393.

[5] N. Ji, T. Zhang, M. Zheng, A. Wang, H. Wang, X. Wang, and J. G. Chen, *Angew. Chem. Int. Ed*. **2008**, 47, 8510-8513.

[6] I. Chorkendorff and J. W. Niemantsverdriet, *Concepts of Modern Catalysis and Kinetics*, Wiley-CH, Weinheim, 2003.

[7] A. J. Bard and L. R. Faulkner, *Electrochemical methods*, 2nd ed., Wiley, 2001, p. 1.

[8] C. M. A. Brett and A. M. O. Brett, *Electrochemistry Principles, Methods, and Applications*, Oxford, 1993, p. 25-26.

[9] A. Ilie, M. Simoes, S. Baranton, C. Coutanceau, S. Martemianov, *J. Power Sources* **2011**, *196*, 4965–4971.

[10] Z. Zhang, L. Xin, J. Qi, Z. Wang and W. Li, *Green Chem*., **2012**, *14*, 2150–2152.

[11] Z. Zhang, L. Xin, W. Li, *Appl. Catal. B-Environ.* **2012**, *119–120*, 40– 48.

[12] Z. Zhang, L. Xin, W. Li, *Int. J. Hydrogen Energ*. **2012**, *37*, 9393-9401.

[13] V. Bambagioni, M. Bevilacqua, C. Bianchini, J. Filippi, A. Lavacchi, A. Marchionni, F. Vizza, P. K. Shen, *ChemSusChem* **2010**, *3*, 851-855.

[14] M. Simoes, S. Baranton, C. Coutanceau, ChemSusChem, **2012**, *5*, 2106-2124.

[15] Y. Sun, J. Cheng, *Bioresour. Technol*. **2002**, *83*, 1-11.

[16] Y. -H. P. Zhang, L. R. Lynd, *Biotechnol. Bioeng*. **2004**, *88*, 797-824.

[17] R. Rinaldi, F. Schuth, *ChemSusChem* **2009**, *2*, 1096-1107.

[18] K. Shimizu, H. Furukawa, N. Kobayashi, Y. Itaya, A. Satsuma, *Green Chem*. **2009**, 11, 1627-1632.

[19] M. Sasaki, Z. Fang, Y. Fukushima, T. Adschiri, K. Arai, *Ind. Eng. Chem. Res.* **2000**, *39*, 2883-2890.

[20] H. Kobayashi, Y. Ito, T. Komanoya, Y. Hosaka, P. L. Dhepe, K. Kasai, K. Hara, A. Fukuoka, *Green Chem*. **2011**, *13*, 326-333.

[21] D. Klemm, B. Heublein, H. -P. Fink, A. Bohn, *Angew. Chem. Int. Ed*. **2005**, *44*, 3358-3393.

[22] J. C. Yu, M. M. Baizer, K. Nobe, *J. Electrochem. Soc.* **1988**, *135*, 83-87.

[23] D. Meng, G. Li, Z. Liu, F. Yang, *Polym. Degrad. Stabil*. **2011**, *96*, 1173-1178.

[24] P. Gallezot, P. J. Cerino, B. Blanc, G. Fleche, P. Fuertes, *J. Catal.* 1994, *146*, 93-102.

[25] K. Park, P. N. Pintauro, M. M. Baizer, K. Nobe, *J. Electrochem. Soc.* 1985, *132*, 1850-1855.

[26] J. C. Yu, M. M. Baizer, K. Nobe, *J. Electrochem. Soc.* **1988**, *135*, 1400-1406.

[27] A. Binkassim, C. L. Rice, A. T. Kuhn, *J. Appl. Electrochem.* **1981**, *11*, 261-267.

[28] C. L. R. Annvar Bin Kassim, Anselm T. Kuhn, *J. Chem. Soc., Faraday Trans.* **1981**, *77*, 683-695.

[29] S. G. Chen, T. Wen, J. H. P. Utley, *J. Appl. Electrochem.* **1992**, *22*, 43-47.

[30] Y. Owobi-Andely, K. Fiaty, P. Laurent, C. Bardot, *Catal. Tod*ay **2000**, *56*, 173-178.

[31] P. N. Pintauro, D. K. Johnson, K. Park, M. M. Baizer, K. Nobe, *J. Appl. Electrochem.* **1984**, *14*, 209-220.

[32] A.T.Kuhn in *Industrial Electrochemical Processes*, Elsevier, Amsterdam, **1971**.

[33] B. Kusserow, S. Schimpf, P. Claus, *Adv. Synth. Catal.* **2003**, *345*, A102-A102.

[34] P. Gallezot, N. Nicolaus, G. Fleche, P. Fuertes, A. Perrard, *J. Catal.* **1998**, *180*, 51-55.

[35] B. J. Arena, *Appl. Catal. A-Gen.* **1992**, *87*, 219-229.

[36] J. M. Chapuzet, A. Lasia, J. Lessard, in Electrocatalysis, ed. J. Lipkowski, P. N. Ross, Wiley-VCH, New York, **1998**, pp. 155-196.

2

Combining voltammetry with HPLC: Application to electro-oxidation of glycerol

Abstract

The combination of cyclic voltammetry and "on-line" chromatographic techniques for product detection is limited by the typically long analysis times in chromatographic columns. Therefore, traditionally, product analysis is performed offline after long bulk electrolysis experiments. To overcome the limitation of the inherently different time scales of voltammetry and HPLC, we suggest here to adopt rapid online sample collection with a micrometer-sized sampling tip placed close to the working electrode, followed by off-line analysis of the sample fractions in an HPLC system. To demonstrate this concept, we applied online fraction collection and offline HPLC analysis to the glycerol electro-oxidation on Au and Pt electrodes in alkaline media, and show that we can successfully follow the concentration changes of glycerol and its reaction products in good correspondence with current profile obtained simultaneously with voltammetry. Moreover, the method allows for a detailed discrimination of the different mechanisms of glycerol oxidation on both electrodes. Therefore, this simple approach enables the monitoring of soluble reaction products during voltammetry with an HPLC system, and thereby allows for new insights into the mechanisms of complex multi-step electrode reactions.

The contents of this chapter have been published: Y. Kwon, M. T. M. Koper, *Anal. Chem.*, **2010**, *82*, 5420-5424.

2.1 Introduction

Voltammetry, or cyclic voltammetry, is a powerful electrochemical measuring technique to study electrode reactions, to distinguish between different reaction mechanisms and to obtain information on the intermediates and products involved in the electrode reactions as well as on possible coupled chemical reactions.[1] However, the fundamental molecular-level understanding of reaction intermediates and products, requires the combination of voltammetry with microscopic, spectroscopic, and chromatographic techniques. There are two main analytical techniques to follow the formation of dissolved products during voltammetry. The first is the Rotating Ring-Disk Electrode (RRDE),[2-4] in which products formed on the disk may be analyzed electrochemically at the ring. Though fast and quantitative, the RRDE method is limited to species with a very well-defined and unique electrochemical response on the ring electrode. The second technique is online or differential electrochemical mass spectrometry (MS), which allows for the identification of volatile intermediates and products simultaneously with the voltammetry, a combination displaying considerable chemical specificity and sensitivity.[5-7] However, this technique only detects volatile species, limiting its versatility. In principle, in situ infrared spectroscopy permits the detection of intermediates and products, but the technique is difficult to quantify in an electrochemical setting, in addition to the frequent overlap of, and uncertainty in the assignment of spectroscopic bands. More recently, Zhao et al.[8] have combined voltammetry with Electrospray Ionization Mass Spectrometry to allow for the detection of non-volatile products. Combining voltammetry with chromatographic techniques such as Gas Chromatography (GC), Ion Chromatography (IC), and High Performance Liquid Chromatography (HPLC) has been limited due to the long analysis times in the column, and existing on-line analysis experiments[9] to understand reaction mechanisms or to identify reaction products have only been applied for prolonged electrolyses. Even though prolonged so-called “bulk electrolysis” experiments at fixed potentials may be helpful in studying reaction pathways and mechanisms, the link with voltammetry and its various applications is essentially lost.

We were confronted with the desire to combine voltammetry with chromatographic techniques in a project studying the electrochemical conversion of biomass and biomass-related compounds. Many industrialized societies are currently developing ways to utilize the abundant and renewable biomass resources more effectively to provide new sources of

energy, food, and value-added chemicals.[10] In order to assess the potential of electrochemistry in biomass conversion, we were in need of an analysis method that is consistent with the time scale of the electrochemist's favorite technique, i.e. voltammetry. Glycerol is an important biomass-related compound, both as a model poly-ol compound, and as an abundant byproduct of biodiesel.[11,12] The catalytic conversion of glycerol into value-added chemicals is a topic of significant current interest in biomass research. In electrochemistry, glycerol has been considered as a potential fuel for fuel cells.[13-16]

To overcome the inherent time-scale differences of voltammetry and chromatographic techniques, especially HPLC, we suggest here to employ rapid sample collection while sweeping the electrode potential, using a very small micrometer-sized tip inlet system placed close to the electrode surface, with the collected sample fractions subsequently analyzed in an HPLC system. As an example of this method, we apply it to the glycerol electro-oxidation on Au and Pt electrodes in alkaline media, visualizing the concentration changes of glycerol and its reaction products in correspondence with the current measured in voltammetry. These materials were chosen as they have been studied before in the literature,[13-16] and they serve as typical examples of catalytically active (Pt) and non-active (Au) electrodes. Alkaline media were chosen as they tend to be particularly active for the oxidation of alcohols.[17] Most importantly, however, we will show that this simple combination of voltammetry and HPLC allows for new insights into the mechanism of glycerol oxidation on platinum and gold, revealing some intriguing differences in product selectivity.

2.2 Experimental

2.2.1 Reagents

All solutions were prepared with 18.2 MΩ/cm water from Millipore MilliQ. Sodium hydroxyde (Sigma-Aldrich, 99.99%), glycerol (Merck, 85%), glyceraldehyde (Sigma, 90%), glyceric acid (Aldrich, 99%), glycolic acid (Across, 99%), formic acid (Merck, 98%), oxalic acid (Riedel-de Haën, 99.5%), tartronic acid (Alfa Aesar, 98%), and argon (purity grade 6.0) were used as received.

2.2.2 Electrochemistry

All measurements were carried out in a conventional single compartment three-electrode glass cell, which was cleaned by a standard procedure[18] to remove all traces of organic contaminations. Glycerol (0.1 M) was dissolved into a 0.1 M NaOH electrolyte solution; prior to the experiments oxygen was removed by bubbling argon through the solution for at least 30 minutes. Working electrodes in the experiment were polycrystalline gold and platinum disks of 5 mm in diameter embedded in PTFE shrouds, which were mechanically polished with alumina (up to 0.05 μm), and cleaned ultrasonically in ultrapure water before use. In all experiments, a platinum plate was used as a counter electrode, while a mercury-mercury oxide electrode (Hg/HgO / 0.5 M KOH) was employed as a reference electrode. All potentials reported here have been converted to the RHE scale ($E_{Hg/HgO} = E_{RHE} - 0.926$ V) in the same electrolyte. Electrochemical cell potentials were controlled with a potentiostat/galvanostat (μ-Autolab Type III).

2.2.3 Fraction collection

The reaction products were collected with a small teflon tip (0.38 mm inner diameter) positioned close (~ 10 μm) to the center of the electrode surface, which was connected to a PEEK capillary with inner/outer diameters of 0.13/1.59 mm. The tip is essentially identical to the tip that we developed previously for our online electrochemical mass spectrometry setup,[7] with the only difference that no hydrophobic membrane is present inside the capillary. The tip configurations were cleaned in a solution of 0.2 M $K_2Cr_2O_7$ and rinsed thoroughly with ultra-pure water before use. The sample volume collected in each well was 60 μL on a 96-well microtiter plate (270 μL/well, Screening Devices b.v.) using an automatic fraction collector (FRC-10A, Shimadzu). The flow rate of sample collection was adjusted to 60 μL/min with a Shimadzu pump (LC-20AT). After collecting samples, the microtiter plate was covered by a silicon mat to prevent the evaporation of collected samples.

2.2.4 Chromatographic determination of products

Collected samples during voltammetry were analyzed by high-performance liquid chromatography (Prominence HPLC, Shimadzu). The microtiter plate with the collected samples was placed in an auto-sampler (SIL-20A) holder and 1 μL of sample was injected into the column. The column used was an Aminex HPX 87-H (Bio-Rad) and diluted sulfuric acid (5 mM) was used as eluent. The temperature of column was maintained at 30°C in column oven (CTO-20A) and the separated compounds were detected with a refractive index detector (RID-10A). The expected products of glycerol oxidation[11] were analyzed as well by HPLC to produce a standard calibration curve at 30°C (i.e., glyceraldehyde, glyceric acid, glycolic acid, formic acid, oxalic acid, and tartronic acid). Since the peaks of glyceraldehyde and glyceric acid strongly overlap at 30°C, the oven temperature was increased to 80°C to effectively separate these products.

2.3 Results and discussion

In order to combine voltammetry with a determination of the product concentration during potential scanning requires optimized conditions: moderate current on the electrocatalyst, a proper flow rate of sample collection, and stability of the intermediates and products in the sampled solution. Especially, the operating conditions in terms of the voltammetric scan rate and sample collecting flow rate should be optimized. With the existing setup, the volume of one droplet from the sample disposal tip is ca. 30 μL in alkaline media, and we collected two drops in each well. Therefore, in the case of glycerol oxidation, optimal scan and flow rates were found to be 1 mV/s and 60 μL/min, respectively. As the collected sample volume per well was 60 μL, each sample represents the average concentration over a 60 mV potential range.

Figure 1 shows the voltammetry of glycerol oxidation on gold (Fig.1a) and platinum (Fig.1b) both in the absence (dashed line) and presence (solid line) of online sample collection. First of all, note that the oxidation current is significantly higher on gold, albeit at higher potentials, making gold a more active catalyst for glycerol oxidation than platinum (in alkaline media). Glycerol oxidation on gold begins at ca. 0.6 V, and the current increases significantly from 0.9 V. However, with sample collection the oxidation of

glycerol appears a little delayed compared to the current without sample collection, particularly in the range of 0.9 ~ 1.1 V. Presumably this happens because of the removal of an intermediate species in the glycerol oxidation, which can be further oxidized. The same tendency was also observed on the Pt electrode, albeit in a different potential window. On Pt, glycerol is oxidized from 0.4 V and the current without sample collection is higher than the current with sample collection in the potential range from 0.4 to 0.7 V (Figure 1(b)). Although onset potentials of each electrode are not identical due to different electrode kinetics,[13-16] we believe that the origin of these current delay phenomena at the onset of glycerol oxidation is the same on both electrodes, i.e. due to the sample collection and the removal of active intermediates. On the other hand, online sample collection caused a higher current density from 1.2 to 1.6 V on the gold electrode and from 0.7 to 1 V on the platinum electrode, respectively. We believe that this current enhancement may be due to the removal of intermediate species that have the tendency to deactivate the electrode because of their poisonous properties. On platinum, especially formic acid, one of the expected products (see below), may cause serious deactivation due to CO formation on the platinum surface.[13,19-21] On gold, CO poisoning is less likely; in this case, carboxylic acids form (see below) that may coordinate to the surface and block the active surface. Also note that on the gold electrode, a voltammetric current with periodic spikes was observed in the presence of online sample collection. Current spikes typically appear at high currents (no spikes were observed with the Pt electrode), and the frequency of the spikes appears to be related to the flow rate of sample collecting pump as shown in Figure 2. The spikes are therefore related to small irregularities in the pumping flow rate. As a general conclusion, the continuous removal of intermediates and products in the presence of online sample collection may result in substantial changes in the measured voltammetry. In the case of glycerol oxidation, both lower and higher currents may be observed, depending on what kind of intermediates and/or products are removed from the solution, and what their role is in the mechanism. Obviously, the exact sampling conditions, in relation to the voltammetric scan rate, should be chosen such that these effects are minimized.

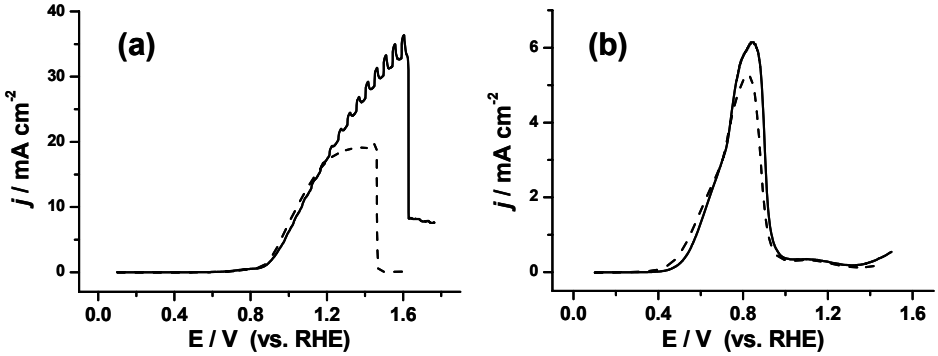

Figure 1. Effect of sample collection on the current density during linear sweep voltammetry. Glycerol oxidation (0.1 M) on (a) Au and (b) Pt electrodes with (solid line) and without (dashed line) sample collection in 0.1 M NaOH. Scan rate is 1 mV/s.

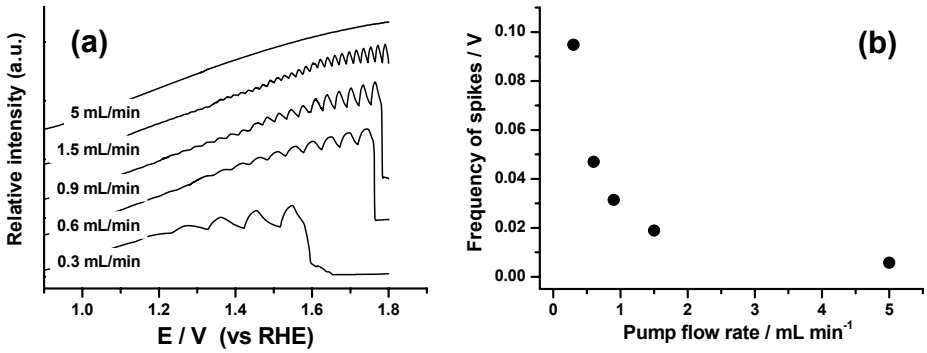

Figure 2. The relationship between pump flow rate of sample collection and frequency of spikes during glycerol oxidation on Au electrode. Scan rate is 10 mV/s.

During voltammetry, samples are continuously collected on a microtiter plate and subsequently analyzed in the HPLC system. All relevant peaks appear to be well separated at column temperature of 30°C as shown in Figure 3. However, the retention times of glyceric acid and glyceraldehyde at 30°C are almost the same (10.414 and 10.475 min, respectively), so all samples obtained for both electrodes were also analyzed at 80°C to clearly separate these species. From the analysis data at 80°C, glyceraldehyde was not detected to any significant extent during the voltammetric glycerol oxidation on Au and Pt electrodes in alkaline media, at variance with previous studies on these systems.[13,22]

However, the absence of glyceraldehyde in our samples could be due to the instability of aldehydes in alkaline media, as suggested by the literature.[23,24]

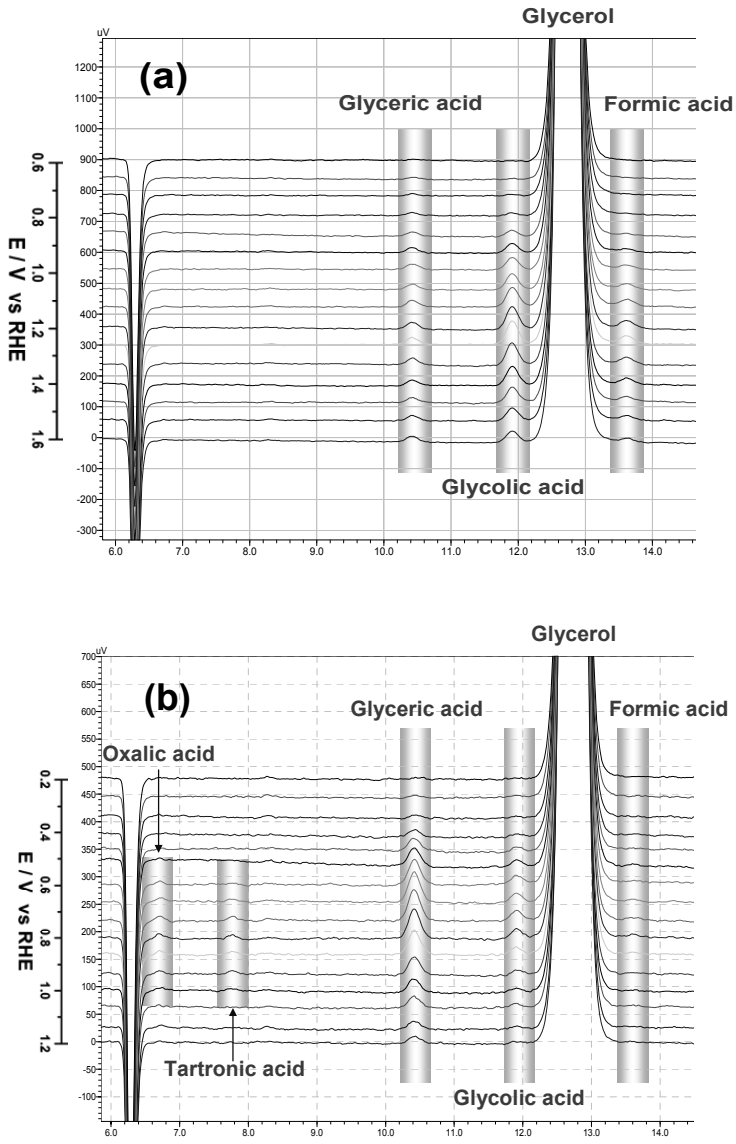

Figure 3. Chromatograms from HPLC analysis at 30ºC with collected samples during voltammetry on (a) Au and (b) Pt electrodes.

The peaks observed in the chromatograms in Figure 3 are converted to the corresponding concentrations of the various compounds, the results of which are shown in Figure 4. The initial concentration of glycerol was a little higher than 0.1 M due to solution evaporation during Ar bubbling on both electrodes. As shown in Figure 4(a), the concentration of glycerol near the Au electrode slowly decreases with the lowest value at around 1.4-1.5 V, after which it increases slightly as the potential is made more positive. The first product of glycerol oxidation on gold, glyceric acid, appears at 0.6 V and its concentration increases until 1.45 V, after which it slowly decreases. From ca. 0.8 V, the secondary products, i.e. glycolic acid and formic acid, are observed, with a concentration ca. three times higher than that of glyceric acid. Both products have an essentially identical concentration as a function of potential. Accordingly, we can conclude that glycerol is first oxidized to glyceric acid from 0.6 V, and next from 0.8 V glyceric acid is further oxidized by C-C bond breaking to equal amounts of glycolic acid and formic acid. It can be clearly seen from Figure 4(a) that these two products are the majority species formed at the electrode, and that their concentrations follow the current profile as observed in the voltammogram in Figure 1(a).

The reaction products of glycerol oxidation and their concentration profiles on the platinum electrode are illustrated in Figure 4(b). The concentration of glycerol decreases until 0.8 V, after which it slowly increases again, in agreement with the maximum in current observed at 0.8 V (Figure 1(b)). The first product of glycerol oxidation, i.e. glyceric acid, agrees with that on the Au electrode, and is detected from potentials as low as 0.35 V with its concentration steeply increasing until 0.8 V, after which it decreases again. The secondary products of glycerol oxidation from the further oxidation of glyceric acid, i.e. glycolic acid and formic acid, appear from 0.4 V. Interestingly, the concentration of formic acid is a little higher than that of glycolic acid from 0.6 to 1.0 V, which can be explained by the further oxidation of glycolic acid to oxalic acid on the Pt electrode, as evidenced by the concentration profile of oxalic acid which exactly compensates for the loss of glycolic acid (line with diamonds in Figure 4(b)). In addition, the formation of tartronic acid was observed in this potential range, which must be the product of glyceric acid oxidation on Pt electrode, as an alternative pathway for the formation of glycolic acid and formic acid. Finally, a remarkable difference with the same measurement on gold is that on platinum, the main product is glyceric acid, and the 2-electron reaction to glycolic acid and formic acid appears much less appreciable on platinum than on gold. This is consistent with the significantly higher currents observed on gold, at least at high overpotentials. A likely

explanation for this difference is the lower surface oxidation potential of platinum compared to gold. Whereas the glycerol and glyceric acid oxidation start at a lower potential on platinum, the platinum electrode becomes deactivated at ca. 0.9 V, the potential at which a surface oxide forms on the platinum electrode and consequently the electrode becomes deactivated. On a gold electrode, the surface oxide formation occurs only at much higher potential, ca. 1.3 V, and as a result there is a wider potential range available for the further oxidation of glyceric acid to glycolic acid and formic acid.

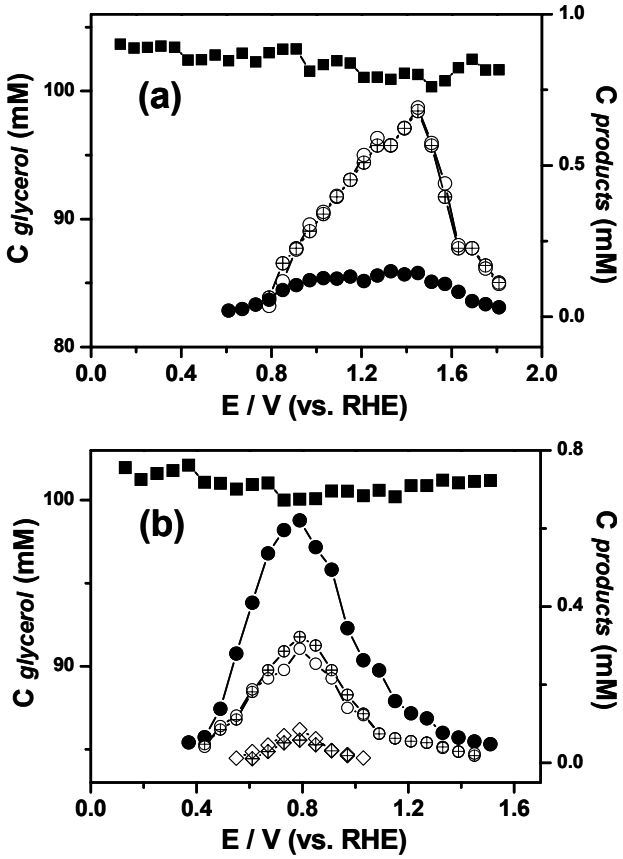

Figure 4. Plots showing the concentrations of glycerol and its electro-oxidation by-products as a function of potential on (a) Au and (b) Pt electrode: ■ glycerol, ● glyceric acid, ○ glycolic acid, ⊕ formic acid, ◇ oxalic acid, ⌖ tartronic acid.

To illustrate the current limitations of the method, we also applied a higher scan rate of 10 mV/s to the Pt electrode, with the sample collecting flow rate also increased to 600 μL/min in order to collect the same number of samples as above. The current density for 10 mV/s is almost twice that of 1 mV/s at highest current ranges in the presence of sample collection. Since the sample collecting rate is now 10 times faster, the product in each well (at 10 mV/s) is 5-10 times more diluted compared to those with 1 mV/s, so that only small peaks of glyceric acid were detected. Using a 5 times higher injection volume into the HPLC, we can obtain a plot very similar to Figure 4(b), but at the price of having a larger difference between the voltammetry with and without sample collection. Therefore, the current limiting factor to go to lower sample collecting flow rates to minimize disturbance in the voltammetry, is the final size of the collected sample drop, which in our commercial instrument is ca. 30 μL in alkaline media.

From the results illustrated in Figures 1 and 4, a reaction mechanism for the glycerol oxidation on Au and Pt electrodes may be suggested, as shown in Figure 5. In alkaline media, glycerol is first oxidized to glyceric acid in a 4-electron transfer step, both on Au and Pt electrodes, though with a lower overpotential on platinum. As a next 2-electron transfer step, glyceric acid is further oxidized by cleavage of a C-C bond into glycolic acid and formic acid on both electrodes. However, on a platinum electrode this process becomes deactivated at potentials close to 0.9 V, where Pt forms an inhibiting surface oxide. On the Au electrode, a much higher conversion activity of glyceric acid to glycolic acid and formic acid than on Pt electrode, which we ascribe to the higher surface oxidation potential of gold. This would suggest that this bond breaking step does not require a highly catalytic material (as it takes place on a relatively inactive surface such as gold), though it does not take place on an oxidized electrode surface. In addition, glyceric acid and glycolic acid may be further oxidized on the Pt electrode to tartronic acid and oxalic acid, respectively, whereas these steps are not observed on the gold electrode.

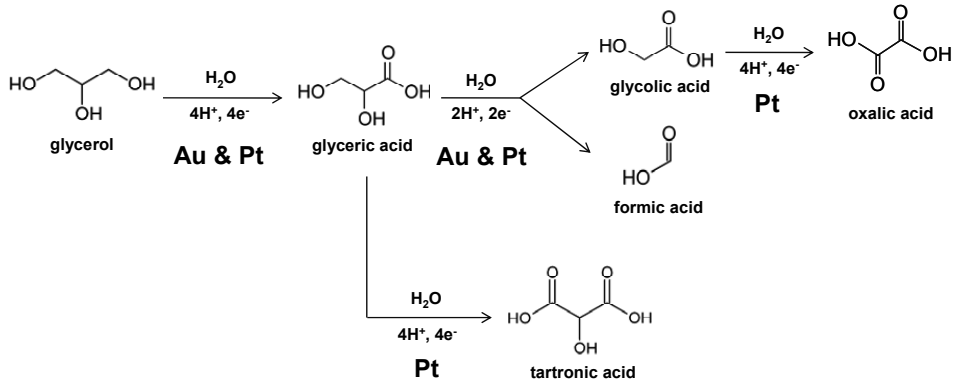

Figure 5. Schematic diagram for the reaction mechanism for the glycerol oxidation on Au and Pt electrode in alkaline media.

2.4 Conclusion

The work described here has demonstrated the possibility and potential of combining voltammetry with a chromatographic technique by online sample collecting during the potential sweep, and offline product analysis in HPLC system. We successfully visualized the relationship between the current observed in voltammetry and the concentration of the various reaction products on the example of glycerol oxidation on a platinum and gold electrode in alkaline media. Significantly, this approach provided a detailed insight into the different mechanisms of glycerol oxidation on the two electrodes. We expect that this combination may be employed for the study of many other multi-electron electrochemical reactions that produce soluble intermediates and products.

At present, this combination is limited by the volume of collected sample. Smaller volumes allow for slower sample collecting flow rates, leading to smaller disturbances on the voltammetry at high scan rates. The highest scan rate at which we have obtained reasonable data is 10 mV/s, which is already quite good, but with further improvements of the setup and a smaller volume of the collected sample (which is essentially determined by the diameter of the capillary dispensing the drop into the wells of the microtiter plate) this situation may still be further improved.

2.5 References

[1] Bard, A. J.; Faulkner, L. R. *Electrochemical methods*, 2nd ed., Wiley, 226-260.

[2] Sánchez-Sánchez, C. M.; Bard, A. J. *Anal. Chem.* **2009**, *81*, 8094–8100.

[3] Nakagawa, T.; Bjorge, N. S.; Murray, R. W. *J. Am. Chem. Soc*. **2009**, *131*, 15578–15579.

[4] Groot, M. T.; Merkx, M; Koper, M. T. M. *J. Am. Chem. Soc.* **2005**, *127*, 16224–16232.

[5] Bruckenstein, R. R.; Gadde, J. *J. Am. Chem. Soc*. **1971**, *93*, 793.

[6] Baltruschat, H. *J. Am. Soc. Mass Spectrom*. **2004**, *15*, 1693.

[7] Wonders, A. H.; Housmans T. H. M.; Rosca, V.; Koper, M. T. M. *J. Appl. Electrochem*. **2006**, *36*, 1215–1221.

[8] Zhao, W.; Jusys, Z.; Behm, R. J. *Anal. Chem.* **2010**, *82*, 2472-2479.

[9] Tarnowski, D. J.; Korzeniewski, C. *J. Phys. Chem. B* **1997**, *101,* 253-258.

[10] Soares, R. R.; Simonetti, D. A.; Dumesic, J. A. *Angew. Chem. Int. Ed.* **2006**, *45*, 3982 –3985.

[11] Pagliaro, M.; Ciriminna, R.; Kimura, H.; Rossi, M.; Della Pina, C. *Angew. Chem. Int. Ed.* **2007**, *46*, 4434-4440.

[12] Zhou, C.; Beltramini, J. N.; Fan, Y-X.; Lu, G. Q. *Chem. Soc. Rev.* **2008**, *37*, 527-549.

[13] Roquet, L.; Belgsir, E. M.; Léger, J. M.; Lamy, C. *Electrochim. Acta* **1994**, *39*, 2387-2394.

[14] Kahyaoglu, A.; Beden, B.; Lamy, C. *Electrochim. Acta* **1984**, *29*, 1489-1492.

[15] Avramov-Ivić, M.; Léger, J. M.; Beden, B.; Hahn, F.; Lamy, C. *J. Electroanal. Chem.* **1993**, *351*, 285-297.

[16] Avramov-Ivić, M. L.; Léger, J. M.; Lamy, C.; Jović, V. D.; Petrović, S. D. *J. Electroanal. Chem*. **1991**, *308*, 309-317.

[17] Lai, S. C. S.; Kleyn, S. E. F.; Oztürk, F. T. Z.; van Rees Vellinga, V. C.; Koning, J.; Rodriguez, P.; Koper, M. T. M. *Catal. Today* **2010**, *154 (1-2)*, 92-104.

[18] Lai, S. C. S.; Koper, M. T. M. *Faraday Discuss*. **2009**, *140*, 399-416.

[19] Capon, A.; Parsons, R. *J. Electroanal. Chem.* **1973**, *44*, 1-7.

[20] Capon, A.; Parsons, R. *J. Electroanal. Chem.* **1973**, *45*, 205-231.

[21] Parsons, R.; VanderNoot, T. *J. Electroanal. Chem.* **1988**, *257*, 9-45.

[22] Beltowska-Brzezinska, M. *Electrochim. Acta* **1978**, *25*, 267-271.

[23] Evans, W. L.; Cornthwaite, W. R. *J. Am. Chem. Soc.* **1928**, *50*, 486-492.

[24] Yaylayan, V. A.; Harty-Majors, S.; Ismail, A. A. *Carbohydr. Res.* **1999**, *318*, 20-25.

3

Mechanism of the catalytic oxidation of glycerol on polycrystalline gold and platinum electrodes

Abstract

This chapter addresses the electro-oxidation mechanisms of glycerol on Au and Pt electrodes under different pH conditions. Intermediates and/or reaction products were detected by an online high-performance liquid chromatography technique (for soluble products) and by online electrochemical mass spectrometry (for CO_2). In alkaline media, the main product of glycerol oxidation on the Pt electrode is glyceric acid produced via glyceraldehyde. Glyceric acid is the primary oxidation product on the Au electrode, and is further oxidized to glycolic acid and formic acid at high potentials ($\geq$ 0.8 V) yielding high current densities. Lowering the pH of the solution, the glycerol oxidation becomes significantly more sluggish on both Au and Pt electrodes, resulting in glyceraldehyde being the main oxidation product in neutral condition, especially on gold. In acidic solution, only the Pt electrode shows catalytic activity with a relatively low conversion rate mainly to glyceraldehyde. At positive potentials corresponding to the formation of a Pt surface oxide, the PtO_x surface catalyzes the conversion from glyceraldehyde finally to formic acid and CO_2, but only in acidic condition. Gold only catalyzes glycerol oxidation under alkaline conditions, in contrast to a "real catalyst", i.e. platinum, which catalyzes glycerol oxidation over the entire pH range.

The contents of this chapter have been published: Y. Kwon, K. J. P. Schouten, M. T. M. Koper, *ChemCatChem*, **2011**, *3*, 1176-1185.

3.1 Introduction

Glycerol is an important biomass-related compound, both as a model poly-ol compound and as an abundant byproduct of biodiesel.[1-3] New applications of glycerol are being sought and have been found as a low-cost feedstock for functional derivatives either for mass consumption, such as additives for concrete, or as a precursor of fine chemicals of added value.[1] For the cogeneration of energy and chemicals, selective electrocatalytic oxidation for converting glycerol into commercially valuable products such as dihydroxyacetone (DHA), glyceraldehyde, glyceric acid etc. is regarded with particular interest.[4,5] Even though most glycerol oxygenated derivatives are of practical value, the fundamental molecular-level understanding of catalytic reaction intermediates and products is still incomplete.[6-8] Since most of the relevant reactions of glycerol in aqueous media are redox reactions, electrochemistry and electrochemical methods are particularly useful in scrutinizing such mechanistic details.

Voltammetric studies of glycerol oxidation have been reported for both alkaline and acidic media.[6-10] However, the disadvantage of purely electrochemical methods is that no specific information on the adsorbates or the (intermediate) oxidation products is obtained. Therefore, a spectroscopic technique, such as Fourier Transform Infrared Spectroscopy (FTIRS)[7,8] has to be applied to probe reaction intermediates/products and mechanisms. Since for the oxidation of glycerol, incomplete oxidation products such as aldehydes, ketones and carboxylic acids tend to dominate the product spectrum, High Performance Liquid Chromatography (HPLC) is the method of choice to study glycerol oxidation products both at a qualitative and quantitative level.

Recently, we introduced a new combination of voltammetry and HPLC by adopting rapid online sample collection with a micrometer-sized sample collecting tip, and we successfully demonstrated the application of the method to the glycerol electro-oxidation on Au and Pt electrodes in alkaline media.[11] The absence of primary oxidation products, i.e. glyceraldehyde and dihydroxyacetone, in the reaction mechanism suggested in that work, was primarily due to the instability of these aldehydes in alkaline media. Therefore, a modification of the sample collection system is necessary to provide clear product detection and separation and their relative selectivity of formation in dependence on the applied electrode potential. Additionally, the very high activity of the Au electrode compared to the

Pt electrode is partially due to the participation of OH^- in the glycerol oxidation mechanism,[8,9,12] and therefore it is worth studying the effect of different pH conditions for both electrocatalysts. Moreover, the online electrochemical mass spectrometry (OLEMS) technique is useful for the identification of volatile intermediates and products and to follow the formation of the complete oxidation product CO_2 during the voltammetry.

In this chapter, we aim at formulating complete reaction mechanisms for the glycerol oxidation on Au and Pt electrodes in alkaline, neutral, and acidic conditions, both with respect to the quantitative and qualitative product distributions, as determined by the combination of voltammetry with online HPLC and OLEMS. We believe these results and mechanisms are very relevant to the aqueous-phase reforming of glycerol on gold and platinum catalysts as depolarized by oxygen.[13-17] The essential electrocatalytic nature of the alcohol oxidation under liquid-phase heterogeneous catalytic conditions was recently confirmed by the groups of Neurock and Davis.[18]

3.2 Experimental Section

3.2.1 Electrochemistry

All measurements were carried out in a conventional single compartment three-electrode glass cell, which was cleaned by a standard procedure[19] to remove all traces of organic contaminations. Glycerol (0.1 M) was dissolved into solutions of different pH (0.1 M NaOH, 0.1 M Na_2SO_4, and 0.5 M H_2SO_4). Prior to the experiments oxygen was removed by bubbling argon through the solution for at least 30 minutes. Working electrodes in the experiment were polycrystalline gold (dia. 5 mm) and platinum disks (dia. 6.1 mm) embedded in PTFE shrouds, which were mechanically polished with alumina (up to 0.05 μm), and cleaned ultrasonically in ultrapure water before use. In all experiments, a platinum plate was used as a counter electrode, while a reversible hydrogen electrode (RHE) was employed as a reference electrode. Electrochemical cell potentials were controlled with a Potentiostat/galvanostat (μ-Autolab Type III). All chemicals used for this work were at least analytical grade.

3.2.2 Fraction Collection

The reaction products in neutral and acidic conditions were collected with the same sample collecting tip as already described in our previous work.[11] Considering the stability of collected products in alkaline solution, in particular glyceraldehyde and dihydroxyacetone, the tip for sample collection was modified as illustrated in Scheme 1. While collecting products from electrode surface, a small amount of stabilizer (i.e. buffer or acidic solution) is injected into the tip-block and immediately mixed with the collected sample. Well mixed and stabilized samples are collected onto the microtiter plate for further analysis in the HPLC system.

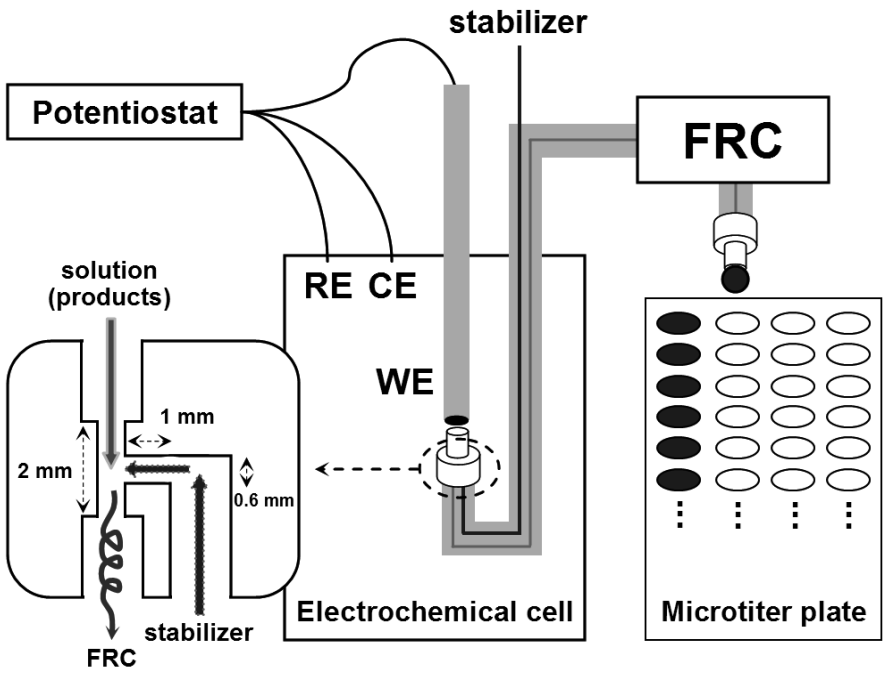

Scheme 1. Schematic diagram of the on-line sample collection by fraction collector (FRC) with a special sample collecting tip for the stabilization of collected samples.
WE - Working Electrode, RE - Reference Electrode, CE - Counter Electrode.

3.2.3 Chromatographic Determination of Products

The samples collected during voltammetry were analyzed in an HPLC system. The microtiter plate with the collected samples was placed in an auto-sampler holder and diverse volumes (2~20 μL) of sample were injected into the column. The columns used were a single Aminex HPX 87-H (Bio-Rad) column or the Aminex with Sugar SH1011 (Shodex) column in series, especially for the detection of dihydroxyacetone. Diluted sulfuric acid (0.5~5 mM) was used as eluent. The selected temperature of column oven was changed from 30 to 85°C in order to confirm reaction products. Details of system configuration are described elsewhere.[11]

3.2.4 On-line Electrochemical Mass Spectrometry (OLEMS)

OLEMS measurements were performed on an EvoLution mass spectrometer system (European Spectrometry Systems Ltd.).[20] The system consists of a Prisma QMS200 (Pfeiffer), brought to vacuum with a TMH-071P turbo molecular pump (60 l/s, Pfeiffer) and a Duo 2.5 rotary vane pump (2.5 m^3/h, Pfeiffer). During measurements, the pressure inside the MS was 1-5 × 10^{-9} bar. Pretreatment procedures and details were explained in a previous paper.[21] For the OLEMS experiments, bead type Au and Pt electrodes were used.

3.3 Results and discussion

3.3.1 Glycerol oxidation in alkaline condition

Considering the glycerol oxidation pathway, glyceraldehyde and/or dihydroxyacetone (DHA) should be produced as intermediate species and/or product. However, in our previous Chapter 2,[11] we assumed that they were not produced during the voltammetric glycerol oxidation on Au and Pt electrodes in alkaline media due to their absence in chromatograms. Generally, however, aldehydes are not stable in alkaline condition, but undergo base-catalyzed dimerization or aldol condensation reactions.[22,23] Therefore, in order to probe the importance of such a non-Faradaic reaction during glycerol oxidation, we investigated the time-dependent degradation of glyceraldehyde (1 mM), an isomer of

dihydroxyacetone, under oxygen-present and -free solutions (0.1 M NaOH). Samples were collected at different reaction times and collected samples were immediately neutralized with the same volume of 50 mM H_2SO_4, and then analyzed in an HPLC system. Figure 1 shows the concentration changes of glyceraldehyde and its chemical reaction products in alkaline condition, both in the absence (Figure 1a) and presence (Figure 1b) of oxygen in solution. Regardless of the presence of oxygen, glyceraldehyde evolves into its isomer (DHA), dimer (incl. fructose) and lactic acid. In a non-deaerated solution, glyceraldehyde decays much faster than in oxygen-free solution, and note that we detected many products that have been claimed as the products of catalytic glycerol oxidation such as glyceric acid, glycolic acid, and formic acid.[6,7,11,24] We note in particular that the concentration of glyceric acid reached 0.35 mM in 15 min, which means glyceraldehyde is predominantly oxidized to glyceric acid, even in the absence of a catalyst. In addition, the concentrations of glycolic acid and formic acid increased gradually, with a constant ratio, but slowly compared to glyceric acid due to the lower rate of C-C bond breaking (glycolic acid and formic acid are formed by decomposition of glyceric acid[6,11]). Even after glyceraldehyde is no longer detected, both the concentrations of glycolic acid and formic acid still increase, which can be explained by the decomposition of fructose after 15 min, since fructose also generally undergoes chemical degradation and oxidation under alkaline conditions.[25,26]

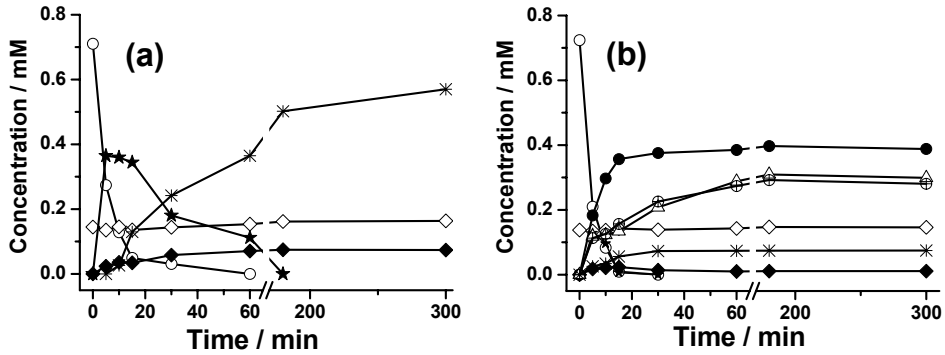

Figure 1. Glyceraldehyde degradation in 0.1 M NaOH as a function of reaction time under (a) argon-saturated and (b) non-deaerated condition. ○ glyceraldehyde, ★ dihydroxyacetone (DHA), ● glyceric acid, △ glycolic acid, ⊕ formic acid, ◇ dimer, ◆ fructose, and ✳ lactic acid.

In our previous work, the samples collected during voltammetry were open to air even in alkaline media, which accelerated the base-catalyzed degradation of unstable glycerol

oxidation intermediates. For an unequivocal understanding of the Faradaic reaction pathways (i.e. those requiring interfacial electron transfer) during glycerol oxidation, the stabilization of collected samples by lowering pH of the collected samples is essential, since the degradation of glyceraldehyde or dihydroxyacetone occurs only under alkaline conditions at room temperature[22,23] or under acidic conditions at high temperature.[27] To improve the existing system, we considered the modified sample collecting-tip illustrated in the Experimental Section (Scheme 1) as an optimal solution, because the collected sample may continue to degrade inside the tubing during the long traveling time (ca. 10 min) from sample collecting-tip to microtiter plate. Therefore, whilst collecting glycerol oxidation products during voltammetry in alkaline solution, a small amount of 0.5 M H_2SO_4 solution was continuously injected into the tip-block and immediately mixed with collected samples. The pH of samples in microtiter plate was ca. 3 ~ 5.

Figure 2 shows the voltammograms recorded in the presence of online sample collection with the modified sample collecting tip, alongside the reaction products of glycerol oxidation on platinum (Figure 2A) and gold (Figure 2B) in alkaline condition as detected by the HPLC system. Note that the voltammograms of glycerol oxidation on both electrodes are similar to the results in our previous paper,[11] which implies that the modified sample collecting tip does not seriously affect the glycerol oxidation reaction. The gold electrode shows an almost 10 times higher current density than the Pt electrode, but only at higher potentials. Both catalysts also have very different onset potentials: ca. 0.4 and 0.8 V for Pt and Au electrodes, respectively. We have ascribed the higher activity of gold to the delayed surface oxidation of Au compared to Pt, which allows for the application of higher effective overpotentials on gold. In the potential region where both Pt and Au are not covered by an oxide layer, platinum is always more active than gold. Both on the Pt and the Au electrode, the onset of glycerol oxidation exhibits a Tafel slope of ca. 120 mV/dec, suggesting that the first electron transfer is rate determining.

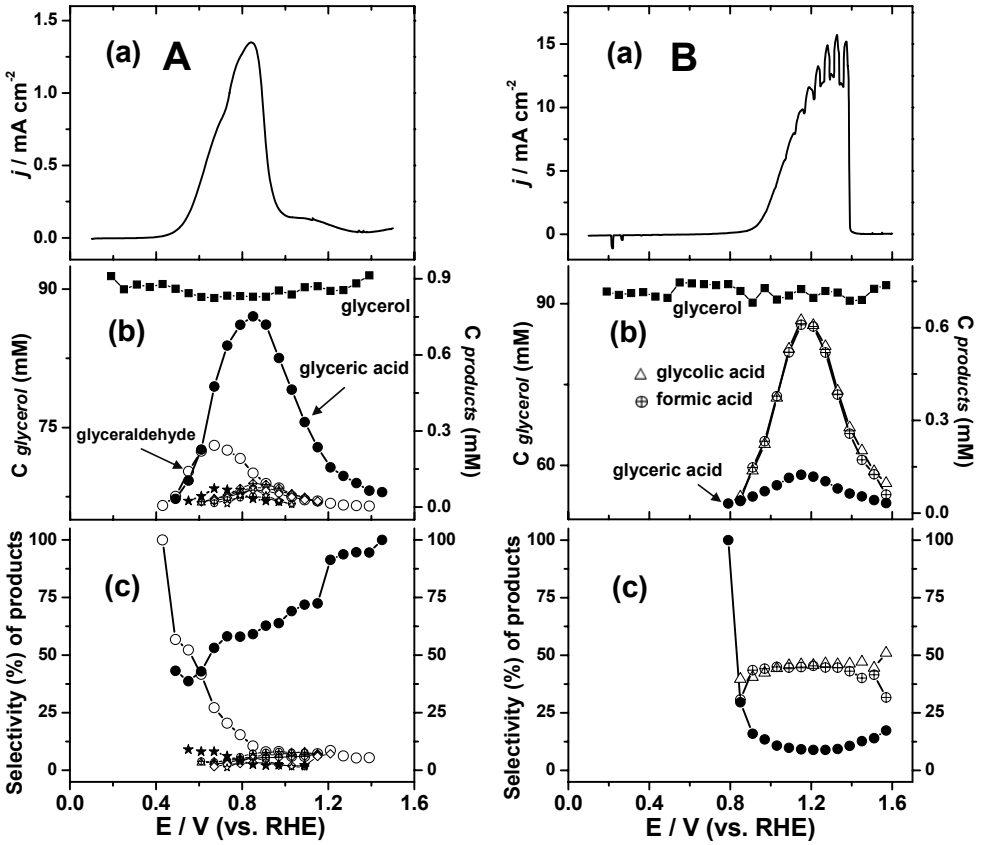

Figure 2. Glycerol oxidation (0.1 M) on (A) Pt and (B) Au electrodes in 0.1 M NaOH: (a) current density during linear sweep voltammetry with scan rate of 1 mV/s, (b) concentration changes of glycerol and its reaction products collected with the modified sample collecting tip and analyzed in an HPLC system, and (c) selectivity (%) of products as a function of potential. ■ glycerol, ○ glyceraldehyde, ★ dihydroxyacetone (DHA), ● glyceric acid, △ glycolic acid, ⊕ formic acid, ◇ oxalic acid, ⌖ tartronic acid, and ☆ hydroxypyruvic acid.

The key result here is that in the product distribution on Pt (Figure 2A-b), glyceraldehyde, dihydroxyacetone, and hydroxypyruvic acid were detected by stabilization of collected samples with the modified sample collecting tip and by an extended product analysis window using two columns in series in the HPLC. These three products are not observed on Au, and were also not observed on Pt in our previous paper using the "old" sample collecting tip.[11] The peaks observed in the chromatograms are converted to the

corresponding concentrations of the various compounds, the results of which are shown in Figure 2A-b and Figure 2B-b. The measured concentration of glycerol was lower than 0.1 M due to the dilution by the continuous injection of stabilizer into the sample collecting tip-block. The concentration of glycerol near the Pt electrode slowly decreases as a function of potential with the lowest value between 0.6 and 1 V, after which it increases slightly as the potential increases positively, although this trend is less clear on the Au electrode. Glyceraldehyde was detected as the first glycerol oxidation product from 0.4 V and observed in whole potential range with its maximum concentration at 0.65 V. As the potential increases, the concentration of glyceric acid steeply increases showing its highest concentration at ca. 0.85 V, which corresponds well with the potential of highest current density in the voltammogram. Based on the sequence of the detected products, we may conclude that glyceric acid is formed from the further oxidation of glyceraldehyde. In addition to glyceraldehyde as the product of primary alcohol oxidation, a relatively low concentration of dihydroxyacetone was also observed and its concentration profile follows that of glyceraldehyde. Especially hydroxypyruvic acid, a compound derived from further oxidation of dihydroxyacetone, was also observed at the highest current values. Interestingly, the concentrations of glycolic acid and formic acid shown in Figure 2A-b are relatively small compared to our previous results,[11] primarily because the stabilized samples containing glyceraldehyde and dihydroxyacetone do not decompose to glycolic acid and formic acid even if samples are open to oxygen. As already mentioned, glyceraldehyde is the first product of glycerol oxidation with close to 100% selectivity at 0.4 V; however, it drops to 10% at 0.8 V in Figure 2A-c because of its conversion to glyceric acid. Therefore, the selectivity toward glyceric acid increases gradually from 40% at 0.6 V to 100 % at the highest potential, though the efficiency at these high potentials is low.

On a gold electrode, we observe only three products as previously reported,[11] and glyceric acid was detected first instead of glyceraldehyde, which means glycerol was oxidized to glyceric acid through glyceraldehyde rapidly, primarily due to the higher overpotentials applicable to gold. The main difference with platinum is that on gold glyceric acid is actively oxidized to glycolic acid and formic acid each with ca. 45 % selectivity after 0.85 V, since there is a wider potential range available for the further oxidation given the higher onset potential of surface oxide formation on gold (~ 1.3 V) compared to platinum (~ 0.85 V).

Based on the results in Figure 2, a reaction mechanism for the glycerol oxidation on Au and Pt electrodes in alkaline media is suggested in Figure 3. In the pathway of primary alcohol oxidation, glycerol is first oxidized to glyceraldehyde in a two-electron transfer step and glyceraldehyde is further oxidized to glyceric acid in a subsequent two-electron transfer step. In the case of the gold electrode, glyceric acid is apparently directly produced from glycerol through glyceraldehyde, because of the high effective overpotential on gold, making glyceraldehyde an unstable intermediate. As a next two-electron transfer step, glyceric acid is further oxidized by cleavage of a C-C bond into glycolic acid and formic acid on both electrodes. However, on the platinum electrode this process becomes deactivated at potentials close to 0.9 V, where Pt forms an inhibiting surface oxide. The Au electrode has a much higher conversion activity of glyceric acid to glycolic acid and formic acid than the Pt electrode, which we ascribe to the higher surface oxidation potential of gold compared to platinum. In addition, glyceric acid and glycolic acid are further oxidized on the platinum electrode to tartronic acid and oxalic acid, respectively. In the pathway of secondary alcohol oxidation, dihydroxyacetone is produced in a two-electron transfer step, but only on the Pt electrode. As a next two-electron transfer step, dihydroxyacetone is oxidized to hydroxypyruvic acid, which can be further oxidized to ketomalonic acid even though it was not detected due to the detection limit of our current system. Recently, the formation of CO_2 as the final oxidation product of glycerol on a gold electrode in alkaline media was observed during FTIR experiments,[7] although CO_2 should appear as carbonate (CO_3^{2-}) in alkaline media by its combination with OH^-. However the assumption of total oxidation of glycerol to CO_2 suggested in that article is unrealistic, because only a limited amount of CO_2 can be produced through formic acid oxidation, considering the similar concentrations of glycolic acid and formic acid in Figure 2B-b. It is also important to point out an important artifact that often appears with the detection of oxidation products using FTIR in the thin-layer configuration. As the oxidation of these organic molecules produces protons which become subsequently trapped in the thin layer, the pH in the thin layer is effectively (much) higher than in the bulk of the solution. Formic acid (or formate) has a very low oxidation activity on gold in alkaline media,[28] but a much better oxidation activity in acidic media.[29] This pH change is probably the main reason why the formic acid intermediate is oxidized on gold and why CO_2 is observed and not carbonate. Normally, in alkaline media, we would expect that only Pt is capable of oxidizing formic acid to carbonate. Therefore, we believe that any complete oxidation of glycerol to carbon dioxide on gold is highly questionable.

As a brief intermediate conclusion concerning alkaline conditions, we can observe both primary and secondary alcohol oxidation pathways on a Pt electrode in alkaline condition with the modified sample collecting-tip. Glyceraldehyde is the main product at low potentials, but is essentially unstable in alkaline media, and is easily oxidized to glyceric acid as the dominant product at higher potentials ($\geq$ 0.6 V). The observation of glyceric acid as the first product on Au electrode shows that glyceraldehyde and dihydroxyacetone are intermediate oxidation products. On gold, glyceraldehyde is oxidized to glyceric acid due to the higher oxidation potentials accessible on Au compared to Pt.

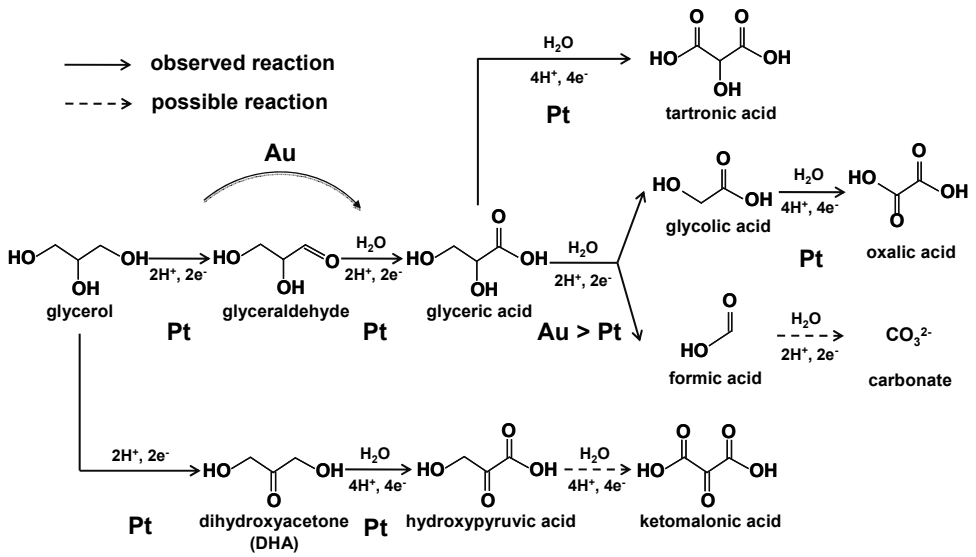

Figure 3. Schematic diagram for the glycerol oxidation mechanism on Au and Pt electrodes in alkaline media.

3.3.2 Glycerol oxidation in neutral condition

The investigation of the electro-oxidation of glycerol in neutral media has been limited to research related to microorganisms, i.e. bio-catalysis in a microbial fuel cell (MFC), to provide optimum pH conditions for bacteria.[30] However, studying neutral conditions as an intermediate between alkaline and acid conditions, is important for the understanding of the catalytic activity changes on gold and platinum electrodes in various media. Below, we report on the oxidation of glycerol in 0.1 M Na_2SO_4. Because of the low sweep rate applied, which should limit the effect of pH changes by the reaction occurring, and because we did

not want to introduce new anion (compared to acidic media), we did not work with buffered solutions. Similar reactivities were found, however, in phosphate buffered solutions, and therefore we believe that the general qualitative conclusions given below are valid.

Figure 4 shows the voltammetry of glycerol oxidation in 0.1 M Na_2SO_4 alongside the concentration profiles of glycerol and its oxidation products on platinum (Figure 4A) and on gold (Figure 4B) electrodes, both in the absence (dotted line) and presence (solid line) of online sample collection. The effect of online sample collection on the voltammogram was described in our previous work.[11] First of all, note that the oxidation current is significantly higher on platinum than on gold, in contrast with the situation in alkaline media. Glycerol oxidation on platinum begins from 0.45 V, and the current increases significantly from 0.6 V. In spite of the presence of sample collection, the oxidation current of glycerol was not delayed compared to the current without sample collection, particularly in the range up to 0.7 V. Presumably this happens because the intermediate species is oxidized further only very slowly. In other words, the first oxidation product (glyceraldehyde) is the final product in that potential range. The same tendency was also observed on the gold electrode, albeit in a different potential window. On Au, glycerol is oxidized from 0.8 V and sample collection did not cause any current changes until 1.1 V. Although the onset potentials of two electrodes are not identical, the kinetics of glycerol oxidation in neutral conditions are significantly slower than in alkaline conditions, and the removal of intermediate species has no effect on current at low potentials. On the other hand, online sample collection caused a small current increase from 0.7 to 1.5 V on the platinum electrode and from 1.1 to 1.5 V on gold electrode, respectively. This current enhancement is probably due to the removal of poisonous intermediate species such as CO on platinum or carboxylic acids on the gold electrode.[11,31-33]

Collected samples during voltammetry were analyzed in an HPLC system, and the peaks observed in the chromatograms were converted to the corresponding concentrations of the various compounds, the results of which are shown in Figure 4A-b and Figure 4B-b. The first product of glycerol oxidation on platinum, glyceraldehyde, appears at 0.43 V and its concentration increases until 0.8 V, after which it decreases due to the formation of surface oxide until 1.1 V. For higher potentials, the concentration of glyceraldehyde increases again slightly until 1.2 V, and then decreases steeply. There is a small disagreement between the potentials of the peak in current density and the maximum glyceraldehyde concentration

near 0.8-0.9 V, due to the further oxidation of glyceraldehyde to glyceric acid. Glyceric acid appears as a product from 0.6 V. The concentration of glyceric acid increases slowly until 0.8 V as the maximum current is observed, after which it shows a plateau, and then steeply increases from 1 V to 1.3 V, implying that the oxidation of glyceraldehyde at these high potentials is accelerated. Interestingly, one of the oxidation products of glyceric acid, glycolic acid, is observed without the observation of formic acid from 0.65 V with a peak in concentration at 0.8 V. Glycolic acid and formic acid appear as a pair from 1.1 V and higher potentials with almost the same concentration profiles. The absence of formic acid until 1.1 V strongly suggests that it is further oxidized to CO_2, probably through the formation of chemisorbed CO which is a poisoning intermediate. To obtain additional evidence for the formation of CO_2, an online electrochemical mass spectrometry (OLEMS) experiment was carried out. Figure 4A-c shows the MS ion current for m/z = 44, which implies CO_2 formation, clearly demonstrating that formic acid is further oxidized to CO_2 at around 0.8 V. Moreover, the steep increase of the CO_2 intensity from 1.4 V should also be ascribed to formic acid oxidation, but it is then hard to explain why there is a slightly higher concentration of formic acid than that of glycolic acid in Figure 4A-b. The reason for this will be further discussed in the next section on the glycerol oxidation in acidic conditions, and it is mainly due to the glycolic acid oxidation to formic acid. As a product of secondary alcohol oxidation, dihydroxyacetone was also observed, but its concentration is negligible in the entire potential range except for the region corresponding to a PtO_x surface. Even though dihydroxyacetone is not produced in great amounts, it was further oxidized to hydroxypyruvic acid, a trace of which was observed in the chromatograms.

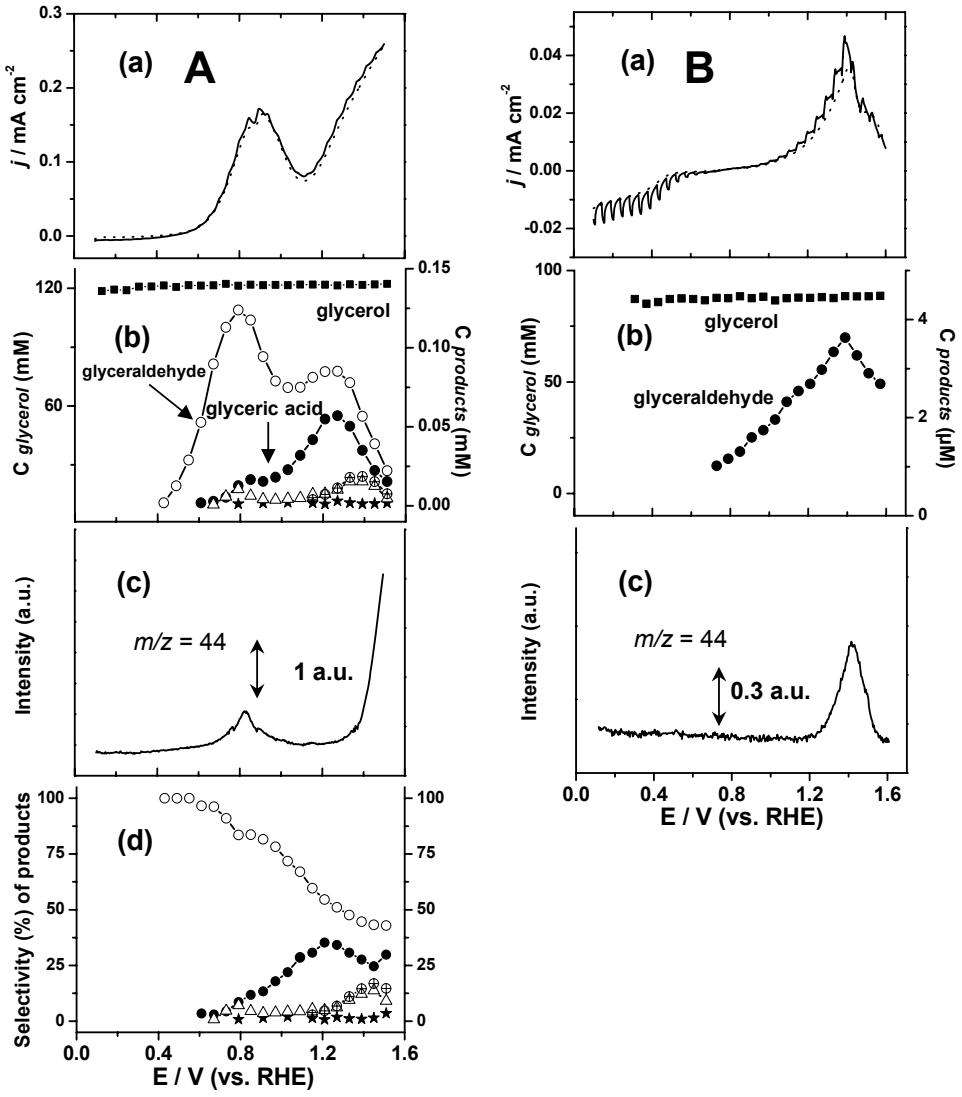

Figure 4. Glycerol oxidation (0.1 M) on Pt (A) and Au (B) electrodes in 0.1 M Na_2SO_4: (a) current density profile with (solid line) and without (dotted line) sample collection during linear sweep voltammetry with scan rate of 1 mV/s, (b) concentration changes of glycerol and its reaction products collected with modified sample collecting tip, (c) ion current profiles for m/z = 44 (CO_2) in OLEMS measured during voltammetry, and (d) selectivity (%) of products as a function of potential. ■ glycerol, ○ glyceraldehyde, ★ dihydroxyacetone (DHA), ● glyceric acid, △ glycolic acid, ⊕ formic acid.

On a gold electrode, only glyceraldehyde was detected as a glycerol oxidation product in the HPLC system. Glyceraldehyde appears from 0.8 V and its concentration slowly increases until 1.4 V, after which it decreases in good correspondence with its current profile. To estimate the detection limit of our current HPLC system, an OLEMS experiment was carried out and disclosed that a relatively small amount of CO_2 is also produced during glycerol oxidation on Au electrode, but only at very high potentials. Considering the high sensitivity of OLEMS for product detection, we can conclude that a small amount of glyceraldehyde must be further oxidized to glyceric acid, glycolic acid and formic acid in this potential range.

The main product of glycerol oxidation on Pt in neutral conditions is glyceraldehyde as shown in Figure 4A-d. The selectivity to glyceraldehyde is over than 80% until 0.8 V, and it is slowly oxidized further to glyceric acid as the potential increases. Interestingly, the amount of glyceric acid decreases from 1.2 V, which matches well with the increase of the selectivity toward glycolic acid and formic acid.

From the results shown in Figure 4, a reaction mechanism for the glycerol oxidation in neutral condition on Au and Pt electrodes is suggested in Figure 5. The general glycerol oxidation pathways in neutral condition are essentially identical to alkaline media, although some products, i.e. oxalic acid and tartronic acid, are absent in the product spectrum. The dominant product of glycerol oxidation is glyceraldehyde formed in a two-electron transfer step on both electrodes. Especially gold shows a very high selectivity to glyceraldehyde in neutral media. Interestingly, the PtO_x surface, though normally considered inactive, shows activity for glycerol oxidation, but its selectivity to glyceraldehyde is less than on a clean Pt surface since glyceraldehyde is further oxidized to glyceric acid, glycolic acid, formic acid and CO_2 on PtO_x. This would suggest that the Pt surface at these high potentials is not fully oxidized to PtO_x in the presence of glycerol, or the high anodic potential makes PtO_x catalytically active. Dihydroxyacetone, the product of secondary alcohol oxidation is produced in small amounts in a two-electron transfer step on the Pt electrode and further oxidized to hydroxypyruvic acid at high potentials.

Although only glyceraldehyde was observed as the glycerol oxidation product on gold electrode in an HPLC analysis, the formation of (small amounts of) CO_2 as the full oxidation product is observed during OLEMS measurements on both electrodes. The

consistency of the appearance of CO_2 with the concentration patterns observed for formic acid (see Figure 4AB-c) prove that CO_2 is formed from formic acid oxidation.

As a general conclusion concerning neutral conditions, we can observe glyceraldehyde as the main oxidation product, although both primary and secondary alcohol oxidation pathways are available on the Pt electrode. The current density of glycerol oxidation on platinum and gold electrodes in neutral conditions is 10 and 50 times lower than in alkaline conditions, respectively, which is well reflected in the product distributions. Furthermore, the onset potential of glycerol oxidation on both electrodes shifted slightly positive. Both observations imply that OH^- strongly encourages the glycerol oxidation reaction and plays an important role as proton acceptor or reaction mediator, especially on an Au electrode.

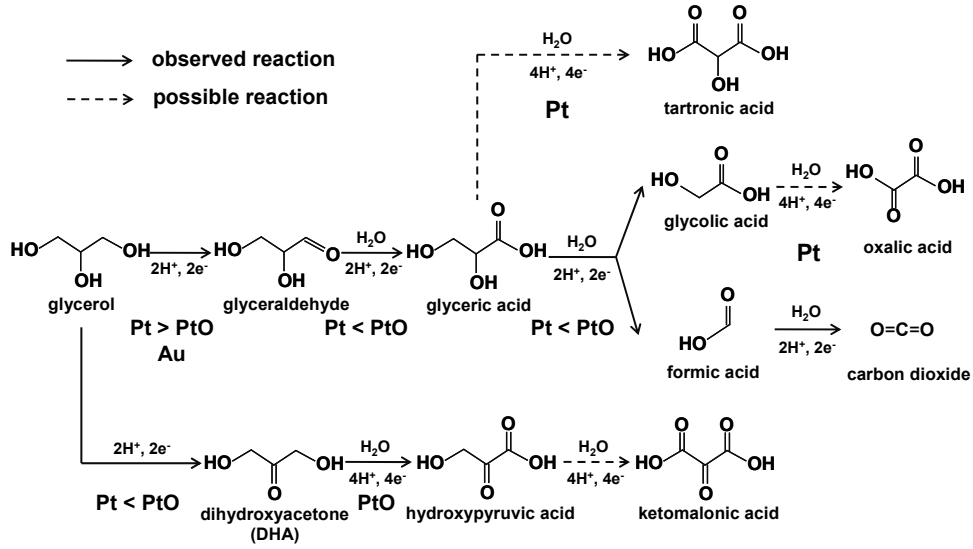

Figure 5. Schematic diagram for glycerol oxidation mechanism on Au and Pt electrodes in neutral media.

3.3.3 Glycerol oxidation in acidic condition

In acid medium, only the platinum electrode shows electrocatalytic activity for the oxidation of glycerol. Figure 6 shows the voltammetry of glycerol oxidation both in the absence (dotted line) and presence (solid line) of online sample collection alongside the concentrations of glycerol and its oxidation products on a platinum electrode in 0.5 M

H_2SO_4 acidic solution. First of all, the general tendency of glycerol oxidation in acidic solution is similar to neutral solution with small deviations of onset potential and maximum current density as shown in Figure 6a. Glycerol oxidation on platinum begins from 0.4 V, and the current increases steeply from 0.55 V, both at ca. 50 mV lower potential than in neutral condition. However, with sample collection the oxidation of glycerol appears a little delayed compared to the current without sample collection, particularly in the range of 0.6-0.9 V. The origin of the current delay during glycerol oxidation is the removal of active intermediates by the sample tip, as supported by the appearance of further oxidation products, i.e. glyceric acid, in that potential range. The current density of the first oxidation feature in the potential range between 0.55 and 1 V, which consists of two peaks, is almost half of that in neutral condition, and it increases to the same values as in neutral solution at high potentials (>1.3 V).

The concentrations of glycerol oxidation products in acidic condition are shown in Figure 6b, as converted from the chromatograms. The first product, glyceraldehyde, appears at 0.37 V and its concentration increases until 0.65 V in good correspondence with the current profile, after which it decreases due to the further oxidation of glyceraldehyde to glyceric acid. The appearance of glyceric acid is observed from 0.6 V and shows a slight first maximum concentration at 0.8 V, coinciding with the current density maximum in that potential range. We point out that the oxidation of glyceric acid to glycolic acid and formic acid in acidic condition is not favored compared to alkaline and neutral solution since no glycolic acid and formic acid were observed until 1.1 V in Figure 6b. This suggests that glyceric acid conversion to glycolic acid and formic acid is strongly base catalyzed. Nevertheless, the formation of CO_2 (presumably from formic acid oxidation) at around 0.65 V is observed in the OLEMS experiment, as shown in Figure 6c. The complete absence of glycolic acid until 1.1 V testifies for the low activity of the Pt electrode for the conversion of glyceric acid. The most interesting observation concerning glycerol oxidation in acidic condition is the potential range above 1.1 V, where a relatively high selectivity to formic acid is observed. The oxidation of glyceric acid to glycolic acid and formic acid on PtO_x was also observed in neutral solution, and the slightly higher concentration of formic acid compared to glycolic acid together with the formation of CO_2 in that potential range was explained by the further oxidation of glycolic acid to formic acid. In acidic solution, the maximum concentration of formic acid is ca. 5 times higher than that of glycolic acid. To prove the importance of the glycolic acid oxidation reaction, the oxidation of glycolic acid

(10 mM) on a Pt electrode was studied separately and it clearly showed the production of formic acid from glycolic acid in the same potential ranges from 1.1 V. Finally, as a product of secondary alcohol oxidation, dihydroxyacetone was observed from 0.5 V to 1.5 V, and its concentration is a little higher on PtO_x than on a clean Pt surface.

The main product of glycerol oxidation on Pt in acidic condition is glyceraldehyde as shown by selectivity patterns in Figure 6d. The selectivity to glyceraldehyde is 100% at 0.4 V and decreases slowly to ca. 80% until 1.1 V, after which its decay is accelerated to ca. 40% at the highest potential, where it matches the selectivity to formic acid.

Based on the results described in Figure 6, a reaction mechanism for the glycerol oxidation on Pt in an acidic medium is suggested in Figure 7. The general glycerol oxidation pathways in acidic condition are essentially identical to in neutral and alkaline media, which means the pH of the solution does not change the existence of the reaction pathways but pH plays an important role in their relative importance. The dominant product of glycerol oxidation is glyceraldehyde and also the PtO_x surface shows activity for glycerol oxidation as in neutral solution (whereas in alkaline it does not). Interestingly, PtO_x encourages the further oxidation of glyceraldehyde and produces mainly formic acid and CO_2 through glyceric acid and glycolic acid intermediates at high potential. Dihydroxyacetone, the product of secondary alcohol oxidation is produced in a two-electron transfer step and its measured concentration is higher than at the other pH's, which suggests that the DHA production is favored in acidic media.[4,34-37]

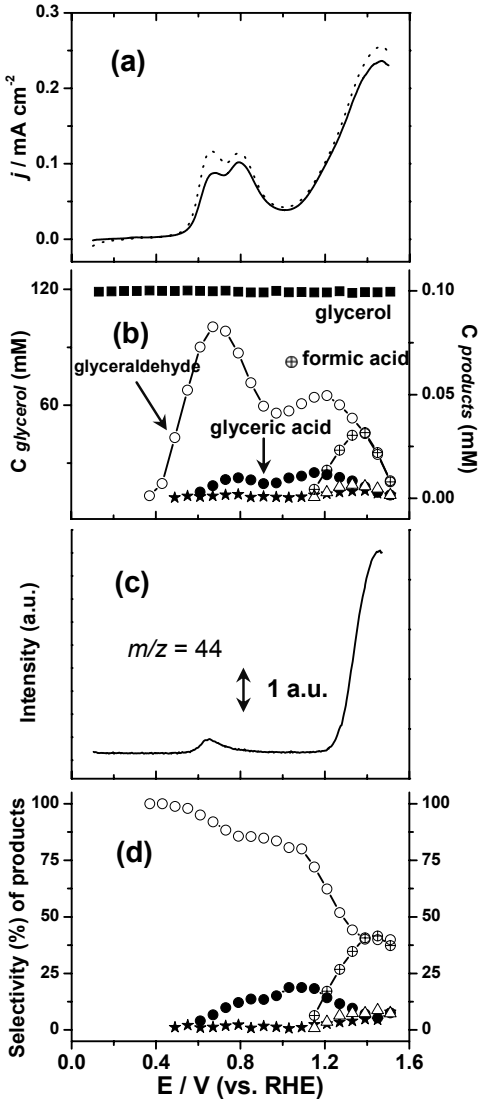

Figure 6. Glycerol oxidation (0.1 M) on a Pt electrode in 0.5 M H_2SO_4: (a) current density profile with (solid line) and without (dotted line) sample collection during linear sweep voltammetry with scan rate of 1 mV/s, (b) concentration changes of glycerol and its reaction products collected with modified sample collecting tip, (c) ion current profiles for m/z = 44 (CO_2) in OLEMS measured during voltammetry, and (d) selectivity (%) of products as a function of potential. ■ glycerol, ○ glyceraldehyde, ★ dihydroxyacetone (DHA), ● glyceric acid, △ glycolic acid, ⊕ formic acid.

As a brief intermediate conclusion concerning acidic media, we observe both primary and secondary alcohol oxidation pathways on Pt electrode. Gold has no activity. The current density of glycerol oxidation on a clean Pt surface in acidic condition is about 2 and 20 times lower than in neutral and in alkaline conditions, respectively. The onset potential of glycerol oxidation on Pt electrode is not seriously affected by the pH of the solution. Acidic media seem to promote the oxidation of the secondary alcohol as compared to alkaline media, and thereby provide more favorable conditions for selective alcohol oxidation.

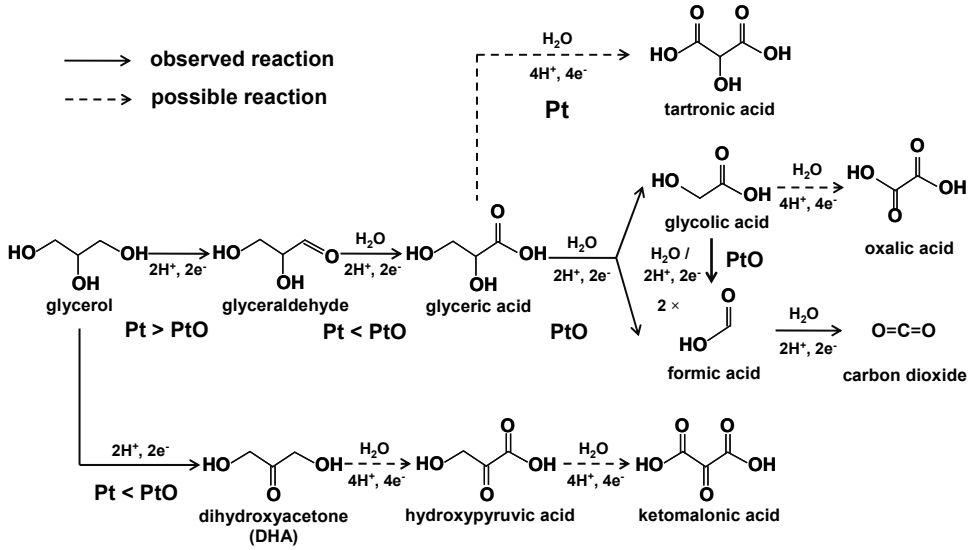

Figure 7. Schematic diagram for glycerol oxidation mechanism on Pt electrode in acidic media.

3.4 Conclusion

This work has elucidated the electro-oxidation mechanisms of glycerol on Au and Pt electrodes under different pH conditions by applying a new HPLC method to study the dissolved reaction products and by online mass spectrometry for CO_2 detection. Our main result is that both the activity and product distributions of glycerol oxidation are strongly dependent on pH and catalyst, however the general reaction pathways do not change. In alkaline media, a modified sample collecting tip for the stabilization of collected samples was applied and successfully allowed for the detection of unstable reaction intermediates,

i.e. glyceraldehyde and dihydroxyacetone, on a Pt electrode. Glyceric acid is the main product on a Pt electrode (with glyceraldehyde as reactive intermediate). Glyceric acid appears as the primary oxidation product on Au electrode in alkaline, but it is rapidly further oxidized to glycolic acid and formic acid due to high oxidation potentials necessary on gold. Interestingly, at these high potentials, gold appears as the most active catalyst for glycerol oxidation, but this is primarily due to the fact that gold stays "clean" even at these high potentials so that turnover can still take place. Lowering the pH significantly deactivates the glycerol oxidation on both Au and Pt electrodes, with Au having lost its activity completely in acidic condition. This effect is very similar to what has been observed for the oxidation of ethanol on Pt and Au,[38] and is believed to be related to the acidity of alcohol groups in glycerol, leading to a deprotonated glycerol species as the main reactant in alkaline media. Interestingly, neutral media appear particularly well suited for a high selectively toward glyceraldehyde, the first oxidation product of glycerol, especially on gold (although the activity is low). The activity and selectivity patterns for Pt are similar in neutral and acidic media (though neutral conditions lead to a slightly higher activity), and remarkably enough the PtO_x surface is active for glycerol oxidation at high potentials, and encourages the conversion of glyceraldehyde through glyceric acid and glycolic acid to formic acid and CO_2 at low pH.

3.5 References

[1] M. Pagliaro, R. Ciriminna, H. Kimura, M. Rossi, C. D. Pina, *Angew. Chem. Int. Ed.* **2007**, *46*, 4434-4440.

[2] C. Zhou, J. N. Beltramini, Y. -X. Fan, G. Q. Lu, *Chem. Soc. Rev.* **2008**, *37*, 527-549.

[3] O. M. Daniel, A. DeLaRiva, E. L. Kunkes, A. K. Datye, J. A. Dumesic, R. J. Davis, *ChemCatChem* **2010**, *2*, 1107-1114.

[4] N. Wörz, A. Brandner, P. Claus, *J. Phys. Chem. C* **2010**, *114*, 1164-1172.

[5] A. Behr, J. Eilting, K. Irawadi, J. Leschinski, F. Lindner, *Green Chem.* **2008**, *10*, 13-30.

[6] L. Roquet, E. Belgsir. J. M. Léger, C. Lamy, *Electrochim. Acta* **1994**, *39*, 2387-2394.

[7] D. Z. Jeffery, G. A. Camara, *Electrochem. Comm.* **2010**, *12*, 1129-1132.

[8] M. Simões, S. Baranton, C. Coutanceau, *Appl. Catal. B: Env.* **2010**, *93*, 354-362.

[9] M. Avramov-Ivić, J. -M. Léger, C. Lamy, V. D. Jović, S. D. Petrović, *J. Electroanal. Chem.* **1991**, *308*, 309-317.

[10] M. Avramov-Ivić, J. -M. Léger, B. Beden, F. Hahn, C. Lamy, *J. Electroanal. Chem.* **1993**, *351*, 285-297.

[11] Y. Kwon, M. T. M. Koper, *Anal. Chem.* **2010**, *82*, 5420-5424.

[12] Z. -Y. Zhou, N. Tian, Y. -J. Chen, S. -P. Chen, S. -G. Sun, *J. Electroanal. Chem.* **2004**, *573*, 111-119.

[13] W. C. Ketchie, Y. -L. Fang, M. S. Wong, M. Murayama, R. J. Davis, *J. Catal.* **2007**, *250*, 94-101.

[14] W. C. Ketchie, M. Murayama, R. J. Davis, *J. Catal.* **2007**, *250*, 264-273.

[15] S. Carrettin, P. Mcmorn, P. Johnston, K. Griffin, G. J. Hutchings, *Chem. Commun.* **2002**, 696-697.

[16] S. Carrettin, P. Mcmorn, P. Johnston, K. Griffin, C. J. Kiely, G. J. Hutchings, *Phys. Chem. Chem. Phys.* **2003**, *5*, 1329-1336.

[17] R. R. Soares, D. A. Simonetti, J. A. Dumesic, *Angew. Chem. Int. Ed.* **2006**, *45*, 3982-3985.

[18] B. N. Zope, D. D. Hibbitts, M. Neurock, R. J. Davis, *Science*, **2010**, *330*, 74-78.

[19] S. C. S. Lai, M. T. M. Koper, *Faraday Discuss.* **2008**, *140*, 399-416.

[20] A. H. Wonders, T. H. M. Housmans, V. Rosca, M. T. M. Koper, *J. Appl. Electrochem.* **2006**, *36*, 1215-1221.

[21] M. Duca, V. Kavvadia, P. Rodriguez, S. C. S. Lai, T. Hoogenboom, M. T. M. Koper, *J. Electroanal. Chem.* **2010**, *649*, 59-68.

[22] W. L. Evans, W. R. Cornthwaite, *J. Am. Chem. Soc.* **1928**, *50*, 486-492.

[23] V. A. Yaylayan, S. Harty-Majors, A. A. Ismail, *Carbohydr. Res.* **1999**, *318*, 20-25.

[24] A. N. Grace, K. Pandian, *Electrochem. Comm.* **2006**, *8*, 1340-1348.

[25] S. P. Moulik, D. Basu, P. K. Bhattacharya, *Carbohydr. Res.* **1978**, *63*, 165-172.

[26] B. Y. Yang, R. Montgomery, *Carbohydr. Res.* **1996**, *280*, 27-45.

[27] G. L. Lookhart, M. S. Feather, *Carbohydr. Res.* **1978**, *60*, 259-265.

[28] J. Hernández, J. Solla-Gullón, E. Herrero, A. Aldaz, J. M. Feliu, *Electrochim. Acta* **2006**, *52*, 1662-1669.

[29] G. L. Beltramo, T. E. Shubina, M. T. M. Koper, *ChemPhysChem* **2005**, *6*, 2597-2606.

[30] R. L. Arechederra, B. L. Treu, S. D. Minteer, *J. Power Sources* **2007**, *173*, 156-161.

[31] A. Capon, R. Parsons, *J. Electroanal. Chem.* **1973**, *44*, 1-7.

[32] A. Capon, R. Parsons, *J. Electroanal. Chem.* **1973**, *45*, 205-231.

[33] R. Parsons, T. VanderNoot, *J. Electroanal. Chem.* **1988**, *257*, 9-45.

[34] H. Kimura, K. Tsuto, T. Wakisaka, Y. Kazumi, Y. Inaya, *Appl. Catal. A* **1993**, *96*, 217-228.

[35] H. Kimura, *Appl. Catal. A* **1993**, *105*, 147-158.

[36] P. Gallezot, *Catal. Tod.* **1997**, *37*, 405-418.

[37] W. Hu, D. Knight, B. Lowry, A. Varma, *Ind. Eng. Chem. Res.* **2010**, *49*, 10876-10882.

[38] S. C. S. Lai, S. E. F. Kleijn, F. T. Z. Öztürk, V. C. Van Rees Vellinga, J. Koning, P. Rodriguez, M. T. M. Koper, *Catal. Tod.* **2010**, *154*, 92-104.

4

Highly selective electro-oxidation of glycerol to dihydroxyacetone on platinum in the presence of bismuth

Abstract

A carbon supported platinum electrode in a bismuth saturated solution at a carefully chosen potential is capable of oxidizing glycerol to dihydroxyacetone with 100% selectivity. In the absence of bismuth, the primary alcohol oxidation is dominant. Using a combination of online HPLC and in situ FTIR, it is shown that Bi blocks the pathway for primary oxidation but also provides a specific Pt-Bi surface site poised for secondary alcohol oxidation.

The contents of this chapter have been published: Y. Kwon, Y. Birdja, I. Spanos, P. Rodriguez, M. T. M. Koper, *ACS Catal.*, **2012**, *2*, 759–764.

4.1 Introduction

In recent years, there has been a growing interest in converting glycerol to valuable chemicals. Glycerol, a surplus byproduct of biodiesel, can be selectively transformed to functionalized feedstocks such as dihydroxyacetone and glyceric acid.[1,2] Especially dihydroxyacetone (DHA), the product of secondary alcohol oxidation, is widely used in the cosmetic industry as a self-tanning agent. It is currently produced by biological fermentation.[3] In spite of its high conversion and selectivity, microbial oxidation suffers from a low glycerol concentration and a long operating time. In heterogeneous catalysis, several monometallic (Pt, Pd, Au)[4,5] and bimetallic catalysts (Pt-Bi, Au-Pt)[4,6-9] have been investigated and revealed that the Pt-Bi bimetallic system shows a promising conversion and selectivity toward DHA at low pH and mild operating conditions.[8] Also homogeneous catalysts have been reported for the selective glycerol oxidation to DHA.[10]

In this chapter, we show that the selective conversion of glycerol to DHA may be achieved by electro-catalytic oxidation on a carbon-supported platinum (Pt/C) electrode in a bismuth-saturated acidic solution. Such a half cell could eventually be incorporated in an electrolysis cell co-producing hydrogen and DHA (incidentally, PtBi is also an active electrocatalyst for hydrogen evolution[11]), or in a fuel cell co-producing electricity and DHA. A previous electro-chemical method employing a glassy carbon electrode for glycerol oxidation mediated by TEMPO showed 30% selectivity to DHA and 35% selectivity to hydroxypyruvic acid after 200 h,[12] which is still inferior to metal-based heterogeneous catalysis. Our results show that by careful selection of the electrode potential, very high selectivity for glycerol conversion to DHA may be achieved. This high selectivity is related to a selective blocking of the Pt electrode by Bi adatoms.

4.2 Experimental

Electrochemical characterization was carried out in a standard three-electrode cell controlled by a potentiostat/galvanostat (μ-Autolab Type III). A thin-film electrode with 3 nm Pt/C nanoparticles (50wt%, Tanaka) was fabricated by loading defined amounts of nanoparticle suspension in water (1 mg mL^{-1}) onto a polished glassy carbon substrate, subsequently dried at room temperature. In order to confirm the electrochemically active

surface area of the loaded catalyst, a blank voltammogram was recorded before each experiment. A large Pt plate was employed as a counter electrode and a reversible hydrogen electrode (RHE) as a reference. Oxidation of glycerol was performed in a mixture of glycerol (0.1 M, analytical grade) and 0.5 M H_2SO_4 under deaerated conditions by purging Ar.

For the Pt/C surface modification, irreversible adsorption of bismuth was performed by placing the freshly prepared Pt/C electrode in contact with a Bi_2O_3-saturated 0.5 M H_2SO_4 solution, and full coverage is determined by a complete suppression of the hydrogen region,[15] and then rinsed with water and transferred to the electrochemical cell. For reversible bismuth adsorption/desorption, a sufficiently large amount of Bi_2O_3 was introduced directly into the electrochemical cell to obtain a bismuth saturated solution, which corresponds to a concentration of ca. 10^{-5}-10^{-4} M.[13]

The reaction products during voltammetry were collected and analyzed with an online HPLC system as described in our previous work.[14,15] Sample volumes of 20 µL were injected into the columns in series of Aminex HPX 87-H (Bio-Rad) and Sugar SH1011 (Shodex) with diluted sulfuric acid (0.5 mM) as eluent. The selected temperature of column oven was 85°C. Details of system configuration are described elsewhere.[14]

The FTIRRAS experiments were carried out with a Bruker Vertex80V IR spectrophotometer; a CaF_2 prism bevelled at 60° was used. Fifty interferograms were averaged for each spectrum, with a resolution of 8 cm^{-1}, resulting in a spectrum every 100 mV. All spectra were recorded using an angle of incidence of 60º, using p- polarised light. The reference spectrum was acquired at the CV starting potential where no Faradaic process takes place and the current is almost zero. Then, spectra at different potentials were collected, and the difference with respect to the reference spectrum was evaluated as the normalised change in reflectivity, $\Delta R/R$. In these difference spectra, negative bands (pointing down) correspond to the generation of species at the electrode-electrolyte interface and positive bands (pointing up) to the consumption of species.

4.3 Results and discussion

On pure Pt electrodes in acidic media, primary alcohol oxidation (to glyceraldehyde and glyceric acid) is favored over secondary alcohol oxidation at all potentials, the selectivity to DHA never exceeding 5% in Chapter 3.[14] The effect of bismuth on the selective oxidation of glycerol is illustrated in Figure 1, which compares the positive-going potential sweeps and the associated product spectrum as detected by online HPLC[15] at 1 mV/s for 0.1 M glycerol oxidation in 0.5 M H_2SO_4 on a Pt/C electrode (A), a bismuth-modified Pt/C electrode as obtained by irreversible Bi adsorption (corresponding to "full" Bi coverage, see experimental section)[13] (B), and for a Pt/C electrode in a solution saturated with Bi (C). The presence of bismuth in solution enhances the glycerol oxidation as shown by a peak at 0.65 V with a ca. 50 mV lower onset potential than that of the Pt/C electrode. The Pt-Bi electrode without Bi in solution exhibits a somewhat lower current density in the potential region of glycerol oxidation. At high overpotential, in the oxygen evolution region, a lower activity is observed in the presence of Bi, both for Bi on the surface and with Bi in solution. We note that the sharp peak at 0.25 V for the Pt/C electrode in Bi-containing solution in Figure 1 is due to oxidative desorption of multilayer bismuth,[16] the peak charge being proportional to the time at which the potential is kept at 0.1 V.

Panels (b) and (c) in Figure 1 compare the concentrations and the corresponding selectivity of the various products of glycerol oxidation as measured by online HPLC[15] for the three different electrodes (A), (B) and (C). The HPLC results confirm that in the absence of Bi, the Pt/C electrode is selective to oxidizing the primary alcohol, and the main products observed are glyceraldehdye and glyceric acid at low potential, and formic acid at high potential.[14] On the other hand, a Bi-modified Pt/C electrode shows a very different selectivity pattern, as one would expect from the results obtained in the heterogeneous catalysis literature.[6-9] At low potential, DHA is formed preferentially, leading to a peak in production and selectivity of ca. 75% at around 0.5-0.6 V. At higher potentials, similar selectivities as on Pt/C are obtained, and the selectivity to DHA drops to zero. It is logical to ascribe this effect to the oxidative desorption of the adsorbed Bi, which according to the literature takes place around 0.6-0.7 V.[13,16,17] As lower overall currents and activities are observed for the Bi-modified Pt/C electrode, the role of Bi seems to be to block the pathway for primary glycerol oxidation, in agreement with the original explanation offered by Kimura[6,7] and supported by Wörz et al..[9] However, in the presence of Bi in solution,

both activity and selectivity are significantly enhanced compared to the Bi-modified Pt/C electrode. Interestingly, the higher current observed at lower potential can be associated with an almost completely selective oxidation to DHA (see Figure 1(c) in column (C)). Even at maximum current, selectivity to DHA is close to 90%. Glyceraldehyde and glyceric acid formation are suppressed over the entire potential range, DHA always being the preferred product, and also much less formic acid is obtained at high potential. We note that, importantly, the enhanced activity and selectivity not only originates from the interaction of Bi with Pt, but also from the interaction of Bi with the carbon-supported Pt nanoparticles.

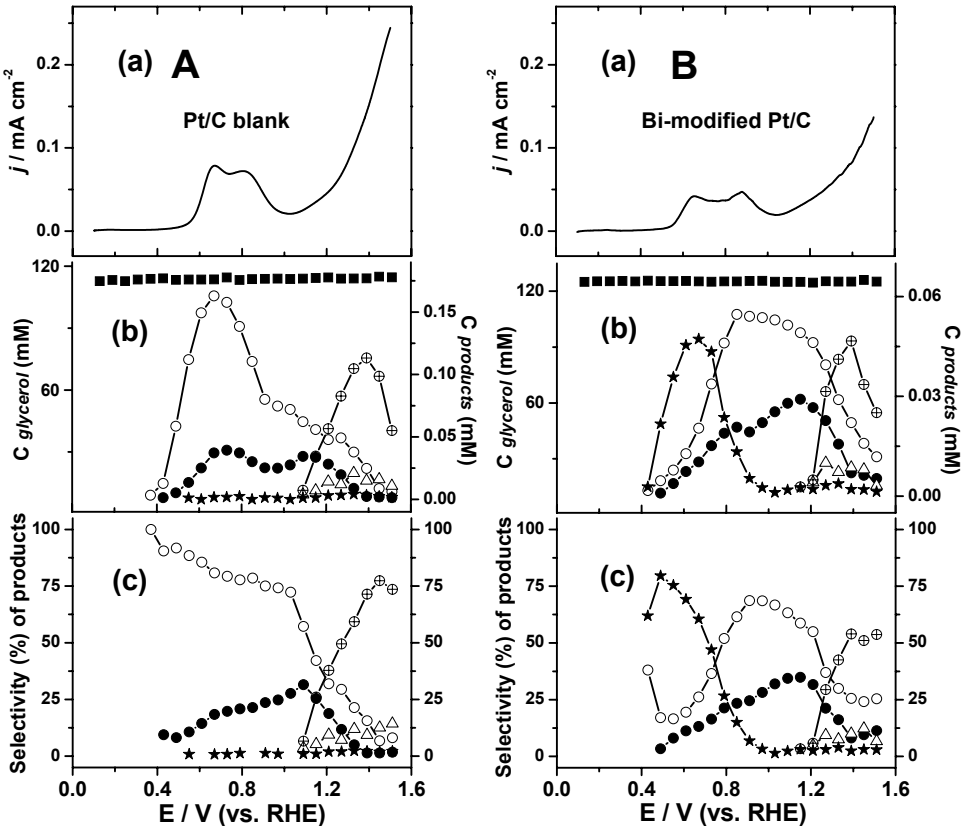

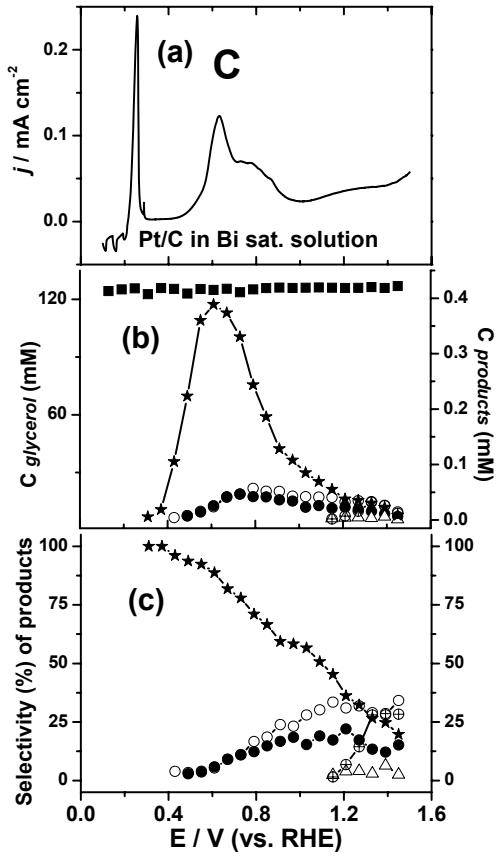

Figure 1. Glycerol oxidation (0.1 M) in 0.5 M H_2SO_4 for (A) a Pt/C electrode, (B) a Bi-modified Pt/C, and (C) a Pt/C electrode in Bi-saturated solution: (a) current density profile at scan rate of 1 mV/s, (b) concentration changes of glycerol and its reaction products, and (c) selectivity (%) of products as a function of potential. ■ glycerol, ○ glyceraldehyde, ★ dihydroxyacetone (DHA), ● glyceric acid, △ glycolic acid, ⊕ formic acid.

Figure 2 shows that in the presence of other supports, such as gold, Bi blocks the active sites of Pt nanoparticles, causing a lower activity and higher overpotential than for glycerol oxidation compared to Bi free solution, even though there is still an enhanced selectivity to DHA at low potentials. Therefore we conclude that Bi-modified Pt surface determines the reaction pathway toward secondary alcohol oxidation and the interaction of carbon

supported Pt with glycerol and Bi lowers the onset potential and thereby enhances the turnover frequency. Returning to Figure 1, note that, although the voltammetric profiles for glycerol oxidation on the three electrodes look rather similar, they actually correspond to significantly different oxidation products. The decrease in overall current for potentials higher than 0.65 V is observed for the oxidation of many organic molecules, and should be ascribed to the initial stages of Pt surface oxidation,[18] in the present case in conjunction with Bi on the surface. We have verified that the selectivity pattern shown in Figure 1 for the Pt/C electrode in Bi-containing solution is not dependent on the number of voltammetric scans. Second voltammetric scan showed essentially identical results (note that at a scan rate of 1 mV/s, as is required for a meaningful online HPLC analysis,[15] a single sweep takes about 20 minutes). Moreover, we have checked the effect of sample collection during voltammetry with the online HPLC system, as the sample collection removes active intermediate species. Various flow rates were applied and verified that the onset potential and the current density are not affected by sample collection. Finally, a lower coverage of Bi (ca. 37% of full coverage) for the Bi-modified Pt/C electrode leads to a severe increase in the primary oxidation products (see Figure 3), showing the importance of a high Bi surface coverage for selective secondary alcohol oxidation.

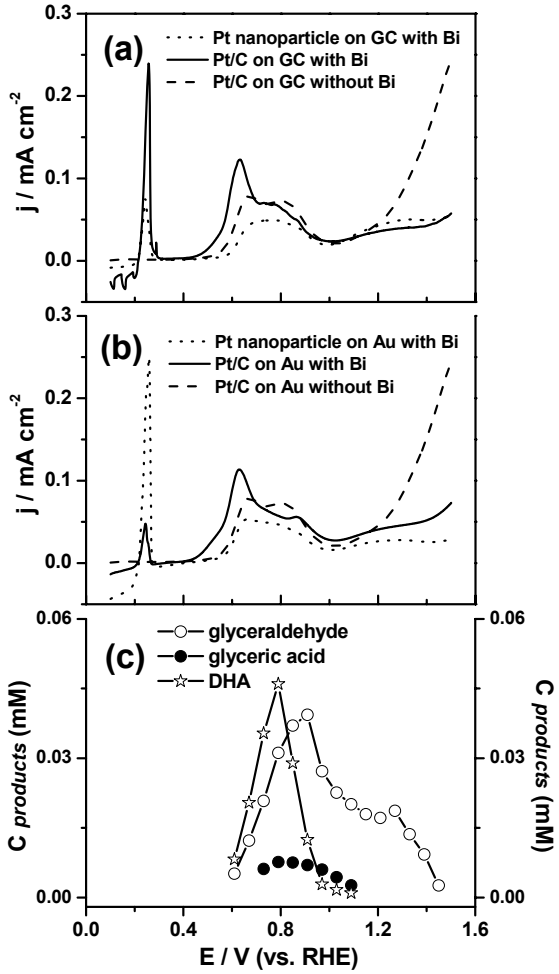

Figure 2. Pt nanoparticles with the effect of carbon support in glycerol oxidation (0.1 M) in Bi-saturated 0.5 M H_2SO_4 on of (a) glassy carbon (GC), (b) gold substrates, and (c) shows the reaction products of Pt nanoparticles in Bi-saturated solution on GC substrate: current density profiles of Pt nanoparticle (– –), Pt/C electrode (—) in Bi-saturated solution, and Pt/C blank (···) without Bi. Thin-film electrodes with Pt nanoparticles (Alfa Aesar) and Pt/C nanoparticles (50wt%, Tanaka) were fabricated by loading defined amounts of nanoparticle suspension in water onto polished glassy carbon and gold substrates, subsequently dried at room temperature. Scan rate is 1 mV/s. ★ dihydroxyacetone (DHA), ○ glyceraldehyde, ● glyceric acid.

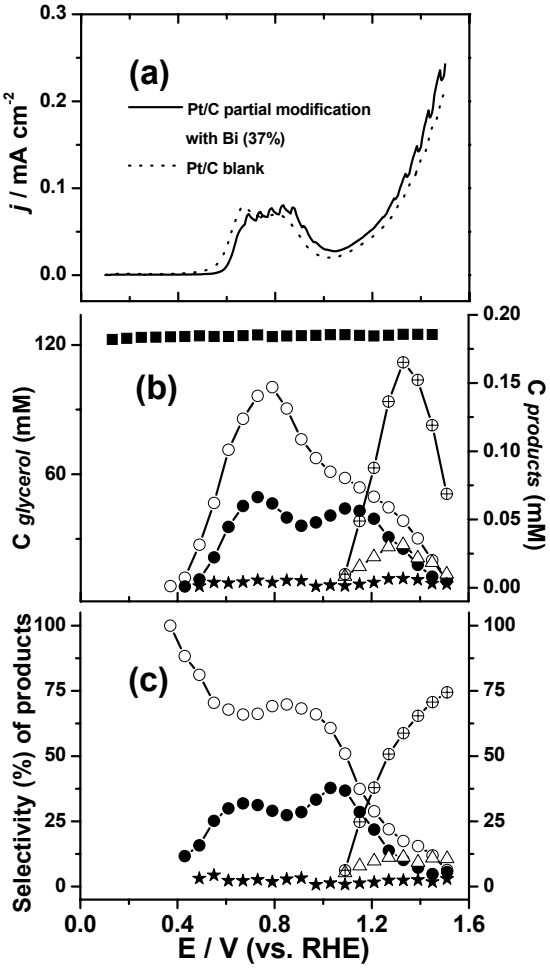

Figure 3. Glycerol oxidation (0.1 M) on a partially Bi modified Pt/C electrode (37% coverage) in 0.5 M H_2SO_4: (a) current density profile with (——) and without (····) Bi modification with scan rate of 1 mV/s, (b) concentration changes of glycerol and its reaction products, and (c) selectivity (%) of products as a function of potential. ■ glycerol, ○ glyceraldehyde, ★ dihydroxyacetone (DHA), ● glyceric acid, △ glycolic acid, ⊕ formic acid.

The continuous oxidation of glycerol at constant potentials was also studied and the corresponding current transients and reaction products are shown in Figure 4. Referring to the peak current density in Figure 1 A(a) and C(a), the potential of 0.65 V was selected to

study product generation for a Pt/C electrode in Bi-free solution (Figure 4b) and a Pt/C electrode in Bi-saturated solution (Figure 4a). A potential of 0.5 V (Figure 4c) was chosen for the Pt/C electrode in Bi-saturated solution for highly selective DHA formation. A comparison of currents and the product formation between (a) and (b) confirms that Bi in the solution enhances the catalytic activity at 0.65 V and predominantly produces DHA (over than 90% selectivity) but still shows some current decay presumably because of the formation of a catalyst poisoning species such as CO at this potential.[14] However, a constant, albeit lower, current was obtained at 0.5 V with an essentially 100% selectivity of DHA (see Figure 4c). This shows that by precise control of the potential, glycerol can be converted to DHA with very high selectivity.

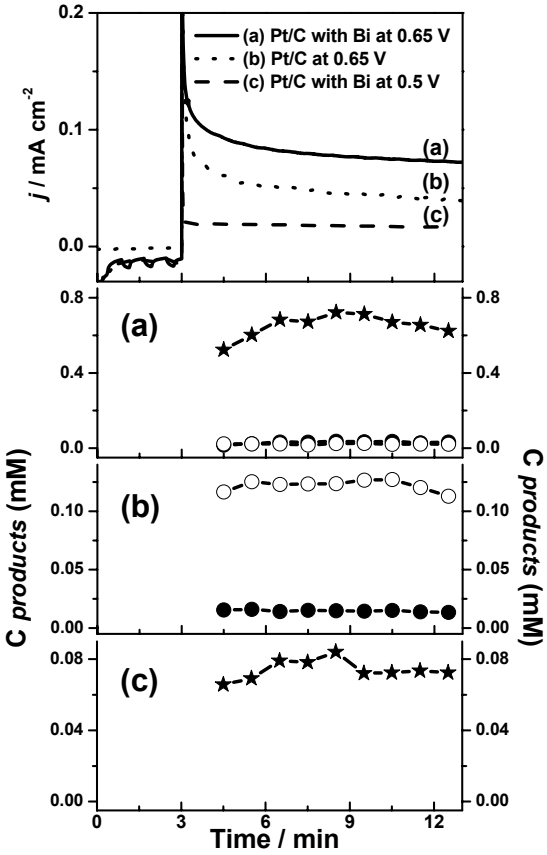

Figure 4. Potentiostatic glycerol oxidation (0.1 M) in 0.5 M H_2SO_4 for (a) Pt/C electrode in Bi-sat. solution at 0.65 V, (b) Pt/C electrode blank at 0.65 V, and (c) Pt/C electrode in Bi-sat. solution at 0.5 V. ★ dihydroxyacetone (DHA), ○ glyceraldehyde, ● glyceric acid.

The results shown in Figure 1 and 4 show that there is a steering role for bismuth in the selectivity of glycerol oxidation. As already referred to, the presence of bismuth on the Pt surface is supposed to block the active sites for primary oxidation.[6,7] To proof such a blocking effect under electrochemical conditions, we have performed in situ Fourier-Transform Infrared (FTIR) spectroscopy. Figure 5 shows the reflection-adsorption spectra obtained at various potentials during glycerol oxidation on a clean Pt electrode and a Pt electrode modified with Bi.[13] We emphasize that these experiments were carried out in the thin-layer configuration in which the electrode is pushed against the CaF_2 window, meaning that the method is less suitable for the quantitative detection of solution species, as these species get trapped in the thin layer. The main interest in Figure 5 lies therefore in assessing any possible differences in the adsorbed species accumulating on the Pt surface during glycerol oxidation in the absence (Figure 5A) and presence (Figure 5B) of Bi on the surface. In the absence of Bi on the Pt electrode, the most conspicuous spectral features are the appearance of (bimodal) bands at ca. 2045 cm^{-1} and 1826 cm^{-1} with increasingly positive potential, ascribable to the build-up of linearly and bridge-bonded adsorbed carbon monoxide resp., and the appearance of carbon dioxide at 2340 cm^{-1} in the thin layer electrolyte. The weak band at 1731 cm^{-1} may be ascribed to the C=O stretching vibration of an aldehyde or ketone species in solution.[19] The results displayed in Figure 5A are in good agreement with earlier FTIR results obtained by Martins et al.,[20] in particular in evidencing the formation of a poisoning surface-adsorbed CO species (though others did not observe adsorbed CO in a similar experiment[19]). In the presence of Bi on the Pt surface (Figure 5B), the IR spectra obtained with increasingly positive potential show that the formation of surface-adsorbed CO is completely suppressed. Carbon dioxide is still observed, but only at higher potentials. The 1734 cm^{-1} feature corresponding to an aldehyde or ketone species in solution is now more pronounced than in the absence of Bi on Pt.

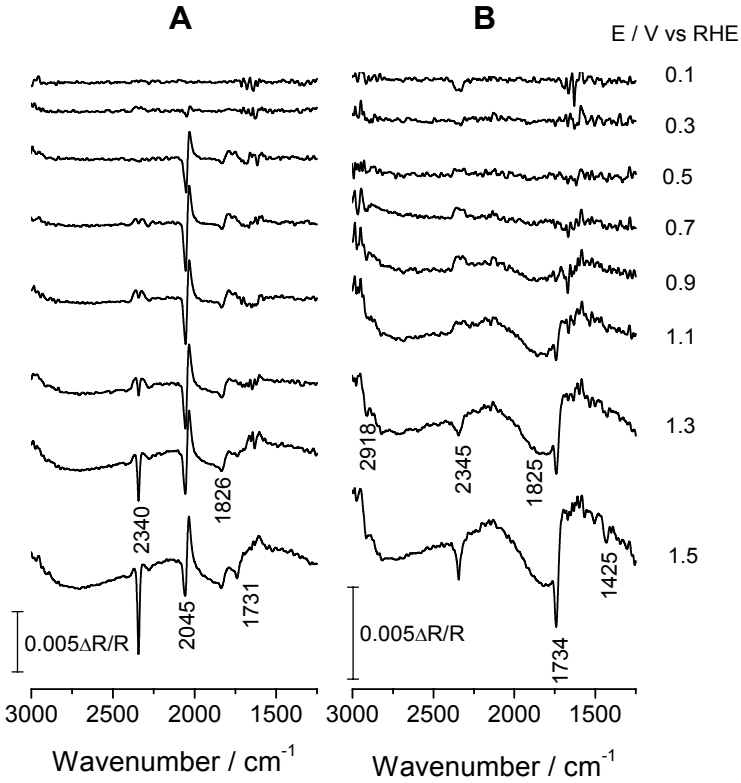

Figure 5. Potential dependent FTIR spectra for (A) clean Pt electrode and (B) Bi modified Pt electrode in 0.01 M $HClO_4$ + 0.1 M glycerol recorded with p-polarized light. E_{ref}= 0.1 V vs. RHE.

The role of Bi in favoring secondary alcohol oxidation can be rationalized by combining the general reaction mechanism for glycerol oxidation on Pt as suggested previously (see Figure 6)[14] with the known effects of Bi adatoms on the oxidation of alcohols and formic acid.[21-23] As Figure 6 illustrates, primary alcohol oxidation leads to the formation of glyceraldehyde and glyceric acid, the latter species being subsequently oxidized to glycolic acid and formic acid. Formic acid has been shown to be the species leading to the formation of CO_2.[14] However, formic acid may also easily dehydrate on Pt to give rise to adsorbed carbon monoxide, and this is the most plausible pathway for the formation of carbon monoxide during glycerol oxidation. In the presence of Bi on the surface, glyceraldehyde and glyceric acid formation is much reduced, and adsorbed carbon monoxide is not observed, which indicates that the pathway for primary alcohol oxidation is blocked at

several stages. However, there is a clearly enhanced formation of DHA, not only relatively, but also in an absolute sense. Various authors have discussed the role of promoters, such as Bi, in the (selective) catalytic oxidation on metal catalysts.[22,23] It is well known that Bi blocks the formation of poisonous CO from small organic molecules, such as formic acid, through a third-body effect.[21,22,24] However, to explain the significantly enhanced activity for secondary alcohol oxidation, one needs to invoke a specific interaction of the glycerol with the adsorbed Bi. Such a specific coordination of glycerol and other poly-ols to Bi[25,26] or PtBi has been suggested by various authors to explain the selective liquid phase oxidation of alcohols promoted by Bi.[27-30] Note that glycerol has been found to coordinate to a zinc cation in a bidentate fashion via its two primary hydroxyl groups.[31] The formation of complexes has also been used to explain the leaching of Bi from the Pt surface.[9] We have studied a possible complexation of Bi by glycerol in the liquid phase by transmission FTIR and NMR, but were unable to obtain direct evidence for the formation of Bi-glycerol complexes in solution under the conditions of our experiment. Further evidence in favour of a surface complexation is provided by the oxidation of 1,3 propanediol in Figure 6. A Pt/C electrode in Bi-saturated solution shows an almost 3 times higher current density compared to Pt/C, but the onset potential of 1,3 propanediol oxidation is identical with that on Bi-free Pt/C, suggesting that the interaction of Bi with the primary alcoholic groups might play an important role in selectively enhancing the activity for secondary alcohol oxidation.

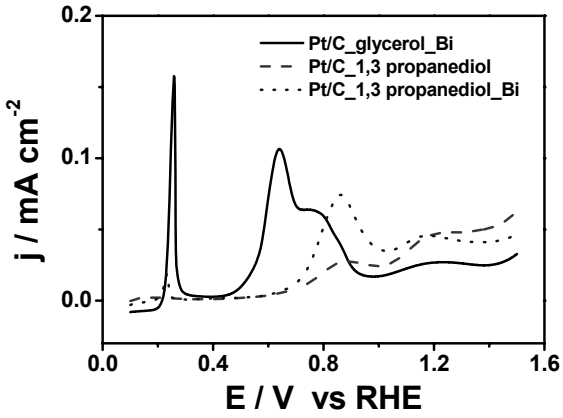

Figure 6. Voltammograms of 1,3 propanediol oxidation (0.1 M) on Pt/C electrode in 0.5 M H2SO4 in comparison with glycerol oxidation at scan rate of 1 mV/s.

4.4 Conclusion

On the basis of the results presented in this chapter, we propose the tentative reaction mechanism for the selective glycerol oxidation to dihydroxyacetone promoted by bismuth shown in Figure 7. Bismuth on the Pt surface blocks the active surface for the primary alcohol oxidation as well as for the formation of adsorbed CO from formic acid. The Pt/C-Bi ensemble on the surface coordinates the glycerol in such a way that oxidation of the secondary alcohol is favored. For optimal activity and selectivity, it is necessary to have a constant and full coverage of Bi on the Pt/C surface, this being a possible explanation why having Bi in solution is important. At higher potentials, Bi desorbs from the surface, and primary oxidation predominates.

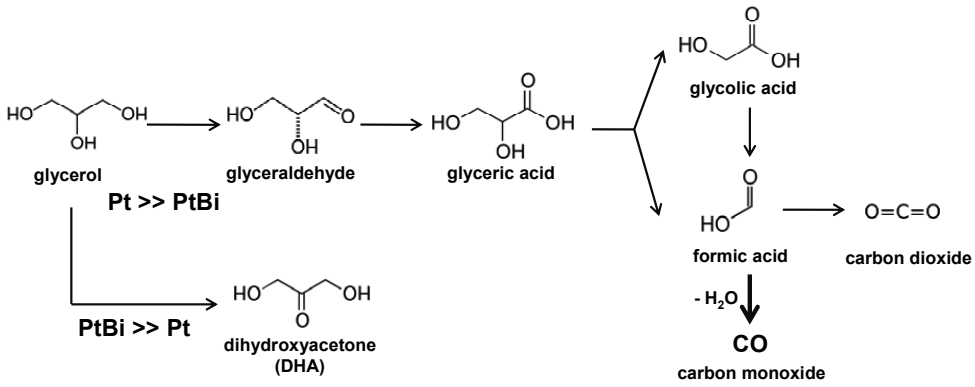

Figure 7. Schematic diagram of the selective oxidation of glycerol.

In conclusion, we have shown that in presence of bismuth in an acidic solution, glycerol may be oxidized to dihydroxyacetone on a Pt/C electrode with very high selectivity. Bismuth blocks the active sites for primary alcohol oxidation on Pt/C electrode, lowers the onset potential, and enhances the turnover frequency by forming a Bi-related active site on the surface poised for secondary oxidation. The mechanistic details and the structure sensitivity of this highly selective catalytic interface remain to be understood in detail. Under the model conditions employed in this experiment, the yield of DHA is still rather low but not unfavourable compared to the only other electrochemical example of selective glycerol oxidation: Ciriminna et al.[12] obtained a maximum current density of ca. 0.24 mA cm^{-2} for a solution of 0.05 M glycerol with 25-30 % selectivity to DHA (but no Faradaic

efficiency was reported) at ca. 1.3 V (vs. NHE), versus our experiment which gives ca. 0.05-0.1 mA cm^{-2} for a solution of 0.1 M glycerol, but with a close to 100% DHA and Faraday efficiency, and a much lower potential (0.5-0.6 V vs. NHE). It remains to be seen whether this same selectivity can be reached at high glycerol concentrations in a batch or continuous reactor process. However, the main purpose of this chapter was to show that bismuth in combination with electrochemical potential control may be used as a highly potent and remarkable steering method for selective oxidation.

4.5 References

[1] Pagliaro, M.; Ciriminna, R.; Kimura, H.; Rossi, M.; Della Pina, C. *Angew. Chem. Int. Ed.* **2007**, *46*, 4434-4440.

[2] Zhou, C. H.; Beltramini, J. N.; Fan, Y-X.; Lu, G. Q. *Chem. Soc. Rev.* **2008**, *37*, 527-549.

[3] Svitel, J.; Sturdik, E. *J. Ferment. Bioeng.* **1994**, *78*, 351-355.

[4] Demirel, S.; Lehnert, K.; Lucas, M.; Claus, P. *Appl. Catal. B* **2007**, *70*, 637-643.

[5] Carretin, S.; McMorn, P.; Johnston, P.; Griffin, K.; Kiely, C. J.; Hutchings, G. J. *Phys. Chem. Chem. Phys*. **2003**, *5*, 1329-1336.

[6] Kimura, H.; Tsuto, K.; Wasisaka, T.; Kazumi, Y.; Inaya, Y. *Appl. Catal. A* **1993**, *96*, 217-228.

[7] Kimura, H. *Appl. Catal. A* **1993**, *105*, 147-158.

[8] Hu, W.; Knight, D.; Lowry, B.; Varma, A. *Ind. Eng. Chem. Res.* **2010**, *49*, 10876-10882.

[9] Wörz, N.; Brandner, A.; Claus, P. *J. Phys. Chem. C* **2010**, *114*, 1164-1172.

[10] Painter, R. M.; Pearson, D. M.; Waymouth, R. M. *Angew. Chem. Int. Ed.* **2010**, *49*, 9456-9459.

[11] Greeley, J.; Jaramillo, T.; Bonde, J.; Chorkendorff, I.; Nørskov, J. K. *Nature Mat*. **2006**, *5*, 909-913.

[12] Ciriminna, R.; Palmisano, G.; Della Pina, C.; Rossi, M.; Pagliaro, M. *Tetrahedr. Lett.* **2006**, *47*, 6993-6995.

[13] Rodriguez, P.; Solla-Gullon, J.; Vidal-Iglesias, F. J.; Herrero, E.; Aldaz, A.; Feliu, J. M. *Anal.Chem*. **2005**, *77*, 5317-5323.

[14] Kwon, Y.; Schouten, K. J. P.; Koper, M. T. M. *ChemCatChem* **2011**, *3*, 1176-1185.

[15] Kwon, Y.; Koper, M. T. M. *Anal.Chem.* **2010**, *82*, 5420-5424.
[16] Cadle, S. H.; Bruckenstein, S. *Anal.Chem.* **1972**, *44*, 1993-2001.
[17] Uhm, S.; Yun, Y.; Tak, Y.; Lee, J. *Electrochem. Commun.* **2005**, *7*, 1375-1379.
[18] Koper, M. T. M.; Lai, S. C. S.; Herrero, E. In *Fuel Cell Catalysis: a Surface Science Approach*; Koper, M. T. M. Ed.; Wiley-VCH: Hoboken NJ, USA, 2009; p.159-207.
[19] Fernandes Gomes, J.; Tremiliosi-Filho, G. *Electrocatal.* **2011**, *2*, 96-105.
[20] Martins, C. A.; Giz, M. J.; Camara, G. A. *Electrochim. Acta* **2011**, *56*, 4549-4553.
[21] Besson, M.; Gallezot, P. *Catal. Today* **2000**, *57*, 127-141.
[22] Climent, V.; Garcia-Araez, N.; Feliu, J. M. In *Fuel Cell Catalysis: a Surface Science Approach*; Koper, M. T. M. ED.;Wiley-VCH: Hoboken NJ, USA, 2009; p.209-244.
[23] Lopez-Cudero, A.; Vidal-Iglesias, F. J.; Solla-Gullon, J.; Herrero, E.; Aldaz, A.; Feliu, J. M. *Phys. Chem. Chem. Phys*. **2009**, *11*, 416-424.
[24] Smith, S.P.E.; Ben-Dor, K.F.; Abruña, H.D., *Langmuir* **2000**, *16*, 787-794.
[25] Angyal, S. J. *Chem. Soc. Rev.* **1980**, *9*, 415-428.
[26] Whitfield, D. M.; Stojkovski, S.; Sarkar, B. *Coord. Chem. Rev.* **1993**, *122*, 171-225.
[27] Smits, P. C. C.; Kuster, B. F. M.; Wiele, K. van der; Baan, H. S. van der *Appl. Catal.* **1987**, *33*, 83-96.
[28] Abbadi, A.; Bekkum, H. van *Appl. Catal. A Gen.* **1995**, *124*, 409-417.
[29] Heinen, A. W.; Peters, J. A.; Bekkum, H. van *Carbohydr. Res.* **1997**, *304*, 155-164.
[30] Wenkin, M.; Ruiz, P.; Delmon, B.; Devillers, M. *J. Mol. Catal. A: Chem*. **2002**, *180*, 141-159.
[31] Ding, Y. S.; Register, R. A.; Nagarajan, M. R.; Pan, H. K.; Cooper, S. L. *J. Polym. Sci., Part B: Polym. Phys.* **1988**, *26*, 289-300.

5

Electrocatalytic oxidation of alcohols on gold in alkaline media: base or gold catalysis?

Abstract

Based on a comparison of the oxidation activity of a series of similar alcohols with varying pK_a on gold electrodes in alkaline solution, we find that the first deprotonation is base catalyzed, and the second deprotonation is fast but gold catalyzed. The base catalysis follows a Hammett-type correlation with pK_a, and dominates overall reactivity for a series of similar alcohols. The high oxidation activity on gold compared to platinum for some of the alcohols is related to the high resistance of gold toward the formation of poisoning surface oxides. These results indicate that base catalysis is the main driver behind the high oxidation activity of many organic fuels on fuel cell anodes in alkaline media, and not the catalyst interaction with hydroxide.

The contents of this chapter have been published: Y. Kwon, S. C. S. Lai, P. Rodriguez, M. T. M. Koper, *J. Am. Chem. Soc.*, **2011**, *133*, 6914–69172.

5.1 Introduction

In recent years, there has been tremendous interest in using gold as a catalyst for various heterogeneously catalyzed oxidation reactions.[1] In gas phase catalysis, gold becomes active towards oxidation reactions, primarily carbon monoxide oxidation,[2] when dispersed as small nanoparticles on an oxidic support.[2-5] Simultaneously, in the area of electrocatalysis, alkaline electrolyte media are receiving increasing attention as a medium offering higher stability to materials and often also higher catalytic activity.[6] Interestingly, there is growing awareness that the alkaline environment is in fact key to making gold, as well as other electrocatalysts such as platinum and palladium, such active oxidation catalysts, without the need for small particles or an oxidic support.[7-13] This has long been known in electrocatalysis,[12] but there is still a lack of detailed understanding as to why the combination of base and gold makes such an active and selective oxidation catalyst.

In alkaline media, many of the organic molecules whose oxidation properties have been studied in the (electro)catalysis literature, such as ethanol and glycerol, take part in an acid-base equilibrium involving the alcoholic group. In relation to the ethanol oxidation on a gold electrode,[13] we have shown that the activity varies in a highly nonlinear fashion with pH, as illustrated in Figure 1. Similar results have been obtained with methanol and glycerol oxidation on gold.[14,15] It is well known that the main products of ethanol oxidation on gold are acetaldehyde and acetic acid,[16] i.e. no catalytic bond breaking takes place. Based on these results, we argued that at a pH higher than ca. 11, the ethoxy anion is the reactive species, its concentration steeply increasing with higher pH. This species is then more easily oxidized to acetaldehyde. As a result, at pH=13, the activity for ethanol oxidation is orders of magnitude higher than in acidic media.
Therefore at high pH the alcohol deprotonates:

$$H_\beta R\text{-}OH_\alpha \leftrightarrows H_\beta R\text{-}O^- + H_\alpha^+ \qquad (1)$$

with the pK_a of this reaction depending on the nature of R, and with HRO^- being significantly more reactive than HROH. This idea is not new (see e.g. refs.8,17,18), but we are not aware of any explicit proof as would be afforded by establishing a Hammett-type relationship[19] between the reactivity of the alcohol and its pK_a, i.e. a lower pK_a leading to a higher reactivity.

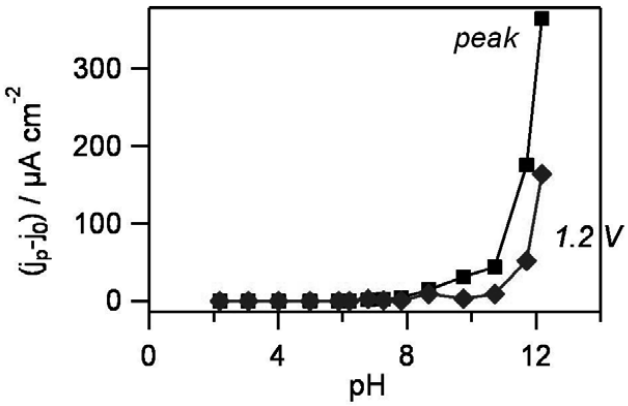

Figure 1. Measured current j_p for 0.5 M ethanol oxidation on a gold electrode at peak potential (solid square) or at 1.2 V vs. RHE (solid diamond) minus the background current j_0 as a function of the electrolyte pH using 0.1 M phosphate buffers. For details, see ref.13.

5.2 Experimental

All measurements were carried out in a conventional single compartment three-electrode glass cell, which was cleaned by employing a standard procedure for removing traces of organic and inorganic contaminants. Oxygen was removed by bubbling argon through the solution prior to the voltammetric experiments. Au electrode in the experiment was mechanically polished with alumina (up to 0.05 μm) and cleaned ultrasonically in pure water (MilliQ gradient A10 system, 18.2 MΩ) followed by electropolishing by cycling 200 times between 0.1 and 1.7 V (vs. RHE) with a scan rate of 1 V s^{-1} in 0.5 M H_2SO_4 solution in order to remove surface impurities and oxide before use. The charge transferred during the reduction of Au monolayer oxide was converted to calculate the electrochemically active surface area (cm^2). A large gold coil was used as a counter electrode while a reversible hydrogen electrode (RHE) was employed as a reference electrode. Electrochemical cell potentials were controlled with a potentiostat/galvanostat (μ-Autolab Type III). All experiments were carried out at room temperature.

5.3 Results and discussion

Figures 2a and b collect the positive-going voltammetric potential sweeps for a number of alkyl-alcohols (at 10 mM concentration) on a gold electrode in 0.1 M NaOH, and Figure 2c plots the onset potential, defined as the potential at which the oxidation current is twice that of the blank background, versus the pK_a of the corresponding alcohol.[20] Alternatively, differences in activity on the potential scale can be appreciated in the Tafel plots of Figure 2d, focusing on the low onset currents. Even though definitions of overall activity are imperfect and ambiguous, Figure 2 by and large confirms the above expectation: alcohols with a low pK_a, such as the sugar alcohols or glycerol, have a high oxidation activity on Au, whereas alcohols with a high pK_a (such as iso-propanol and tert-butanol), are significantly less active at pH=11. To activate such an alcoholic group, a "real" catalyst, such as platinum, is much better suited. Methanol seems to deviate somewhat from the main trend, a possible reason for which will be discussed below.

We note that we have confirmed by online HPLC[21] or literature data that the main oxidation products of the alcohols in Figures 2a and b are their corresponding aldehydes. However, aldehydes are unstable in alkaline media[20] and, especially in the presence of oxygen, decompose into a variety of products even without a catalyst.

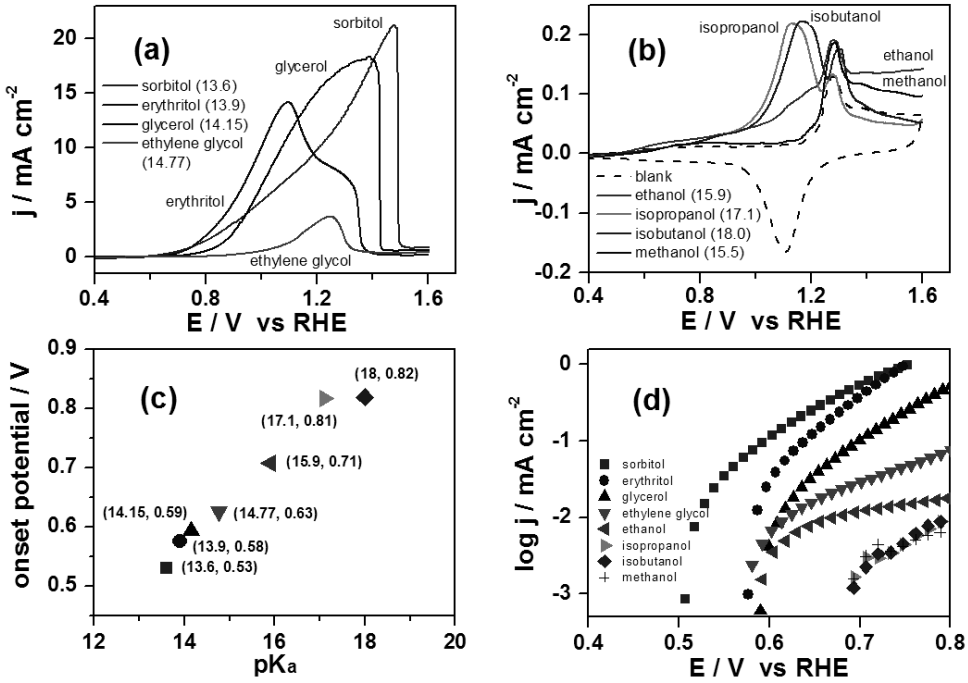

Figure 2. Linear sweep voltammograms of (a) alcohols with high **j**, (b) alcohols with low **j** on Au electrode in 0.1 M NaOH with a scan rate of 50 mV s^{-1}, (c) plots of the onset potential versus the pK_a, and (d) Tafel plots of the corresponding alcohols.

Figure 3 illustrates the temporal evolution of the products of the decomposition of glyceraldehyde and glycolaldehyde, the primary oxidation products of glycerol and ethylene glycol, resp., in a non-deaerated 0.1 M NaOH solution *in the absence of gold*. Note that this Figure includes products that have been observed as the gold-catalyzed oxidation products of the corresponding alcohols.[8] Figure 3 justifies the conclusion that the role of gold in the oxidation of the aldehydes must be very limited (similar plots for glycerol oxidation on gold are available in ref.14). For the oxidation of the alcohols, the catalytic role of gold is weak but not absent: in the presence of strongly adsorbing anions, it is well known that under electrochemical conditions gold is much less active,[13,15] suggesting that some interaction with the gold surface is still necessary.

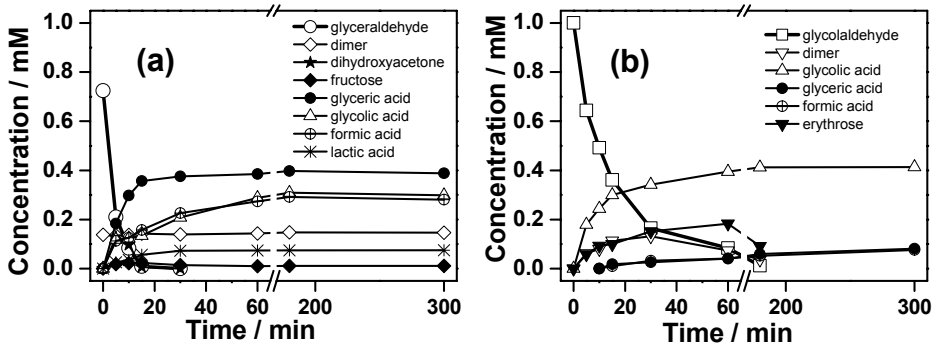

Figure 3. Decomposition of (a) glyceraldehyde and (b) glycolaldehyde, the primary oxidation products of glycerol and ethylene glycol, resp., in a non-deaerated O_2-containing 0.1 M NaOH solution in the absence of gold, as determined by HPLC.

Figure 2 collects our results obtained with alkyl-alcohols. We have also considered and studied the oxidation of alcohols whose pK_a is lowered by functionalization with fluoride, amines or unsaturated carbon-carbon bonds. Such alcohols typically do not follow the trend illustrated in Figure 2. Fluoroethanols show hardly any oxidation activity on gold in alkaline media as shown in Figure 4, even though fluoroalcohols are textbook examples[20] of alcohols with a low(er) pK_a.

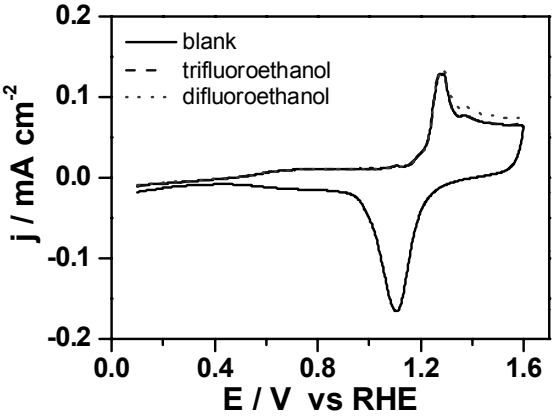

Figure 4. Linear sweep voltammograms of fluoroethanols (10 mM) on Au electrode in 0.1 M NaOH with a scan rate of 50 mV s^{-1}.

Gellman et al.[22] have also observed that the tendency of fluoroethanol to form an adsorbed alkoxide on copper surfaces is increased compared to ethanol, but conversely, the abstraction of the beta hydrogen to form the corresponding aldehyde through

$$H_\beta R\text{-}O_{ads} \rightarrow R{=}O_{ads} + H_{\beta,ads} \qquad (2)$$

was slowed down significantly (the labelling of α and β hydrogen was borrowed from ref.22,23). Cong and Masel[23] have confirmed this observation for platinum surfaces, but also observed enhanced beta-hydrogen elimination on oxidized platinum. Under electrochemical conditions, (gold)oxides appear to show only a small though noticeable activity, in particular for methanol and ethanol. A reaction similar to reaction 2 may explain the electrocatalytic oxidation activity of unsaturated alcohols, i.e. allylalcohol (2-propenol) and propargyl alcohol (2-propyn-1-ol), on gold in alkaline media as observed by Holze et al.[24] Compared to propanol, 1-propenol is more reactive, but 1-propynol is less reactive.[24] This trend would agree with the higher reactivity of an allylic H_β compared to an propargylic H_β.[25] We note, however, that these compounds also show oxidation activity on gold in acidic media, so the real story may well be more complicated.[26] Finally, in agreement with a previous report by Luczak,[27] we found that amino-alcohols have a very high oxidation activity in alkaline media, with an oxidation potential as low as 0.4 V in Figure 5.

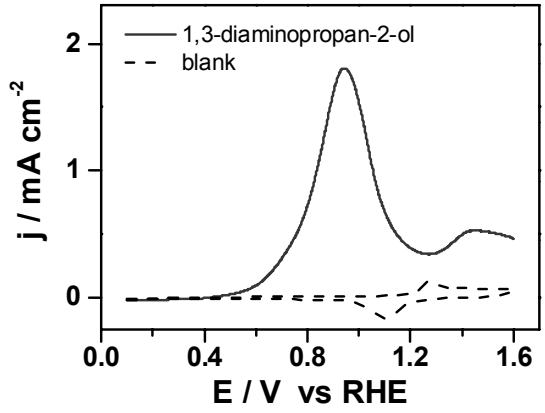

Figure 5. Linear sweep voltammograms of 1,3-diaminopropan-2-ol (10mM) on Au electrode in 0.1 M NaOH with a scan rate of 50 mV s^{-1}.

However, in situ FTIR spectroscopy suggests that both the alcohol and the amino groups are involved in the first stages of the oxidation, and therefore it is unlikely that amino-alcohols are oxidized easily only because of their increased alcoholic acidity.

From the results illustrated in Figs.1-5, the following picture emerges for the catalytic oxidation of alcohols in alkaline media. At sufficiently high pH, where "sufficiently" depends on the pK_a of the alcohol, the alcohol deprotonates into its corresponding alkoxide through reaction 1. The alkoxide is thought to be more active towards oxidation and therefore acts as a precursor to aldehyde formation:

$$H_\beta R\text{-}O^- \rightarrow R{=}O + H_\beta^+ + 2\ e^- \qquad (3)$$

We believe that some of the deviations from the simple Hammett relationship may be traced back to the different leaving ability of the H_β. For instance, methanol, having a pK_a of 15.5, would be expected to be more reactive than ethanol (pK_a = 15.9), but the C-H_β bond in methanol is stronger than the C-H_β bond in ethanol[28] (we have not been able to find similar data for the corresponding alkoxides). In reaction 3, there may therefore be an important role of the catalyst, though Figure 2 strongly suggests that base catalysis dominates the overall reactivity. As mentioned, Cong and Masel[23] found that beta-elimination is enhanced on platinum oxide vs. platinum, and recent DFT calculations suggest that adsorbed OH on gold lowers the barrier for beta-elimination significantly,[9] suggesting that some interaction of the alkoxide with the (hydroxylated) gold surface is mandatory. This is also evidenced by the inhibiting role of strongly adsorbing anions in the electrochemical oxidation reaction, and by the fact that carbon is not a good electrode material for alcohol oxidation in alkaline media. However, if the alcohol is to be oxidized catalytically, a "real" catalyst, such as Pt or Pd, is needed. Aldehydes are not stable in alkaline media, and will react quickly in the presence of oxygen or other electron acceptors, such as positively polarized gold. These reactions determine the final products of the oxidation reaction on gold. Still, the activity of gold in alkaline media can be very high, even higher than that of platinum. The main reason for this is that gold is much less prone to the formation of poisoning oxides. Under electrochemical conditions, gold oxidizes at 0.4-0.5 V more positive potentials than platinum. For an electron transfer reaction with a Butler-Volmer transfer coefficient of 0.5, this translates into a rate enhancement of three to four orders of magnitude! This effect has been observed for the oxidation of glycerol,

which shows much higher current densities (turnover numbers) on gold than on platinum in alkaline media,[14,15,21] but only at high overpotentials for which Pt is oxidized and hence not active.

5.4 Conclusion

In conclusion, the oxidation of the alcohol to an aldehyde involves the transfer of two protons and two electrons. The first "alpha" proton transfer is base catalyzed, with no essential role of the (gold) catalyst. The second combined "beta" proton – electron transfer (reaction 3) is fast, provided the leaving ability of the "beta" hydrogen is good, and gold primarily acts as an electron acceptor, although this step likely involves a catalytic interaction with surface bonded hydroxide. If the H_β is bound strongly, deviations to the "pK_a rule" are expected, to the extent that oxidation activity can even be completely absent (such as for fluoroethanol). This picture of alcohol oxidation is similar to that recently suggested by Davis et al.[9], who suggest that both solution-mediated and metal-catalyzed steps are involved. This chapter makes an important and crucial addition by the establishment of a Hammett relationship as illustrated in Figure 2c, which shows that the OH^- in solution could be more important for the overall reactivity than OH bound to the gold catalyst. We emphasize that OH can be formed on gold in acidic media at a sufficiently positive potential (for instance CO may be oxidized on gold in perchloric acid at potentials as low as 0.6 V_{RHE}[10,29]), but it does not lead to any appreciable alcohol oxidation activity such as that observed in alkaline media. The further reaction of the aldehyde into other products is also strongly if not entirely base catalyzed. Certain implications of this model can be transferred to the platinum- or palladium-catalyzed alcohol oxidation in alkaline media, even if such reactions involve additional catalyzed steps, especially related to C-C bond breaking. One often reads that alkaline media are highly active for the oxidation of alcohols on Pt and Pd because of the high coverage of hydroxide on the electrocatalyst surface. However, OH is adsorbed on a Pt electrode in acidic and alkaline in the same potential region (vs.RHE), and still alkaline media are significantly more reactive towards ethanol oxidation than acidic media.[30,31] Therefore, we believe that it is really the solution hydroxide that promotes the initial deprotonation, and thereby the important first step of the overall oxidation reaction, and that the explicit formulation of this idea is important for the future development of alkaline electrocatalysts.

To summarize our main points once more:

• The first deprotonation step in the electrocatalytic oxidation of an alcohol is base catalyzed, resulting in the reactive alkoxide intermediate.
• The second deprotonation (to the aldehyde) depends on the ability of the electrode material to abstract the H_β. If this is fast, the "pK_a rule" applies.
• On gold, the overall reaction rate is determined by the more sluggish of the two. On the other metals, further oxidation pathways will be important. However, in alkaline media, aldehydes are not stable and their degradation products should not be misinterpreted as resulting from the catalytic activity of gold.

5.5 References

[1] G. C. Bond, C. Louis, D. T. Thompson, *Catalysis by Gold*, Imperial College Press, London, **2006**.

[2] M. Haruta, T. Kobayashi, H. Sano, M. Yamada, *Chem. Lett*. **1987**, *16*, 405; M. Haruta, *Nature* **2005**, *437*, 1098.

[3] R. Grisel, K. J. Weststrate, A. Gluhoi, B. E. Nieuwenhuys, *Gold Bull*. **2002**, *35*, 39.

[4] A. S. K. Hashmi, G. J. Hutchings, *Angew. Chem. Int. Ed.* **2006**, *45*, 7896.

[5] M. Valden, X. Lai, D. W. Goodman, *Science* **1998**, *281*, 1647.

[6] J. R. Varcoe, R. C. T. Slade, *Fuel Cells* **2005**, *5*, 187.

[7] L. Prati, M. Rossi, *J. Catal*. **1998**, *176*, 552.

[8] W. Ketchie, Y. -L. Fang, M. Wong, M. Murayama, R. J. Davis, *J. Catal*. **2007**, *250*, 94.

[9] B. N. Zope, D. D. Hibbits, M. Neurock, R. J. Davis, *Science* **2010**, *330*, 74.

[10] J. L. Roberts, Jr., D. T. Sawyer, *Electrochim. Acta* **1965**, *10*, 989; H. Kita, H. Nakajima, K. Hayashi, *J. Electroanal. Chem*. **1985**, *190*, 141.

[11] P. Rodriguez, A. A. Koverga, M. T. M. Koper, *Angew. Chem. Int. Ed.* **2010**, *49*, 1241.

[12] M. Betowska-Brzezinska, T. Uczak, R. Holze, *J. Appl. Electrochem.* **1997**, *27*, 999.

[13] S. C. S. Lai, S. E. F. Kleijn, F. T. Z. Öztürk, V. C. van Rees Vellinga, J. Koning, P. Rodriguez, M. T. M. Koper, *Catal. Today* **2010**, *154*, 92.

[14] Y. Kwon, K. J. P. Schouten, M. T. M. Koper, *ChemCatChem* **2011**, *3*, 1176.

[15] B. Beden, I. Cetin, A. Kahyaoglu, D. Takky, C. Lamy, *J. Catal.* **1987**, *104*, 37.

[16] G. Tremiliosi-Filho, E. R. Gonzalez, A. J. Motheo, E. M. Belgsir, J. M. Leger, C. Lamy, *J. Electroanal.Chem.* **1998**, *444*, 31.

[17] J. Szammer, M. Jáky, O. Gerasimov, *Int. J. Chem. Kin.* **1992**, *24*, 145.

[18] V. R. Gangwal, J. van der Schaaf, B. F. M. Kuster, J. Schouten, *J. Catal*. **2005**, *229*, 389.

[19] L. P. Hammett, *Chem. Rev*. **1935**, *17*, 125.

[20] J. E. McMurry, *Organic Chemistry*, Brooks/Cole, 6th ed., **2003**.

[21] Y. Kwon, M. T. M. Koper, *Anal. Chem.* **2010**, *82*, 5420.

[22] A. J. Gellman, Q. Dai, *J. Am. Chem. Soc.* **1993**, *115*, 714.

[23] Y. Cong, R. I. Masel, *Surf. Sci.* **1998**, *396*, 1.

[24] R. Holze, T. Luczak, M. Beltowska-Brzezinska, *Electrochim. Acta* **1994**, *39*, 991.

[25] M. M. Martin, E. B. Sanders, *J. Am. Chem. Soc.* **1967**, *89*, 3777.

[26] E. Pastor, V. M. Schmidt, T. Iwasita, M. C. Arevalo. S. Gonzalez, A. J. Arvia, *Electrochim. Acta* **1993**, *38*, 1337.

[27] T. Luczak, *J. Appl. Electrochem.* **2007**, *37*, 653.

[28] L. A. Gribov, I. A. Novakov, A. I. Pavlyuchko, O. Yu. Shumovskii, *J. Struct. Chem.* **2007**, *48*, 607.

[29] P. Rodriguez, N. Garcia-Araez, M. T. M. Koper, *Phys. Chem. Chem. Phys*. **2010**, *12*, 9373.

[30] S. C. S. Lai, M. T. M. Koper, *Faraday Disc*. **2008**, *140*, 399.

[31] S. C. S. Lai, M. T. M. Koper, *Phys. Chem. Chem. Phys*. **2009**, *11*, 10446.

6

Cellobiose hydrolysis and decomposition by electrochemical generation of acid and hydroxyl radicals

Abstract

This chapter addresses the hydrolysis of cellobiose to glucose and its further decomposition with electrochemically generated acid (H^+) on a platinum electrode, and with electrochemically generated hydroxyl radical (OH•) on boron-doped diamond (BDD). Results are compared with the hydrolysis promoted by conventional acid (sulfuric acid) and OH• (from Fenton's reaction) with support of product analysis by online high-performance liquid chromatography (for soluble products) and online electrochemical mass spectrometry (for CO_2). Cellobiose hydrolysis follows a first-order reaction obeying Arrhenius' law over the temperature range from 25°C to 80°C with different activation energies for the acid- and radical-promoted reaction, i.e. ca. 118±8 kJ mol^{-1} and ca. 55±1 kJ mol^{-1}, respectively. The high local acidity with electrochemically generated acid (H^+) on the Pt electrode increases the rate of glucose formation, however the active electrode (PtO_x) interacts with glucose and decomposes it further to smaller organic acids. In addition, the molecular oxygen formed during oxygen evolution reaction (OER) lowers the selectivity for glucose by forming side-products. The hydroxyl radical (OH•) generated on a BDD electrode first hydrolyzes the cellobiose to glucose, but rapidly attacks the aldehyde on glucose, which is further decomposed to smaller aldoses and finally formaldehyde, which is subsequently oxidized electrochemically to formic acid.

The contents of this chapter have been published: Y. Kwon, S. E. F. Kleijn, K. J. P. Schouten, M. T. M. Koper, *ChemSusChem*, **2012**, *5*, 1935-1943.

6.1 Introduction

Cellulose is the most abundant source of biomass, and holds widespread recognized potential as an alternative carbon source to fossil fuels for the sustainable production of fuels and chemicals.[1-3] However, the utilization of cellulose as a major renewable energy source is restricted by its crystalline structure of β-1-4-glycosidic linkages by the tight packing of cellulose chains in microfibrils.[2] Although the hydrolysis of cellulose produces glucose, which is a versatile precursor to fuels, plastics, pharmaceuticals, and other value-added chemicals, the efficient hydrolysis of cellulose to glucose with low environmental impact remains a challenge.[4] An extensive number of works have been devoted to the hydrolysis of cellulose using enzymes, mineral acids, supercritical water, and heterogeneous catalysts.[5-10] However, the application of electrochemical methods for cellulose hydrolysis has been limited mainly by the low solubility of cellulose in aqueous media.[2] Baizer and Nobe[11] introduced many years ago the acid-catalyzed cellulose hydrolysis by electrochemically generated acid (H^+) at the platinum anode in an electrochemical cell. Recently, Li[12] reported the effect of hydroxyl radical (OH•) generated on a Pb/PbO_2 anode for depolymerization of cotton cellulose. In these cases, the electrode provides the active homogeneous catalysts or promoters (i.e. H^+, OH•) for the reaction. However, more detailed studies of reaction kinetics, intermediate species, and the effect of heterogeneous reactions between reactants and electrode have not been reported.

In this chapter, we selected cellobiose, which consists of two glucose molecules linked by a β-1-4-glycosidic bond, as a model of cellulose, and aim at understanding the cellobiose hydrolysis by electrochemically generated acid (H^+) on a Pt electrode, and hydroxyl radical (OH•) on boron-doped diamond (BDD) electrode, in comparison with hydrolysis by conventional acid (sulfuric acid) and OH• radical generated from Fenton's reaction. The details of the reaction pathways are discussed with the support of both quantitative and qualitative product distributions, as determined by using a combination of voltammetry with online high-performance liquid chromatography (HPLC) for soluble reaction products and online electrochemical mass spectroscopy (OLEMS) mainly for CO_2. Finally, the potential of the electrochemistry-assisted hydrolysis and decomposition of cellobiose and cellulose are discussed.

6.2 Experimental

6.2.1 Chemical reactions

10 mM cellobiose in sulfuric acid (0.5, 1, 2, 5, and 10 M) was prepared in 5 mL vials for acid cellobiose hydrolysis and reaction temperature was controlled in an oven (25, 60, and 80^{o}C). Reaction products were collected at different reaction times (0, 0.5, 1, 2, 3, and 22 hr) and cooled down immediately to room temperature to prevent further reaction. For radical cellobiose hydrolysis, 2 mM Fe(II) was introduced into a solution of hydrogen peroxide (5, 10, and 20 mM H_2O_2) and experiments were carried out under the same conditions as for the acid-catalyzed hydrolysis (i.e. temperature and sample collection). Residual hydroxyl radical was quenched by adding a stoichiometric excess of Na_2SO_3 after the sample collection. Selectivity to glucose was calculated by the following equation, involving the measured concentrations of glucose and cellobiose:

$$\frac{\text{glucose (mM)}}{\text{2 x converted cellobiose (mM)}} \text{ x } 100\%$$

6.2.2 Electrochemical reactions

All measurements were carried out in a conventional single compartment three-electrode glass cell, which was cleaned by a standard procedure[13] to remove all traces of organic contaminations. Cellobiose (10 mM) was dissolved into solutions of neutral (0.1 M Na_2SO_4) and acid (0.5 M H_2SO_4). Prior to the experiments oxygen was removed by bubbling argon through the solution for at least 20 minutes. The working electrode for acid cellobiose hydrolysis was a polycrystalline Pt plate. A boron-doped diamond electrode (Windsor Scientific Ltd, 0.2%) was applied for radical cellobiose decomposition. In all experiments, a platinum plate was used as a counter electrode, while a reversible hydrogen electrode (RHE) was employed as a reference electrode. Electrochemical cell potentials were controlled with a potentiostat/galvanostat (μ-Autolab Type III). Reaction temperatures were controlled with a heating bath (Lauda E100, Ecoline). All chemicals used for this work were at least analytical grade.

6.2.3 Fraction Collection and Product Analysis

The reaction products from acid-catalyzed (H_2SO_4) and radical-promoted (Fenton's reaction) cellobiose hydrolysis were collected at different reaction time (i.e. 0, 0.5, 1, 2, 3, and 22 hr) and further reaction was quenched immediately. The reaction products from electrochemical acidic and radical cellobiose hydrolysis were collected with a micro-sized sample collecting tip[14] close to electrode surface. Collected samples during chemical and electrochemical reactions were analyzed in an HPLC system as already described in Chapter 2~3.[14,15] The microtiter plate with the collected samples was placed in an auto-sampler holder and 20 μL of sample was injected into the column. The columns used were a single Aminex HPX 87-H (Bio-Rad) column or a series of two columns of an Aminex and a Sugar SH1011 (Shodex). Diluted sulfuric acid (0.5 and 5 mM) was used as eluent. The selected temperature of column oven was adjusted to 85°C. Details of the system configuration are described in Chapter 2~3.[14,15]

6.2.4 On-line Electrochemical Mass Spectrometry (OLEMS)

OLEMS measurements were performed on an EvoLution mass spectrometer system (European Spectrometry Systems Ltd.).[16] The system consists of a Prisma QMS200 (Pfeiffer), brought to vacuum with a TMH-071P turbo molecular pump (60 l/s, Pfeiffer) and a Duo 2.5 rotary vane pump (2.5 m^3/h, Pfeiffer). During measurements, the pressure inside the MS was $1\sim5\times10^{-9}$ bar. Pretreatment procedures and details were explained in a previous paper.[17]

6.3 Results and discussion

6.3.1 Hydrolysis of cellobiose in acid

The molecular mechanism of acid-catalyzed hydrolysis of cellulose (cleavage of β-1-4-glycosidic bond) proceeds in three steps: 1) a proton interacts with the glycosidic oxygen linking two glucose units to form the corresponding conjugate acid, 2) C-O bond cleavage and breakdown of the conjugate acid into the cyclic carbonium ion, and 3) glucose and a proton are liberated after the rapid addition of water.[7,18] From the reaction mechanism, the

hydrolysis conditions (i.e. acid concentration) strongly influence the physical and chemical stability of cellulose. Apart from the acidity of the solution, reaction temperature also plays a key role in accelerating the rate of cellulose hydrolysis. Acidity and temperature are typically applied in two combinations: strong acid hydrolysis at ambient temperature (25~45^{o}C) and dilute acid hydrolysis at moderate temperature (170~240^{o}C).[7,11] Strong acid breaks down cellulose into oligosaccharides and glucose within a few hours without formation of large amounts of dehydration products, such as 5-hydroxymethylfurfural (HMF), levulinic acid, and formic acid.[19] Dilute acid hydrolysis is efficient because of the short residence time of the hydrolysis products (i.e. glucose) in the continuous reactor minimizing the formation of degradation products from glucose.[11]

Cellobiose, a glucose dimer connecting two glucose units by a glycosidic bond, is selected as a model molecule in order to understand the mechanism of cellulose hydrolysis. The effect of acid concentration and reaction temperature were studied for later comparison to the electrochemistry-assisted hydrolysis. We investigated the time-dependent hydrolysis and degradation of cellobiose (10 mM) at several concentrations of sulfuric acid (0.5, 1, 2, 5, and 10 M) and reaction temperatures (25, 60, and 80^{o}C). The reaction temperature was limited to below 100^{o}C considering standard electrochemical reaction conditions in aqueous media. Samples were collected at different reaction times (0, 0.5, 1, 3, and 22 hr), and collected samples were immediately cooled down to room temperature and diluted with water to less than 0.5 M in order to prevent further reactions, after which they were analyzed in an HPLC system.

The amount of remaining cellobiose (%) as a function of reaction time summarized in a logarithmic plot follows first-order reaction kinetic as confirmed by the linearity of the plots for all temperatures, and the slope of the plot indicates the first-order rate constant (k, s^{-1}). Based on the obtained rate constant, Arrhenius plots, ln(k, s^{-1}) vs. 1/T (1/K) are drawn in Figure 1a. Even though three data points are not sufficient for an accurate determination of the activation energy, the values obtained from Figure 1, ca. 118±8 kJ mol^{-1}, is within the error range of the value, 110±30 kJ mol^{-1}, reported by Mosier.[20] It is also significantly lower than the value reported for conventional cellulose hydrolysis (ca. 176 kJ mol^{-1}).[11,21,22] Interestingly, the activation energy for glucose degradation is ca. 138 kJ mol^{-1},[11,21] which means cellobiose hydrolysis is more facile than glucose degradation during

the acid-catalyzed reaction, and therefore we can obtain a higher selectivity toward glucose in dilute acid hydrolysis.

The rates of glucose formation, ln(R, mM s^{-1}) vs. 1/T (1/K), based on the HPLC results are shown in Figure 1b. The values for high concentration of sulfuric acid (i.e. 5 and 10 M) are extracted from the initial glucose formation rate before decomposition of glucose. We note that the rate of glucose formation also follows the type of Arrhenius plots as shown in Figure 1a, since cellobiose converts to glucose with high selectivity. The activation energy obtained from Figure 1b is ca. 110±7 kJ mol^{-1}, which is consistent with the value from Figure 1a. Especially low concentrations of sulfuric acid and low temperature lead to a very low activity for cellobiose conversion, which indicates that acid-catalyzed cellulose hydrolysis is hardly applicable to electrochemical reactions at room temperature. At elevated temperatures, for example at 80°C, however, even 0.5 M sulfuric acid actively hydrolyzes cellobiose to glucose since the reaction rate increases exponentially as the reaction temperature increases, with high selectivity (> 98%) to glucose.

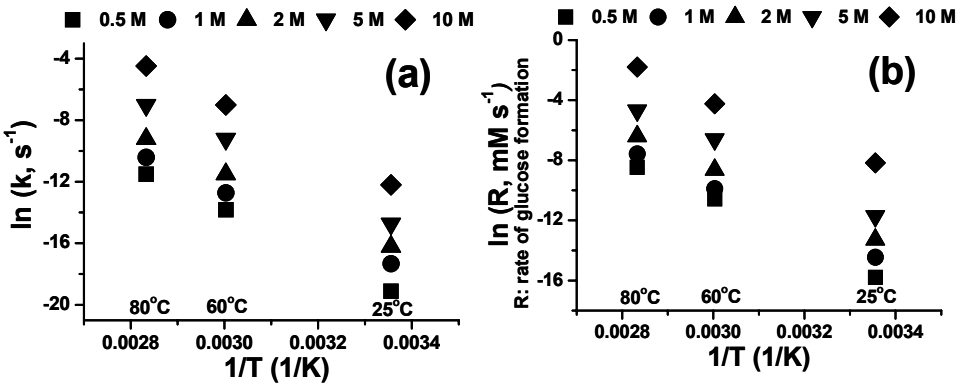

Figure 1. (a) Arrhenius plots for the acid-catalyzed cellobiose hydrolysis and (b) the rates of glucose formation at diverse concentrations of sulfuric acid (■ 0.5 M, ● 1 M, ▲ 2 M, ▼ 5 M, and ◆ 10 M) at different temperatures (25, 60, and 80°C).

Although the condition of 10 M sulfuric acid at 80°C shows extremely high cellobiose conversion and glucose formation rate in a short reaction time (2.6 mM cellobiose converted to glucose within 30 s corresponding to a rate of glucose formation of ca. 10 mM/min, and the conversion of cellobiose complete within 0.5 hr), the subsequent degradation of glucose lowers the yield and selectivity. The results from the HPLC analysis

reveal that glucose is ultimately decomposed to equal amounts of levulinic acid and formic acid. However 5-hydroxymethylfurfural (HMF), a key intermediate species, was not observed. In general, the pathway for glucose decomposition is believed to be initiated by fructose isomerization from glucose, which is subsequently dehydrated to give HMF or humin (a carbonaceous hydrocarbon)-type side products due to condensation reactions of intermediates during fructose dehydration.[23] Next, HMF is further rehydrated to give levulinic acid and formic acid.[24] Since we observed the formation of humin at 60°C and 80°C from 5 and 10 M sulfuric acid, we are convinced that the two reaction steps of glucose isomerization to fructose and fructose dehydration to HMF must have taken place. Therefore, as illustrated in Scheme 1, a cellobiose molecule is hydrolyzed to two molecules of glucose, then glucose isomerizes to fructose, followed by dehydration to HMF and humin, and finally HMF is hydrolyzed to levulinic acid and formic acid in strong acid and at high temperature.

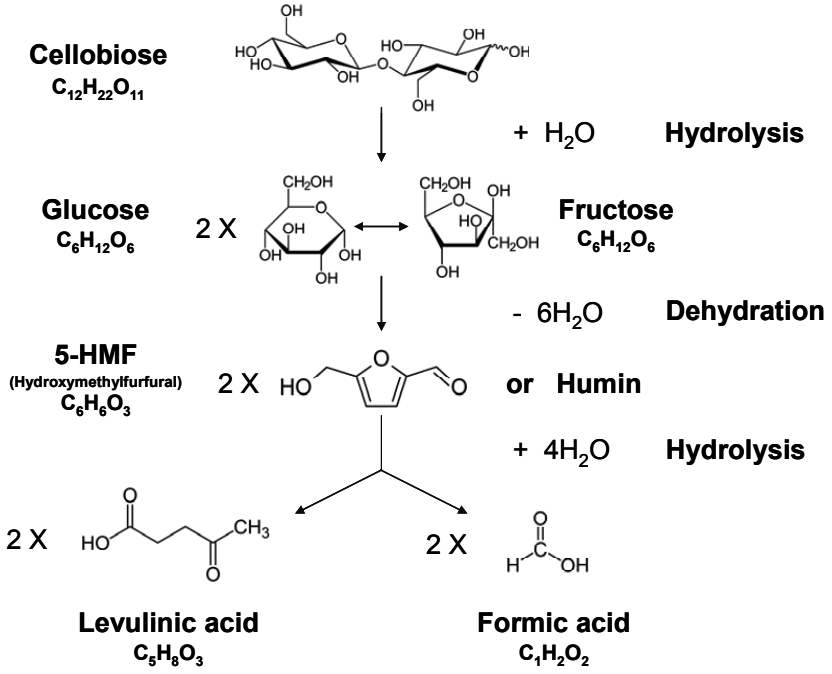

Scheme 1. Reaction pathway for acid-catalyzed cellobiose hydrolysis to glucose and its decomposition.

As a general conclusion, cellobiose is hydrolyzed by acid with a lower activation energy (118±8 kJ mol^{-1}) than conventional cellulose hydrolysis (ca. 176 kJ mol^{-1} [11,21,22]). Cellobiose hydrolysis is strongly dependent on reaction temperature and concentration of acid. Higher concentration of acid and higher temperature accelerate the rate of cellobiose conversion, however glucose is not stable under these conditions, as it may isomerize to fructose, followed by dehydration to 5-HMF or humin, and finally hydrolyzes to levulinic acid and formic acid.

6.3.2 Cellobiose hydrolysis by electrochemically generated acid

The easiest way to generate acid (H^+) in an electrochemical cell is by the oxygen evolution reaction (OER) at an anode. The main potential advantage of using an electrochemical method for cellobiose hydrolysis is that we can control the local acidity during oxygen evolution by applying a controlled potential or current. Based on the experimental results obtained from chemical (H_2SO_4) cellobiose hydrolysis in the previous section, we selected a relatively low concentration of sulfuric acid (0.5 M) as electrolyte with high reaction temperature (80°C), in order to examine whether the electrochemically generated acid can accelerate the rate of cellobiose hydrolysis, in a background electrolyte in which the further degradation of glucose may be limited.

First of all, a blank experiment was carried out without electrochemical reaction and without the electrode in solution, and the concentrations of cellobiose and its reaction products were obtained by continuous fraction collection and subsequent analysis in an HPLC system, as shown in Figure 2a. Note that the concentration of cellobiose decreases linearly, and was hydrolyzed and converted mainly to glucose with only a small amount of side-product. The rate of glucose formation starts at 1.87 mM/hr and decreases to 1.27 mM/hr after one hour, but it is higher than the decomposition rate from chemical cellobiose hydrolysis (0.94 mM/hr) under the same conditions in 0.5 M H_2SO_4 at 80°C (see previous section), most likely due to the convection of solution introduced by the continuous sample collection.[14] For the generation of acid at the anode by water electrolysis, a platinum electrode was applied as working electrode using different current densities, i.e. 10, 30, 60, and 120 mA cm^{-2} as shown in Figure 2b. As expected, a higher applied current causes a faster conversion of cellobiose to glucose at the initial stage of the reaction (< 30 min) since

an applied current of 120 mA cm^{-2} shows the highest concentration of glucose in Figure 2b. However, after 30 min, the rate of glucose formation decreases as the applied current increases. Interestingly, only a current of 10 mA cm^{-2} shows an overall enhanced rate for glucose formation (1.73 mM/hr on average) in comparison with the blank (1.57 mM/hr on average), whilst higher applied currents cause lower rates of glucose formation, on average 1.56, 1.54, and 1.3 mM/hr for 30, 60, and 120 mA cm^{-2}, respectively. The reason for this lower glucose yield is that the glucose hydrolyzed from cellobiose degrades to by-products, i.e. glyceric acid and formic acid on the activated Pt surface by electro-oxidation.

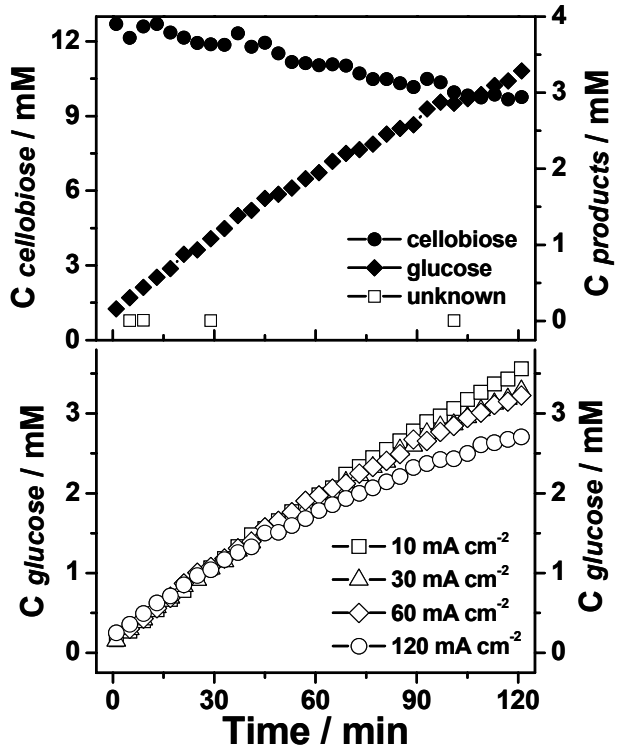

Figure 2. Cellobiose conversion to glucose in 0.5 M H_2SO_4 at 80°C in (a) blank and (b) with support of electrochemically generated acid by applying different current densities (10, 30, 60, and 120 mA cm^{-2}) on Pt electrode.

A similar effect was observed during glycerol oxidation,[15] in which glycerol oxidizes dominantly to glyceraldehyde and glyceric acid on a clean Pt surface, and further oxidizes

to glycolic acid and formic acid on a PtO_x surface (> 1.2 V vs. RHE). The applied currents on the Pt electrode cause the corresponding potential to range from 1.6 to 1.9 V (vs. RHE), at which potentials the Pt electrode is oxidized to PtO_x, leading to C-C bond breaking, i.e. glucose to form smaller organic molecules. In a related experiment, Baizer and Nobe[11] separated the electrochemically generated acid from the platinum anode and introduced it to a high-pressure autoclave, obtaining 98% glucose selectivity with 29% of cellulose conversion at 160°C under optimized operating conditions. In our experiment, the concentration of unknown side-product increases at higher applied currents, which also produces a large amount of molecular oxygen. This "unknown" side product was also seen in an oxygen bubbled blank experiment, indicating oxygen produced during water electrolysis decreases the glucose selectivity.

As a brief conclusion, electrochemically generated acid can be applied to hydrolyze cellobiose to glucose during oxygen evolution reaction on a Pt anode. However, the interaction between reactants (cellobiose or glucose) and the activated Pt electrode decomposes glucose to smaller organic molecules in case of high applied potential or current. In addition, the oxygen produced during water electrolysis produces side-products and lowers the selectivity to glucose. Therefore, for a higher yield of glucose, an active catalyst for the oxygen evolution reaction is needed which is not-active towards glucose. Also separation of evolved oxygen will be important. Besides that, in order to achieve total cellobiose conversion in solution with our electrochemical method, one will need a large electrode area within a limited volume of solution.

6.3.3 Cellobiose decomposition by Fenton's reaction

Hydrogen peroxide has been used for the pretreatment of cellulose to solubilize the cellulosic matrix and reduce the cellulose crystallinity thus improving enzyme digestibility.[25,26] The advanced oxidation process (AOP) (i.e. wet air oxidation) utilizes hydrogen peroxide or hydroxyl radical (OH•) as an active intermediate species to oxidize cellulose at high temperature (150-350°C) with high pressure of O_2 (5-20 MPa).[27] However, only a few reports have studied the effect of the hydroxyl radical on cellulose hydrolysis and degradation.[12,28,29] In an attempt to achieve cellobiose hydrolysis, we employed hydroxyl radical (OH•) from Fenton's reaction as follows[30]:

$$Fe^{2+} + H_2O_2 \rightarrow Fe^{3+} + OH\bullet + OH^- \quad (1)$$

$$Fe^{3+} + H_2O_2 \rightarrow Fe^{2+} + OOH\bullet + H^+ \quad (2)$$

In reaction (1) the iron(II) introduced into the solution is oxidized by hydrogen peroxide to the ion iron(III), a hydroxyl radical, and a hydroxyl anion. In reaction (2) the iron(III) is subsequently reduced back to iron(II) by hydrogen peroxide, forming a peroxide radical and a proton,. Therefore the iron(II) is regenerated during the cycle and only hydrogen peroxide is consumed in the overall reaction. As the typical ratios of Fe(II) and H_2O_2, we chose 1:5-10, and the time dependent hydrolysis of 10 mM cellobiose in water was investigated with 2 mM Fe(II) and 5, 10, and 20 mM of H_2O_2 at three different temperatures, i.e. 25, 60, and 80^{o}C. Samples were collected at different reaction times (0, 0.5, 1, 2, 3, and 22 hr), and residual H_2O_2 was immediately quenched by using a stoichiometric excess of Na_2SO_3 in order to prevent further reactions, and subsequently analyzed in an HPLC system.

Similar results compared to the acid-catalyzed cellobiose hydrolysis were observed with the radical reaction. The amount of remaining cellobiose (%) plotted logarithmically as a function of time represents a first-order reaction as confirmed by the linearity of the plots for all temperatures, and the slope of the plot gives the first-order rate constant (k, s^{-1}). From the obtained rate constant, Arrhenius plots of ln(k, s^{-1}) vs. 1/T (1/K) are shown in Figure 3a. High reaction temperature and high concentration of hydrogen peroxide accelerate the cellobiose conversion, with glucose as initial product, indicating that the hydroxyl radical generated during Fenton's reaction cleaves the β-1-4-glycosidic bond of cellobiose to form glucose. Interestingly, the activation energy derived from the slope of the Arrhenius plots in Figure 3a is ca. 55±1 kJ mol^{-1}, about twice lower than that of acid-catalyzed reaction (ca. 118±8 kJ mol^{-1}), indicating that the application of hydroxyl radicals for cellulose hydrolysis can be a very promising technique with enhanced cellobiose conversion compared to acid catalysis. However, the glucose is also fractionized by radicals to smaller molecules as observed in the product spectra showing glyceric acid, glycolic acid, acetic acid, and formic acid. In contrast to the acid-catalyzed hydrolysis, in which the proton is not consumed, the hydroxyl radical is continuously consumed and needs to be generated by the cycles of reaction (1) and (2), which is limited by the residual amount of H_2O_2. In addition, the stability of H_2O_2 is dependent on the pH of solution and it decomposes easily to O_2 and H_2O at pH>1.[31]

Concerning the neutral condition for our experiment, H_2O_2 is not stable and therefore decomposes, which causes a lower conversion of cellobiose during long-term reaction. Therefore, after consumption of all H_2O_2 in the solution, cellobiose conversion does not proceed anymore. In addition, the rate of hydroxyl radical formation, which determines the rate of cellobiose conversion, is mainly dependent on the concentration of H_2O_2 and temperature. Figure 3b clearly shows that a higher concentration of H_2O_2 and a higher reaction temperature generate more hydroxyl radicals, which results in higher conversion of cellobiose to glucose with Arrhenius-type temperature dependence. The activation energy obtained from Figure 3b is ca. 54±2 kJ mol^{-1}, which value is consistent with that from Figure 3a. Room temperature is almost inactive for cellobiose conversion, however at high temperature (at 80^{o}C), the conversion ratio of cellobiose increases to 28, 45, and 70% with 5, 10, and 20 mM H_2O_2, respectively. Interestingly, a higher conversion of cellobiose does not lead to a higher selectivity for glucose as shown in Figure 3c, since the hydroxyl radical further decomposes glucose into smaller fractions. Therefore, in general, the selectivity (%) of glucose is less than 30% under all reaction conditions studied, and decreases as the rate of hydroxyl radical formation increases.

As an intermediate conclusion, the hydroxyl radical generated by Fenton's reaction initially hydrolyzes cellobiose to glucose with the activation energy of ca. 55±1 kJ mol^{-1}, but it further decomposes glucose to smaller organic molecules. The rate of cellobiose conversion is dependent on the rate of hydroxyl radical formation mainly determined by the amount of H_2O_2 and reaction temperature, and the selectivity of glucose is less than 30% in general, and inversely proportional to the rate of reaction.

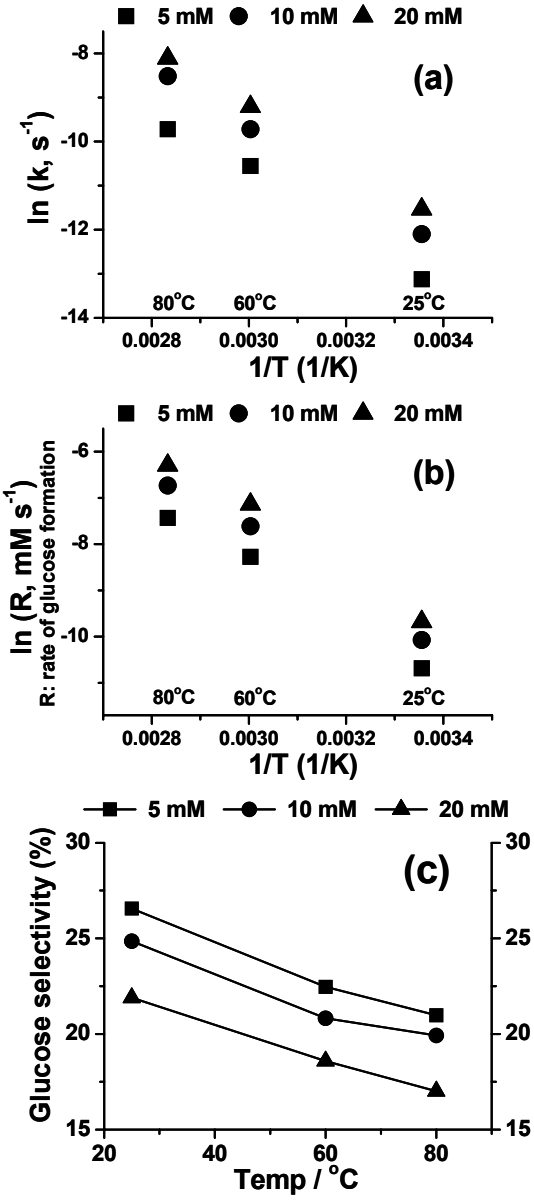

Figure 3. (a) Arrhenius plots for the first-order rate constants in radical-enhanced cellobiose hydrolysis, (b) the rates of glucose formation, and (c) glucose selectivity (%) at different concentrations of hydroxyl radical generated by Fenton's reaction (2 mM Fe(II) with 5, 10, and 20 mM H_2O_2) at 25, 60, and 80°C.

6.3.4 Electrochemical cellobiose decomposition on BDD

Boron-doped diamond (BDD) seems a suitable anode to produce large amounts of OH• to hydrolyze cellobiose to glucose as shown in the previous section with hydroxyl radicals generated from Fenton's reaction. BDD shows a higher O_2 evolution overvoltage than conventional anodes such as PbO_2, doped SnO_2, IrO_2, and Pt. The OH• formation follows from the reaction[32]:

$$H_2O \rightarrow OH_{ads}\bullet + H^+ + e^- \quad (3)$$

This formation of a hydroxyl radical has been confirmed by electron paramagnetic resonance spectroscopy.[27,33] The hydroxyl radical is considered as a non-selective, very powerful oxidant.[34] Here we will demonstrate its reactivity toward cellobiose hydrolysis to glucose and the further decomposition of glucose. As the hydroxyl radical from Fenton's reaction is highly active for cellobiose hydrolysis and accelerates the glucose decomposition at high reaction temperature, which lowers the selectivity toward glucose, we only show the electrochemical results obtained at room temperature. Also note that the number of protons generated by reaction (3) will be too small to lead to significant pH changes, so that we disregard any acid-catalyzed decomposition induced by reaction (3).

Shown in Figure 4 are the voltammograms of cellobiose decomposition in 0.1 M Na_2SO_4 (Figure 4A) and in 0.5 M H_2SO_4 (Figure 4B) alongside the concentration profiles of the reaction products, both in the absence (dashed line) and in the presence (solid line) of cellobiose (10 mM) in the solution. First of all, the blank voltammograms (dashed line) seem to have a higher overpotential for oxidation than the voltammogram with cellobiose in solution. However, we note that the potential for the formation of hydroxyl radical (blank, dash line) on the BDD electrode is identical with the onset potential of the oxidation current with cellobiose (solid line) in the solution (see insets in Figure 4A-a, and 4B-a), since hydroxyl radical initiates the cellobiose hydrolysis and further oxidizes its fractions. Also note that the onset potential of radical formation depends on the acidity of the solution. The oxidation current on BDD with cellobiose in neutral solution begins from 2.15 V, and the current increases significantly from 2.7 V. In acidic condition, 2.05 V is the onset potential for the oxidation with cellobiose, and the current increases exponentially. Comparing the current density at 3 V clearly shows that the current in acid

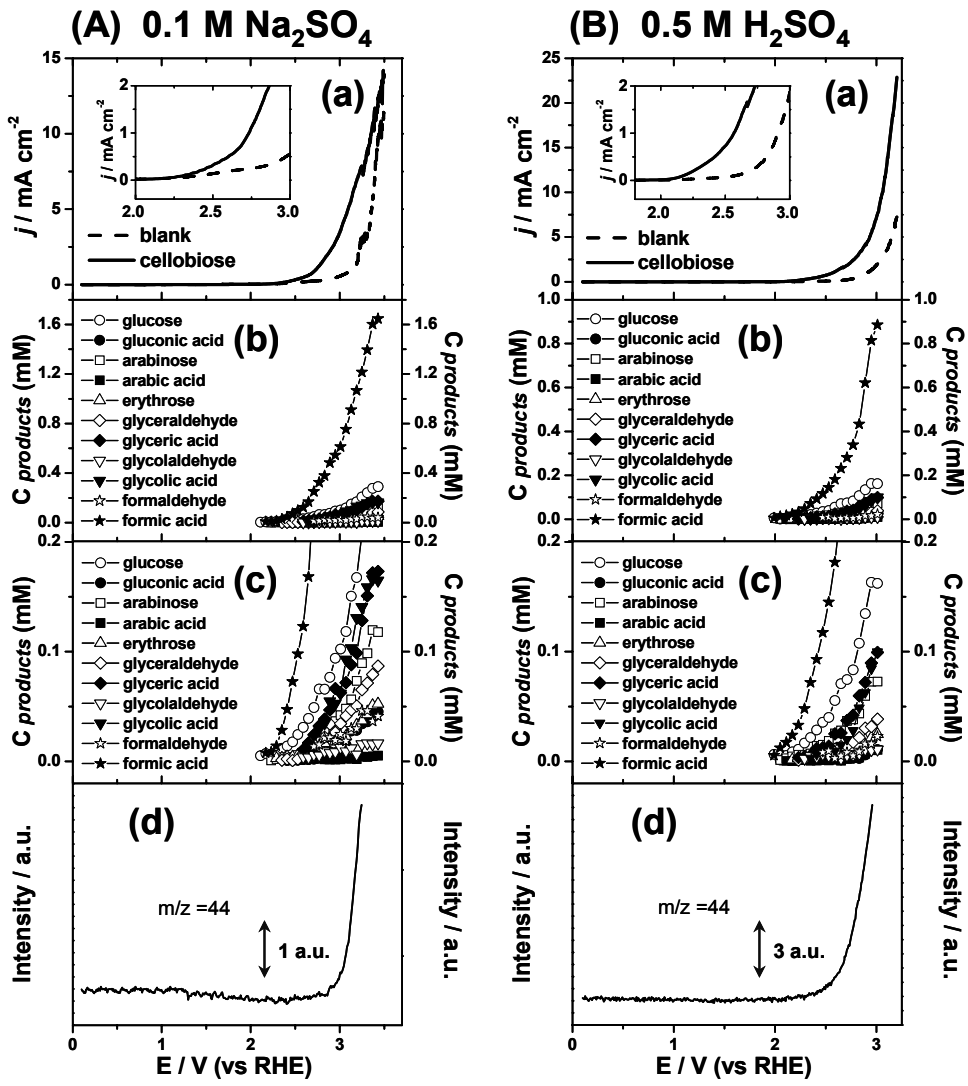

Figure 4. Cellobiose (10 mM) decomposition on boron-doped diamond (BDD) under (A) neutral (0.1 M Na_2SO_4) and (B) acidic (0.5 M H_2SO_4) conditions: a) current density measured with (solid line) and without (dash line) cellobiose in the solution during linear sweep voltammetry with a scan rate of 1 mV s^{-1}; b) concentration profiles of reaction products collected with the fraction collection system; c) enlargement of b) with different scale; and d) ion current profiles for *m/z*=44 (CO_2) obtained with OLEMS measured during voltammetry.

solution is almost twice of that in neutral solution, which indicates that the oxidation or decomposition of cellobiose and its by-products by hydroxyl radicals on BDD is enhanced under acidic conditions.

To study the formation of gaseous products, in particular CO_2, an online electrochemical mass spectrometry experiment was carried out.[16] Figure 4 A-d and B-d shows the MS ion current for *m/z*=44, which implies CO_2 formation, clearly demonstrating that formic acid is further oxidized to CO_2 from ca. 2.8 V in neutral and from ca. 2.5 V in acidic condition, respectively. The potential for CO_2 formation indicates that formic acid is relatively stable at low potentials (< ca. 2.5 V), but it is oxidized to CO_2 at high concentration of hydroxyl radical at high potentials. The electro-oxidation of formaldehyde (10 mM) and formic acid (10 mM) on a BDD electrode were studied in separate experiments, the results of which are shown in Figure 5. Formaldehyde clearly shows a higher oxidation current and a lower onset potential than formic acid, especially in neutral condition, suggesting that the CH_2O detached from aldose is easily oxidized to formic acid, but the oxidation of formic acid is sluggish. Interestingly, from the OLEMS experiment, we did not observe the formation of O_2, *m/z*=32, during cellobiose decomposition even at higher potentials (> 3 V), which implies that the oxygen evolution reaction is sluggish on a BDD electrode and the blank currents in Figure 4 A-a and B-a are mainly due to the water oxidation to hydroxyl radical following the one electron transfer reaction (3).

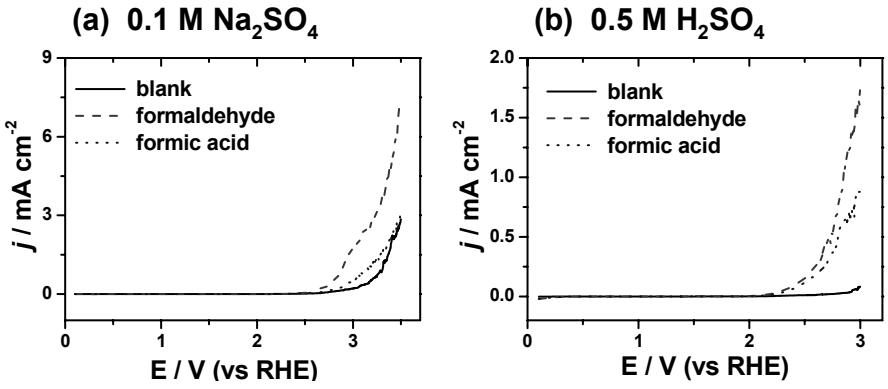

Figure 5. Formaldehyde (10 mM) and formic acid (10 mM) oxidation on boron-doped diamond (BDD) in (a) neutral (0.1 M Na_2SO_4) and (b) acidic (0.5 M H_2SO_4) conditions with a scan rate of 1 mV s^{-1}.

Turning our attention to the detailed reaction pathway, Figure 6 shows the onset potentials for the observed reaction products in 0.1 M Na_2SO_4 and in 0.5 M H_2SO_4 from panel (b) in Figure 4. First of all, we can clearly see how the sequence of product formation depends on the applied potential. For the formation of aldoses under neutral conditions, Figure 6a shows that glucose ($C_6H_{12}O_6$) hydrolyzed from cellobiose appears as the first product from ca. 2.11 V, followed by arabinose ($C_5H_{10}O_5$, 2.23 V), erythrose ($C_4H_8O_4$, 2.29 V), glyceraldehyde ($C_3H_6O_3$, 2.35 V), glycol-aldehyde ($C_2H_4O_2$, 2.59 V), and formaldehyde (CH_2O, 2.71 V), indicating that the hydroxyl radical selectively attacks the aldehyde on the aldose and breaks the nearby C-C bond, thereby producing a smaller aldose and formic acid (as formed by oxidation of CH_2O). This is evidenced by the observation of formic acid from 2.17 V, the potential in between the formation of glucose and arabinose, with the CH_2O detached from aldose immediately oxidized to formic acid. We also observed several organic acids oxidized from their corresponding aldoses, which enhances the total current density compared to the blank. The formation of organic acids follows the same potential dependence as the aldoses, i.e. gluconic acid was observed from 2.41 V, followed by arabic acid (2.47 V), glyceric acid (2.59 V), and glycolic acid (2.65 V).

The onset potentials of the observed aldoses and their corresponding organic acids in acidic solution (Figure 6b) are shifted to lower potentials compared to neutral solution (Figure 6a), however they also follow the general trend described above. The first reaction products from cellobiose decomposition by hydroxyl radical are glucose and formic acid observed from 1.99 V, with other aldoses observed at consecutively higher potentials, i.e. arabinose (2.05 V), erythrose (2.17 V), glyceraldehyde (2.23 V), glycolaldehyde (2.29 V), and formaldehyde (2.47 V), and the organic acids, i.e. gluconic acid (2.05 V), arabic acid (2.11 V), glyceric acid (2.23 V), and glycolic acid (2.35 V). Therefore we conclude that acidic conditions are preferred to generate hydroxyl radicals on BDD,[35] which actively hydrolyze cellobiose to glucose, and then further decompose and oxidize glucose to smaller aldoses and their corresponding organic acids at lower potentials than in neutral condition.

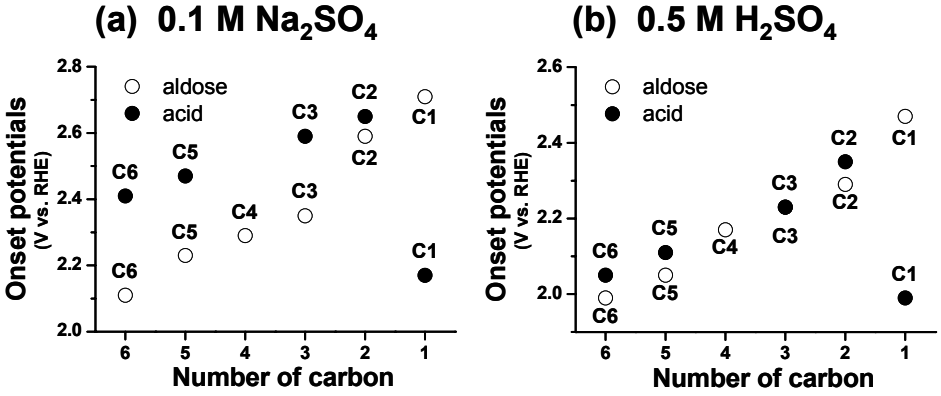

Figure 6. The onset potentials for observed reaction products as a function of the number of carbon atoms of the aldoses and their corresponding acids on a BDD electrode in (a) neutral (0.1 M Na_2SO_4) and (b) acidic (0.5 M H_2SO_4) solution.

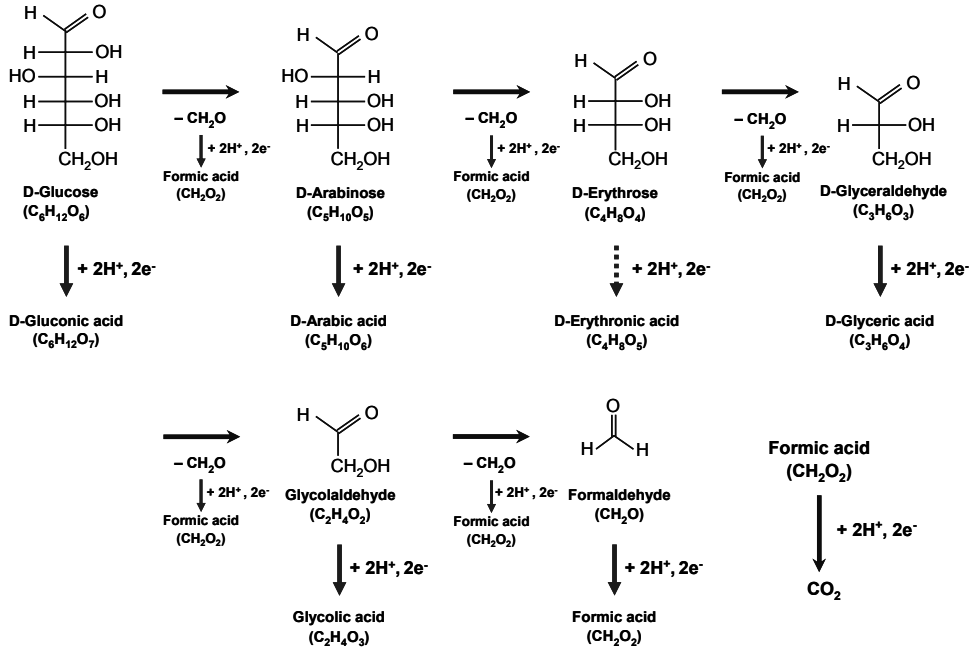

Scheme 2. Reaction pathway for radical cellobiose decomposition on BDD electrode.

On the basis of the results shown in Figure 4~6, we suggest a general reaction pathway for the cellobiose hydrolysis to glucose and its further decomposition by the hydroxyl radicals generated on a BDD electrode as shown in Scheme 2. First of all, the hydroxyl radical generated on a BDD surface depolymerizes cellobiose to glucose. A possible pathway for the cleavage of cotton cellulose was proposed recently by Li et al.,[12] suggesting that the hydroxyl radical extracts the hydrogen atom from the C4 of D-anhydroglucopyranose unit forming a carbon radical, which is subsequently oxidized to form a superoxide radical of cellulose by addition of molecular oxygen. This is followed by the cleavage of the glycosidic bond to form glucose after the leaving of superoxide anion radical. However, this suggestion does not fit our case since there is no molecular oxygen in our experiment, as confirmed by the OLEMS measurements. After the hydrolysis of cellobiose by the hydroxyl radical, glucose is subsequently decomposed to arabinose, erythrose, glyceraldehyde, glycol-aldehyde, and formaldehyde, which indicates that the hydroxyl radical selectively attacks the C-C bond of the aldehyde to break it to smaller aldoses. After the C-C bond cleavage, CH_2O is detached from the aldose molecule, which is immediately oxidized to formic acid. We note that, however, the formation of CO_2 from formic acid oxidation is a bit sluggish on the BDD electrode (see Figures 4A-d, 4B-d, and 5), even at high potential. In addition, we did not observe stereoisomers, but only D-aldose during hydrolysis and decomposition, indicating that the hydroxyl radical does not change the configuration of sugar molecules.

6.4 Conclusion

This work has described the potential of cellobiose hydrolysis and decomposition by electrochemical methods. We investigated the cellobiose hydrolysis to glucose and its further decomposition during the acid-catalyzed reaction by comparison of sulfuric acid vs. electrochemically generated acid, and the radical reaction by hydroxyl radicals from Fenton's reaction vs. hydroxyl radicals from water oxidation on a BDD electrode. The reaction products were determined by (online) HPLC for dissolved reaction products and by OLEMS for CO_2. The experiments with homogeneous chemical reactions provided the key reaction parameters for cellobiose conversion to glucose, i.e. concentration of acid and radical, and reaction temperature. The hydrolysis of cellobiose follows a first-order reaction with Arrhenius-type temperature dependence for the various concentrations of sulfuric acid

and hydroxyl radicals with different activation energies of ca. 118±8 kJ mol^{-1} and ca.55±1 kJ mol^{-1}, respectively. The main advantage of electrochemical approach would be to steer the reaction rate by controlling the amount of acid or radical formation at the electrode surface. The electrochemically generated acid during the oxygen evolution reaction (OER) only marginally increases the rate of glucose formation, but lowers the selectivity towards glucose since the electrode (PtO_x) interacts with glucose and decomposes it further to smaller organic acids. In addition, the oxygen formed during OER lowers the selectivity of glucose, since oxygen causes the formation of side-products. Therefore, an electrode with high activity for OER and low activity for glucose decomposition is necessary for such an application. Hydroxyl radicals generated on a BDD electrode first hydrolyze the cellobiose to glucose, and then attacks the aldehyde group on the glucose species, which is then further fractionized to smaller aldoses and formic acid. The application of hydroxyl radicals may be a promising technique with lower activation energy than that of the acid-catalyzed reaction, provided the hydrolyzed glucose is immediately separated from the active radical. In combination with the ability of potential-controlled electrolysis, as recently demonstrated for the oxidation of glycerol,[15,36] it may be possible to use this method to achieve higher selectivity towards certain interesting end products.

6.5 References

[1] G. W. Huber, S. Iborra, A. Corma, *Chem. Rev.* **2006**, *106*, 4044-4098.

[2] D. Klemm, B. Heublein, H. -P. Fink, A. Bohn, *Angew. Chem. Int. Ed*. **2005**, *44*, 3358-3393.

[3] C. Luo, S. Wang, H. Liu, *Angew. Chem. Int. Ed*. **2007**, *46*, 7636-7639.

[4] H. Kobayashi, T. Komanoya, K. Hara, A. Fukuoka, *ChemSusChem* **2010**, *3*, 440-443.

[5] Y. Sun, J. Cheng, *Bioresour. Technol*. **2002**, *83*, 1-11.

[6] Y. -H. P. Zhang, L. R. Lynd, *Biotechnol. Bioeng*. **2004**, *88*, 797-824.

[7] R. Rinaldi, F. Schuth, *ChemSusChem* **2009**, *2*, 1096-1107.

[8] K. Shimizu, H. Furukawa, N. Kobayashi, Y. Itaya, A. Satsuma, *Green Chem*. **2009**, 11, 1627-1632.

[9] M. Sasaki, Z. Fang, Y. Fukushima, T. Adschiri, K. Arai, *Ind. Eng. Chem. Res.* **2000**, *39*, 2883-2890.

[10] H. Kobayashi, Y. Ito, T. Komanoya, Y. Hosaka, P. L. Dhepe, K. Kasai, K. Hara, A. Fukuoka, *Green Chem*. **2011**, *13*, 326-333.

[11] J. C. Yu, M. M. Baizer, K. Nobe, *J. Electrochem. Soc.* **1988**, *135*, 83-87.

[12] D. Meng, G. Li, Z. Liu, F. Yang, *Polym. Degrad. Stabil*. **2011**, *96*, 1173-1178.

[13] S. C. S. Lai, M. T. M. Koper, *Faraday Discuss*. **2008**, *140*, 399-416.

[14] Y. Kwon, M. T. M. Koper, *Anal. Chem.* **2010**, *82*, 5420-5424.

[15] Y. Kwon, K. J. P. Schouten, M. T. M. Koper, *ChemCatChem* **2011**, *3*, 1176-1185.

[16] A. H. Wonders, T. H. M. Housmans, V. Rosca, M. T. M. Koper, *J. Appl. Electrochem*. **2006**, *36*, 1215-1221.

[17] M. Duca, V. Kavvadia, P. Rodriguez, S. C. S. Lai, T. Hoogenboom, M. T. M. Koper, *J. Electroanal. Chem*. **2010**, *649*, 59-68.

[18] Q. Xiang, Y. Y. Lee, P. O. Petterson, R. W. Torget, *Appl. Biochem. Biotechnol.* **2003**, *107*, 505-514.

[19] F. Bergius, *Ind. Eng. Chem.* **1937**, *29*, 247-253.

[20] N. S. Mosier, C. M. Ladisch, M. R. Ladisch, *Biotech. Bioeng*. **2002**, *79*, 610-618.

[21] I. A. Malester, M. Green, G. Shelef, *Ind. Eng. Chem. Res.* **1992**, *31*, 1998-2003.

[22] J. F. Saeman, *Ind. Eng. Chem.* **1945**, *37*, 43-52.

[23] E. A. Pidko, V. Degirmenci, R. A. van Santen, E. J. M. Hensen, *Angew. Chem. Int. Ed.* **2010**, *49*, 2530-2534.

[24] B. Girisuta, L. P. B. M. Janssen, H. J. Heeres, *Ind. Eng. Chem. Res*. **2007**, *46*, 1696-1708.

[25] P. Martel, J. M. Gould, *J. Appl. Poly. Sci*. **1990**, *39*, 704-714.

[26] R. A. Silverstein, Y. Chen, R. R. Sharma-Shivappa, M. D. Boyette, J. Osborne, *Biores. Tech*. **2007**, *98*, 3000-3011.

[27] R. Robert, S. Barbati, N. Ricq, M. Ambrosio, *Water Res*. **2002**, *36*, 4821-4829.

[28] V. Arantes, A. M. F. Milagres, *J. Chem. Technol. Biotechnol*. **2006**, *81*, 413-419.

[29] E. Akio, I. Shuji, T. Hiromi, *J. Biotechnol.* **1997**, *53*, 265-272.

[30] C. W. Jones, in *Applications of Hydrogen Peroxide and Derivatives*, The Royal Society of Chemistry, Cambridge, **1999**, p. 44.

[31] M. L. Kremer, *J. Phys. Chem. A* **2003**, *107*, 1734-1741.

[32] E. Brillas, B. Boye, I. Sires, J. A. Garrido, R. M. Rodriguez, C. Arias, P. -L. Cabot, C. Comninellis, *Electrochim. Acta* **2004**, *49*, 4487-4496.

[33] B. Marselli, J. Garcia-Gomez, P. -A. Michaud, M. A. Rodrigo, C. Comninellis, *J. Electrochem. Soc.* **2003**, *150*, D79-D83.

[34] B. Boye, E. Brillas, B. Marselli, P. -A. Michaud, C. Comninellis, G. Farnia, G. Sandon, *Electrochim. Acta* **2006**, *51*, 2872-2880.

[35] S. C. B. Oliveira, A. M. Oliveira-Brett, *Electrochim. Acta* **2010**, *55*, 4599-4605.

[36] Y. Kwon, Y. Birdja, I. Spanos, P. Rodriguez, M. T. M. Koper, *ACS Catal.* **2012**, *2*, 759-764.

7

Electrocatalytic hydrogenation and deoxygenation of glucose on solid metal electrodes

Abstract

This chapter addresses the electrocatalytic hydrogenation of glucose to sorbitol or 2-deoxysorbitol on solid metal electrodes in neutral media by combining voltammetry and online product analysis with high-performance liquid chromatography, which provides both qualitative and quantitative information of the reaction products as a function of potential. Three groups of catalysts in the Periodic Table regarding to reaction products clearly show their affinities toward: 1) hydrogen formation on early transition metals (Ti, V, Cr, Mn, Zr, Nb, Mo, Hf, Ta, We, and Re) and platinum group metals (Ru, Rh, Ir, and Pt), 2) sorbitol on late transition metals (Fe, Co, Ni, Cu, Pd, Au, and Ag) and Al (*sp* metal), and 3) sorbitol and 2-deoxysorbitol on post-transition metals (In, Sn, Sb, Pb, and Bi) as well as Zn and Cd (*d* metals). Ni shows the lowest overpotential for sorbitol formation from -0.25 V whereas Pb generates sorbitol with the highest yield (< 0.7 mM cm^{-2}). Different from a smooth Pt electrode, a large surface-area Pt/C electrode hydrogenates glucose to sorbitol from -0.21 V with relatively low current, which emphasizes the importance of the active sites and the surface area of the catalyst. The mechanism to form 2-deoxysorbitol from glucose and/or fructose is discussed according to the observed reaction products. The yield and selectivity of hydrogenated products is highly sensitive to the chemical nature and state of the catalyst surface.

The contents of this chapter have been published: Y. Kwon, M. T. M. Koper, *ChemSusChem*, **2013**, *6*, 455-462.

7.1 Introduction

Catalytic conversion of biomass to fuels and chemicals has attracted great attention as one of the future technologies for mitigating global warming and for building up a carbon-neutral energy cycle.[1,2] Glucose, as the monomer of the cellulose, plays a central role in biomass conversion. In particular, hydrogenation of glucose to sorbitol is a very important reaction from the synthetic and hydrogen storage points of view. Sorbitol is a promising platform polyol used as additives in foods, drugs, cosmetics, and various chemicals including vitamin C.[3] Using electrochemical approaches, sorbitol has been produced from aqueous glucose solution by applying certain current or potential on large-surface-area catalysts such as Raney-Ni[4,5] or poor metals at moderate pH (3~11)[4,6-8] and temperature (<60°C)[4-8] in a flow reactor.[4-6,9] Especially controlling pH and temperature during hydrogenation process is a key issue to obtain high yield of sorbitol since strong acid leads to only H_2 formation and alkaline pH and high temperature cause mutarotation of glucose to by-products. Although electrocatalytic synthesis of sorbitol from glucose was once applied on an industrial scale,[10] since 1950 sorbitol has been produced by catalytic hydrogenation on Raney-Ni and with modifiers (W, B, P etc.)[3,11-13] or noble metals such as Ru[14-16] under hydrogen pressure (1~350 atm) at various temperatures (ambient to 400°C).[17]

Recently, one-pot conversion of cellulose into sorbitol under high H_2 pressure has been introduced,[18,19] which consists of the hydrolysis of cellulose to glucose *via* water-soluble oligo-saccharides, followed by the hydrogenation of glucose to sorbitol.[19] Precious metals such as Pt, Rh, Ir etc. on oxidic supports promote the rate-determining step of the hydrolysis of cellulose to glucose and subsequently reduce glucose to sorbitol.

In addition to Raney-Ni[4,5], the most applied catalysts for the electrocatalytic hydrogenation of glucose are poor metals such as Pb,[6-8], Hg,[20] Pb(Hg)[6,20], and Zn(Hg)[4,20] since they suppress the hydrogen evolution reaction (HER). In electrocatalytic glucose hydrogenation, the chemisorbed hydrogen on electrode surface (M-H) is generated by electroreduction of water (under ambient pressure and temperature) as follows:

$$H_2O + e^- + M \rightarrow M\text{-}H + OH^- \qquad \text{(Volmer reaction)} \qquad (1)$$

In competition with electrochemical (Eq. 2) and chemical (Eq. 3) hydrogen generation, adsorbed glucose on the electrode surface (M-glucose) is hydrogenated to sorbitol (Eq. 4) or deoxygenated to 2-deoxysorbitol (Eq. 5) following:

$$M\text{-}H + H_2O + e^- \leftrightarrow M + H_2 + OH^- \quad \text{(Heyrovsky reaction)} \tag{2}$$

$$2M\text{-}H \leftrightarrow M + H_2 \quad \text{(Tafel reaction)} \tag{3}$$

$$M\text{-glucose} + 2M\text{-}H \leftrightarrow 3M + \text{sorbitol} \tag{4}$$

$$M\text{-glucose} + 4M\text{-}H \leftrightarrow 5M + \text{2-deoxysorbitol} + H_2O \tag{5}$$

where we have assumed that glucose reacts in its adsorbed state with hydrogen adsorbed on the metal catalyst. Because of the co-production of hydrogen, careful selection of the electrocatalyst as well as the applied potential/current is very important in order to obtain high yield and selectivity towards sorbitol, since the overpotential for water reduction (Eq. 1~3) and the adsorption energy of glucose depend strongly on the nature of catalyst. Although electrocatalytic glucose hydrogenation to sorbitol has been applied on an industrial scale,[10] unfortunately, a fundamental understanding of the reactions linking catalysts and voltammetry has not been reported mainly due to existing technical limitations regarding the online analysis of products. For instance, conventional bulk electrolysis requires a long operating time to find the optimum potential or current for a high yield of sorbitol,[6-9] and moreover such studies yield little insight into the mechanistic aspects of the reaction. We believe this lack of insight into the mechanistic aspects of glucose reduction, and sugar compounds in general, hampers the application of electrochemical methods in their conversion, and therefore a detailed study, such as reported herein, is warranted.

In this chapter, we investigate the electocatalytic glucose hydrogenation to sorbitol or 2-deoxysorbitol on a large number of pure solid metal electrodes from across the Periodic Table, aiming at understanding the activity and selectivity of catalysts by correlating the voltammetry and online product analysis. Glucose reduction is carried out in neutral solution deliberately as the local alkalinity generated during H_2 evolution helps in mutarotating glucose into an electro-active form, whereas the pH neutrality of the bulk

avoids product degradation. Acidic solutions are not active for glucose reduction. Reaction products are determined both quantitatively and qualitatively by using a combination of voltammetry and online high-performance liquid chromatography (HPLC).[21-26] Since the expected products are soluble, HPLC is the most suitable analysis technique. The application of in situ spectroscopic techniques such as in situ Infrared or Raman spectroscopy is problematic due to concurrent hydrogen evolution. Finally, a possible mechanism of electrocatalytic hydrogenation of glucose is discussed based on the observed reaction products and the pH changes during electrolysis.

7.2 Experimental

7.2.1 Electrochemical procedures

All measurements were carried out in a conventional single compartment three-electrode glass cell, which was cleaned by employing a standard procedure[27] for removing traces of organic and inorganic contaminants. Oxygen was removed by bubbling argon through the solution prior to the voltammetric experiments. All transition and post-transition metals (≥99.5%) used as working electrodes in the experiment were polycrystalline wires/ rods/plates, which were mechanically polished with alumina (up to 0.05 μm) and cleaned ultrasonically in pure water (MilliQ gradient A10 system, 18.2 MΩ) followed by electropolishing by cycling 5 times between -1.5 and 0 V (vs. RHE) with a scan rate of 50 mV s^{-1} in 0.1 M Na_2SO_4 solution in order to remove surface impurities and oxide before use.[28,29] The surface area (cm^2) of the catalysts used to calculate the current density (mA cm^{-2}) and concentration yield of reaction products (mM cm^{-2}) was obtained based on geometric area except for Pt and Pt/C catalysts for which we considered the electrochemically active surface area by the hydrogen desorption charge in 0.5 M H_2SO_4. A thin-film electrode with 3 nm Pt/C nanoparticles (50 wt %, Tanaka) was fabricated by loading 3 μl and 20 μl of nanoparticle suspension in water (1 mg mL^{-1}) onto a polished Pt plate substrate, subsequently dried at room temperature. For the Pt and Pt/C catalysts, the electrochemically active surface area was recorded before experiment. In all experiments, a large platinum plate was used as a counter electrode while a reversible hydrogen electrode (RHE) was employed as a reference electrode. Glucose (0.1 M, Merck) was dissolved into a solution of 0.1 M Na_2SO_4 (Merck, pH 7). Electrochemical cell potentials were controlled

with a potentiostat/galvanostat (μ-Autolab Type III). All experiments were carried out at room temperature.

7.2.2 Fraction collection and product analysis

For the detection of intermediates and products by HPLC, samples of the electrolyte solution were collected with a small Teflon tip (inner diameter, 0.38 mm) positioned close (10 μm) to the center of the electrode surface, the tip being connected to a PEEK capillary with inner/outer diameters of 0.13/1.59 mm.[21] The tip was cleaned in a solution of 0.2 M $K_2Cr_2O_7$ and rinsed thoroughly with ultrapure water before use. The sample volume collected in each well was 60 μl on a 96-well microtiter plate (270 μl/well, Screening Devices b.v.) using an automatic fraction collector (FRC-10A, Shimadzu). The flow rate of sample collection was adjusted to 60 ml min^{-1} with a Shimadzu pump (LC-20AT). Collected samples were immediately neutralized by adding 60 μl of 10 mM phosphate buffer. After collecting samples, the microtiter plate was covered by a silicon mat to prevent the evaporation of collected samples.

Samples collected during voltammetry were analysed using a Shimadzu Prominence HPLC. The microtiter plate with the collected samples was placed in an autosampler (SIL-20A) holder, and 20 μl of sample was injected into the column. The column (Shodex SP0810) used for the analysis used pure water as the eluent. The temperature of the column was maintained at 80^{o}C in an oven (CTO-20A), and the separated compounds were detected with a refractive index detector (RID-10A). The main reaction products analysed by HPLC, i.e. sorbitol and 2-deoxysorbitol, were confirmed by a FINNIGAN LTQ + LTQ ORBITRAP LC-MS equipped with two columns in series configuration (Aminex HPX 87-H+Shodex SH1011) using dilute sulfuric acid (5 mM) as the eluent at room temperature.

7.3 Results and discussion

Metal catalysts are divided into three groups based on the reaction products from glucose reduction; i) metals forming sorbitol, as well as some dihydrogen gas (Fe, Co, Ni, Cu, Pd, Au, Ag, and Al), ii) metals forming sorbitol and 2-deoxysorbitol, with very little hydrogen

(Zn, Cd, In, Sn, Sb, Pb, and Bi), and iii) metals forming solely H_2 (Ti, V, Cr, Mn, Zr, Nb, Mo, Hf, Ta, We, Re, Ru, Rh, Ir, and Pt).

7.3.1 Sorbitol forming metals

Figure 1 shows the voltammograms of the glucose-free "blank" solution (dashed line) and 0.1 M glucose (solid line) reduction in 0.1 M Na_2SO_4 alongside the concentration profiles of the reaction product, sorbitol, on (a) Fe, Co, Ni, and Cu, and (b) Pd, Au, Ag, and Al. In general, the increase of cathodic current observed in the blank experiment is attributed to the evolution of H_2 and the solid line represents the formation of both sorbitol from glucose reduction and H_2 evolution. First of all, note that all catalysts in Figure 1 show different onset potential for H_2 evolution from blank scans, which clearly indicates that the formation of chemisorbed hydrogen (M-H, Eq. 1) and molecular H_2 (Eq. 2 and 3) is strongly dependent on the properties of the catalyst. For most metals, the cathodic current in the presence of glucose in solution is smaller compared to the reduction current in the blank, especially at high overpotentials, although the onset potentials are often quite close. From this observation, we can conclude that the presence of glucose inhibits hydrogen evolution, presumably by adsorbing onto the electrode surface. The two exceptions to this rule appear to be gold and especially copper, which exhibit higher cathodic currents in the presence of glucose. These are also the two metal electrodes with the highest sorbitol yield in their potential range of activity. Figure 1a also shows that the cathodic current on Ni increases from ca. -0.25 V, which is the lowest onset potential among all transition metals forming sorbitol, and the maximum concentration of sorbitol is observed at -0.41 V, after which it significantly decreases. This indicates that the optimum ratio between Ni-H and Ni-glucose is at -0.41 V, after which H_2 evolution becomes predominant. Although Raney-typed Ni catalysts are widely applied for heterogeneous hydrogenation reactions in industry, previous reports emphasize that Ni shows hardly any electrocatalytic activity for glucose reduction to sorbitol.[6,7] However, the applied current (> 10 mA cm^{-2}) or potential (< -1 V vs. RHE) in these works will yield only H_2 according to Figure 1a. Therefore, this observation confirms the importance of providing fundamental information correlating voltammetry and product formation. In addition to Ni electrode, Figure 1a shows that sorbitol is formed on Co, Fe, and Cu from -0.51, -0.63, and -0.75 V, and exhibit maximum yields at -1 V or -5 mA cm^{-2} for Co, -0.75 V or -2 mA cm^{-2} for Fe, and -1.3 V or -10 mA cm^{-2} for Cu electrodes, respectively. As mentioned, on a Cu electrode, the cathodic current

with glucose in solution is significantly higher compared to blank, which must be mainly attributed to the formation of sorbitol.

Pd, one of the platinum group metals (Pt, Pd, Rh, Ir, Ru, and Os), adsorbs and also absorbs hydrogen, which changes the shiny surface to a highly porous structure after the cathodic reaction. On Pd, sorbitol is generated from -0.45 V and maximum concentration was observed at -0.87 V with a current density of -7 mA cm^{-2}, after which the concentration of sorbitol decreases (see Figure 1b). The special hydrogenation capacity of Pd, and also Ni, which have also been applied for electrocatalytic hydrogenation of ketone (C=O), aldehyde (CHO), alkene (C=C), and alkyne (C≡C) functionalities using i.e. Raney-type materials or supported nanoparticles,[17] is often ascribed to absorbed hydrogen. Nogerbekov et al.[30] showed that absorbed hydrogen in Pd black is able to carry out chemical hydrogenation of *p*-nitrophenol in 0.1 M NaOH to *p*-aminophenol and Sykes et al.[31] observed subsurface hydrogen atoms in a Pd(111) surface by using low-temperature scanning tunnelling microscopy. Also in heterogeneous catalysis it is well known that Pd-based catalysts selectively hydrogenate the triple bonds of carbon in a mixture of alkynes and alkenes, governed by the population of either hydrogen or carbon on subsurface sites of Pd.[32,33]

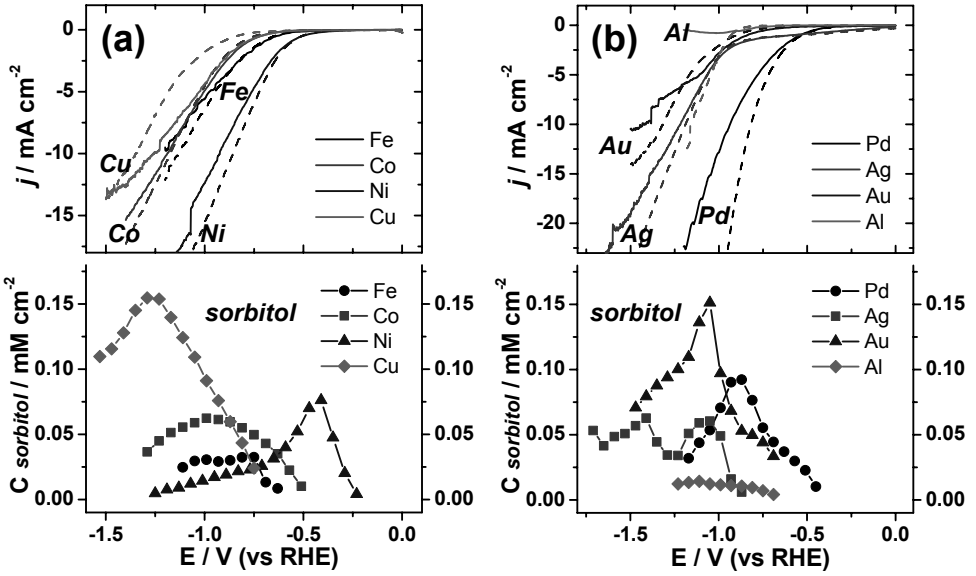

Figure 1. Electrocatalytic glucose (0.1 M) reduction on (a) Fe, Co, Ni, and Cu, and (b) Pd, Ag, Au, and Al in 0.1 M Na_2SO_4. Current density profiles (upper panels) with (solid line) and without (dashed line) glucose in the solution during linear sweep voltammetry with a scan rate of 1 mV s^{-1}, and concentration profiles (lower panels) of corresponding reaction product, sorbitol, as a function of potential.

On Ag, sorbitol is detected from -0.9 V and two maxima in the production of sorbitol were observed at -1.05 V or -3 mA cm^{-2} and -1.41 V or -16 mA cm^{-2}. The potential at which sorbitol appears on Au and Al is -0.69 V, with -1.05 V the optimum potential for sorbitol formation on both metals with current densities of -3 mA cm^{-2} on Au and -3.5 mA cm^{-2} on Al, respectively. Although Al is the only *sp* metal in Figure 1, it shows some, albeit comparatively low, activity for glucose reduction to sorbitol.

As an intermediate conclusion, Ni exhibits the lowest potential, -0.25 V, to form sorbitol. Au and Cu show the highest yield of sorbitol (0.15 mM cm^{-2}) at -1.05 V and -1.3 V, respectively. Concerning the concentrations of sorbitol with corresponding current densities for each metal in Figure 1, we can conclude that each catalyst has an optimum potential or a current density to maximize the yield of sorbitol. Pd and Ni are active hydrogenation

catalysts in heterogeneous catalysis, and also require relatively low overpotentials for maximum sorbitol yield, but this is accompanied by the formation of H_2 at low overpotentials. Therefore, the efficiency of the electrochemical hydrogenation is determined by the competition between the glucose reduction to sorbitol (Eq. 4) and the evolution of hydrogen (Eq. 2 or 3).

7.3.2 Sorbitol and 2-deoxysorbitol forming metals

In contrast to transition *d* metals which produce H_2 and sorbitol during glucose hydrogenation reaction, the post-transition *sp* metals also deoxygenate glucose to 2-deoxysorbitol as shown in Figure 2. Moreover, the higher overpotential or cathodic current applied to post-transition metals results in higher concentration of products in general. This high potential is made possible by the fact that these metals are typically poor hydrogen evolution catalysts. In the rest of this section, we will use the term 'selectivity' as the percentage of sorbitol or 2-deoxysorbitol generated from glucose, regardless of hydrogen generation.

Zn and Cd are included in Figure 2a, as they show similar reactivity as the other post-transition metals, although they are sometimes considered transition metals. Both Zn and Cd form reaction products from -1 V. Interestingly, the concentrations of sorbitol and 2-deoxysorbitol increase continuously as the cathodic potential increases, which is different from the sorbitol formation trend observed with the transition metals, which always show a maximum (Figure1). We note that the cathodic current on Zn is higher than that on Cd, however, the yield of reaction products on Cd is higher than on Zn, which indicates that Cd hydrogenates glucose more efficiently than Zn by suppressing the hydrogen evolution reaction. On Cd, the selectivity to sorbitol is 61±2% vs. 39±2% to 2-deoxysorbitol. On the other hand, 2-deoxysorbitol (65±7%) is the preferred product on Zn vs. 35±7% sorbitol. Even though Zn itself shows lower activity than Cd, adding Zn^{2+} to the solution significantly enhances the current efficiency by enlarging the surface area during electrodeposition or by accelerating the rate of the isomerisation of glucose.[6]

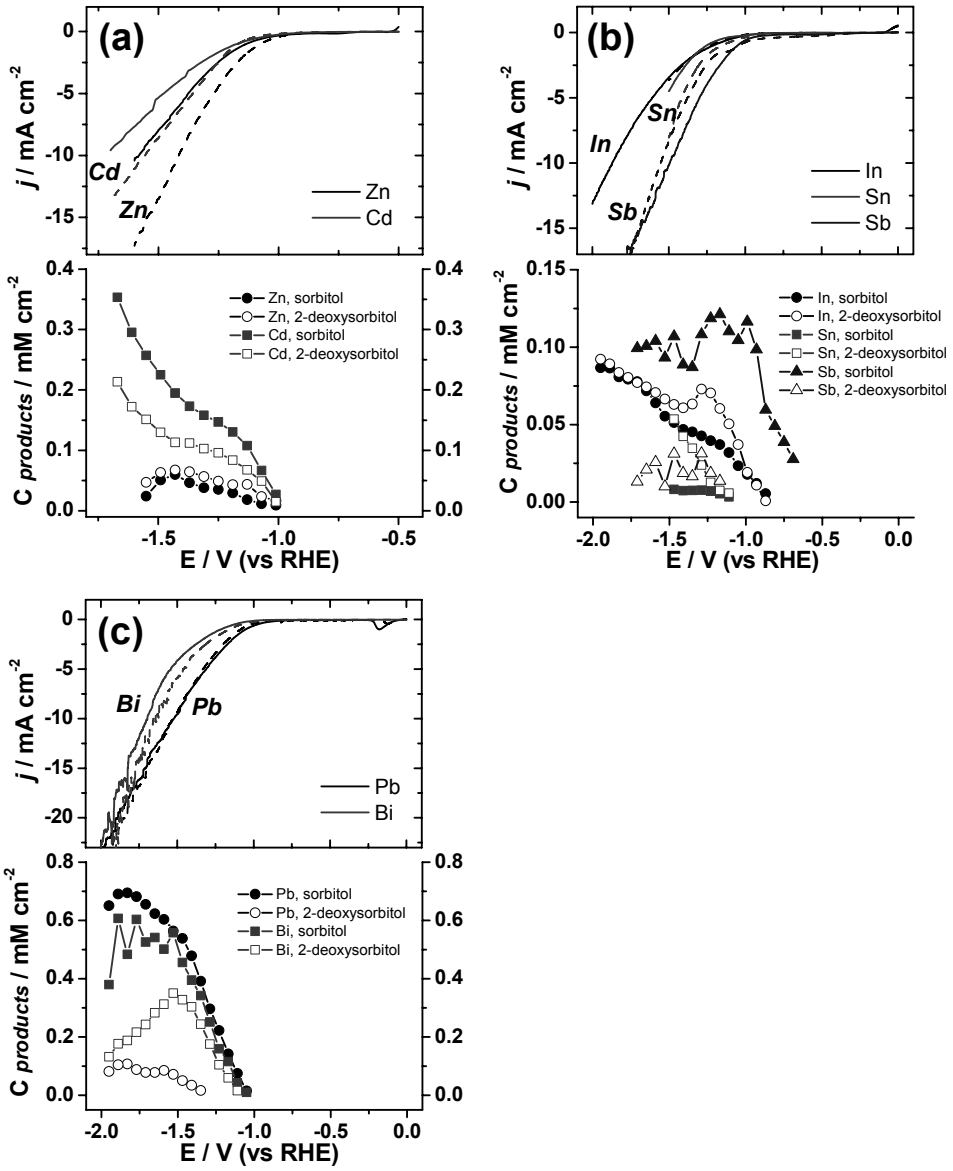

Figure 2. Electrocatalytic glucose (0.1 M) reduction on (a) Zn and Cd, (b) In, Sn, and Sb, and (c) Pb and Bi in 0.1 M Na_2SO_4. Current density profiles with (solid line) and without (dashed line) glucose in the solution during linear sweep voltammetry with a scan rate of 1 mV s^{-1} and concentration profiles of corresponding reaction products, sorbitol and 2-deoxysorbitol, as a function of potential.

The activity of the period 5 metals In, Sn, and Sb for glucose reduction is shown in Figure 2b. Based on current profiles, Sb shows the lowest overpotential and the main product on Sb, sorbitol, is observed from -0.7 V. The concentration of sorbitol on Sb increases until -1 V, after which it fluctuates mainly due to vigorous hydrogen evolution at higher overpotentials (< -1 V). 2-deoxysorbitol on Sb appears from -1.17 V with low selectivity (< 20%) in the entire potential range, thus sorbitol is the dominant hydrogenation product (> 80%) on the Sb electrode. On Sn the collected samples clearly show that sorbitol and 2-deoxysorbitol are generated from -1.1 V to -1.5 V, with 2-deoxysorbitol being the dominant product, although vigorous hydrogen evolution limits sample collection at high cathodic potential ranges. Note that the selectivity of 2-deoxysorbitol on Sn is higher than 90% at -1.5 V, even though the absolute concentration of 2-deoxysorbitol is not that high. On In, sorbitol and 2-deoxysorbitol appear at ca. -0.87 V and their concentrations increase roughly linearly as the cathodic potential increases. Between -1.4 V and -1 V the concentration of 2-deoxysorbitol is higher than that of sorbitol and the highest selectivity (65%) is reached at -1.3 V, whereas for E < -1.5V the selectivities are approximately equal.

Figure 2c shows the results of glucose reduction on Pb and Bi catalysts. Sorbitol is observed as the first reduction product at -1.05 V on both electrodes, although the onset potential on Bi seems to be a bit more negative as compared to Pb. The concentration of sorbitol strongly increases until ca. -1.5 V, after which the sorbitol production slows down, mainly due to the hydrogen evolution reaction, and reaches to the highest concentration yield of 0.7 mM cm^{-2} on Pb at -1.83 V (or -17.5 mA cm^{-2}) and 0.6 mM cm^{-2} on Bi at -1.89 V (or -20 mA cm^{-2}), respectively. Note that the concentration of 2-deoxysorbitol on Bi follows the trend of sorbitol until -1.53 V with a selectivity of ca. 40%, after which it decreases as the cathodic potential increases. On the Pb electrode 2-deoxysorbitol is first observed at -1.35 V and reaches a maximum with ca. 13% selectivity as the cathodic potential increases. This makes Pb the most active and selective catalyst for glucose hydrogenation to sorbitol.

As a general conclusion, poor metals, both post-transition metals ("poor metals") and Zn and Cd, show a high overpotential for the hydrogen evolution reaction, thus leading to a relatively high activity and selectivity toward glucose hydrogenation to sorbitol and 2-deoxysorbitol. The formation of sorbitol is highest on Pb (> 87% selectivity) with high yield (< 0.7 mM cm^{-2}). The Sn electrode has the highest selectivity towards 2-deoxysorbitol

(> 90%) though the overall yield is rather low. Figure 2 does not show a clear trend of reactivity and selectivity of the various surfaces based on their electronic structure. As an important difference to the reactivity of transition metals, the concentration of reaction products on poor metals tends to continuously increase as the cathodic potential increases.

7.3.3 Metals producing only H_2

Non-active catalysts for glucose hydrogenation can be divided into two groups; 1) early transition metals (Ti, V, Cr, Mn, Zr, Nb, Mo, Hf, Ta, We, and Re) as shown in Figure 3a~c and 2) platinum group metals (Ru, Rh, Ir, and Pt) as shown in Figure 3d. Early transition metals require high overpotentials for the hydrogen evolution reaction (dashed line, blank) and the onset potentials are in between -0.8 and -0.5 V (vs. RHE). Although in 0.1 M glucose solution, the current densities near the onset potentials on Ti, V, Cr, Mo, Nb, Mo, Hf, W, and Re are a bit higher than those of the blank, similar to the general trends of sorbitol forming catalysts in Figure 1, we did not observe any trace of sorbitol either due to the inactivity of the catalysts or to the limitation of the HPLC analysis (a concentration of > 1 μM is required). Therefore, we conclude that although a certain minimum applied overpotential is important to obtain hydrogenation products, as shown in Figure 1 and 2, a highly negative potential itself does not automatically imply glucose hydrogenation and needs to be accompanied by a reaction product analysis.

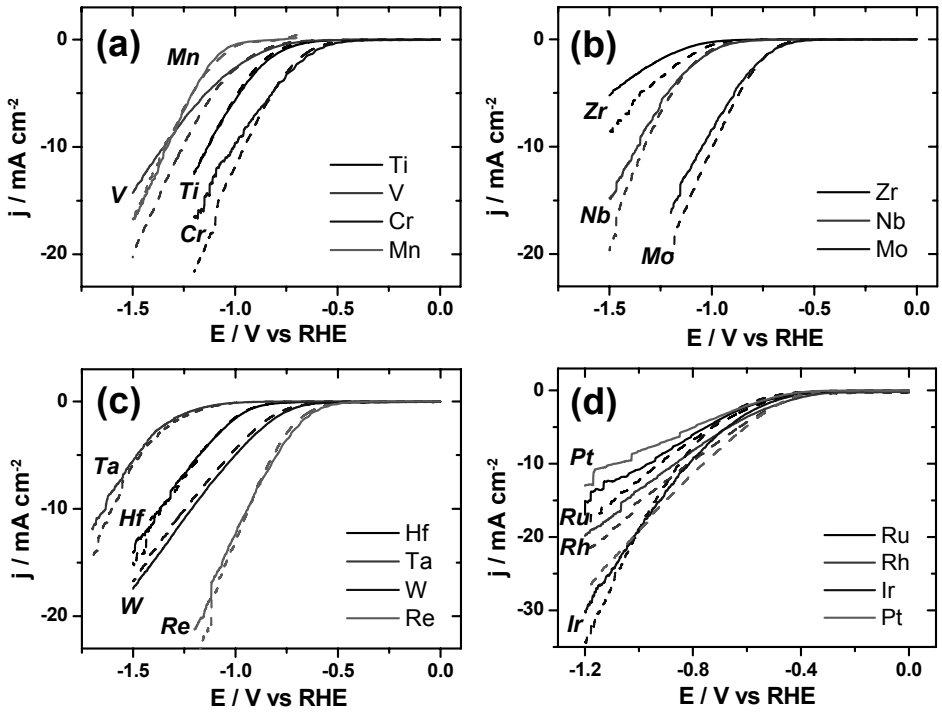

Figure 3. Voltammograms of electrocatalytic glucose reduction (0.1 M) on (a) Ti, V, Cr, and Mn, (b) Zr, Nb, and Mo, (c) Hf, Ta, W, and Re, and (d) Ru, Rh, Ir, and Pt in 0.1 M Na_2SO_4. Current density profiles with (solid line) and without (dashed line) glucose in the solution during linear sweep voltammetry with a scan rate of 1 mV s^{-1}.

In contrast to the early transition metals, the onset potential for hydrogen evolution reaction on platinum group metals is less negative (close to -0.4 V) as shown in Figure 3d. Interestingly, Pt[18,34] and Ru[3,14,18,34,35] are the most well-known active catalysts in the heterogeneous glucose hydrogenation reaction, however there is no evidence in our experiments that glucose is hydrogenated to sorbitol or 2-deoxysorbitol under electrochemical conditions at room temperature. The general hydrogenation mechanism considered in the heterogenous catalysis literature is that the adsorbed hydrogen on active Pt or Ru under high H_2 pressure hydrogenates the C=O bond stabilizing glucose to its hydrogenated alcohol form, i.e. sorbitol.[18,19] The inactivity of Pt and Ru during electrohydrogenation might be due to the fact that the kinetics of hydrogen evolution (H_2,

Eq. 2 or 3) is faster than the hydrogenation reaction (Eq. 4 or 5). However, it is known that e.g. cinnamic acid can be only reduced on platinized, i.e. rough, platinum.[36] In general, the hydrogenation of carbohydrates is carried out on platinized Pt in organic solvents such as methanol.[37]

To investigate the influence of the catalyst surface condition or the number of active sites, the activity of carbon-supported Pt nanoparticles with the identical active surface area (3µg Pt/C loading) compared to smooth Pt for glucose hydrogenation was studied separately, and we could only observe the trace of sorbitol. In order to clarify the influence of the active surface area of the catalyst, a 7 times higher loading of Pt/C (20µg) was also investigated, the results of which are shown in Figure 4.

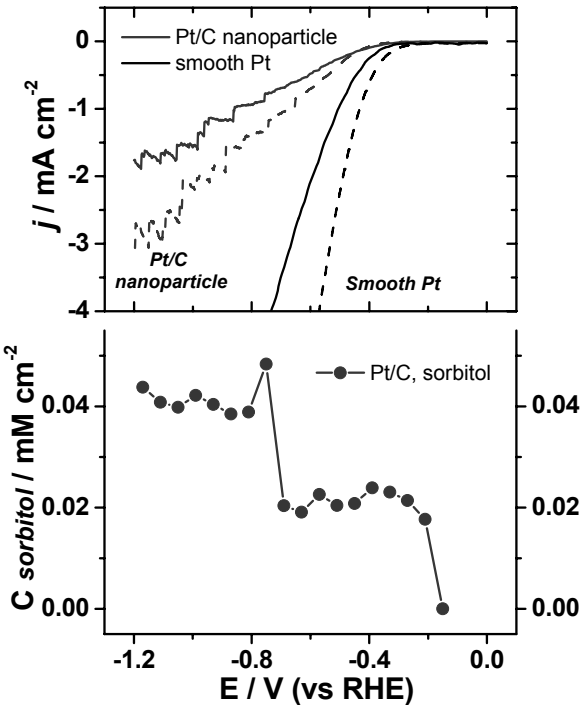

Figure 4. Electrocatalytic glucose (0.1 M) reduction on Pt/C in 0.1 M Na_2SO_4. Current density profiles with (solid line) and without (dashed line) glucose in the solution during linear sweep voltammetry with a scan rate of 1 mV s^{-1} and the concentration profile of sorbitol as a function of potential.

Although the current density on Pt/C with glucose in solution (solid line) is ca. 4 times lower than on smooth Pt (at -0.6 V) due to the loss (ca. 70%) of Pt/C and the formation of hydrogen bubbles which adsorb stronger than on the smooth surface, we can observe the formation of a small but significant amount of sorbitol from -0.21 V. A sudden increase of the concentration of sorbitol was observed from -0.75 V, which was mainy due to the removal of a hydrogen bubble from the catalyst surface. Below -0.75 V, the yield of sorbitol stabilizes to ca. 0.04 mM cm^{-2}. Therefore this observation implies that a large active surface area on Pt is necessary for glucose hydrogenation as well as a roughened catalyst surface in order to generate a measurable amount of sorbitol in our HPLC. Owobi-Andely et al.[9] reported that a Pt-Rh catalyst, which was prepared by calcination after substituting Sn ions for Pt and Rh on the electrode, electroreduces fructose selectively to mannitol (60%) and sorbitol (40%) with a 60% conversion of fructose at -1.25 V (SCE) in a electrocatalytic membrane reactor, which supports our observation, although there is no explicit evidence that the synthesized Pt-Rh catalyst is Sn-free. Apart from metalic catalysts, we tested boron-doped diamond (BDD), a material which shows a high overpotential for water electrolysis but also some electrocatalytic activity toward nitrate reduction,[38] for glucose hydrogenation. However, BDD does not generate sorbitol or 2-deoxysorbitol in spite of the negative onset potential of -1.2 V (RHE) for hydrogen evolution, which clearly emphasizes again that the feasibility of glucose hydrogenation is mainly determined by the nature of catalyst, and much less by the applied overpotential.

Based on the reactivities of the catalysts as reported above, the potential ranges for formation of sorbitol and/or 2-deoxysorbitol as well as hydrogen evolution are summarized in the Periodic Table in Figure 5. The metals forming only hydrogen shown in Figure 3 are the early transition metals with overpotentials of between -1.0 and -0.5 V, and the Pt group metals with hydrogen evolution potentials higher than -0.5 V. The other transition metals shown in Figure 1 hydrogenate glucose to sorbitol with low cathodic potentials (> -0.5 V) on Ni and Pd, and intermediate overpotentials (-1 V to -0.5 V) on Fe, Co, Cu, Ag, and Au catalysts. Post-transition metals (*sp* orbital) including Zn and Cd (*d* orbital) as shown in Figure 2 generate sorbitol and 2-deoxysorbitol in combination with suppressing the hydrogen evolution reaction resulting in a high overpotential (< -1 V).

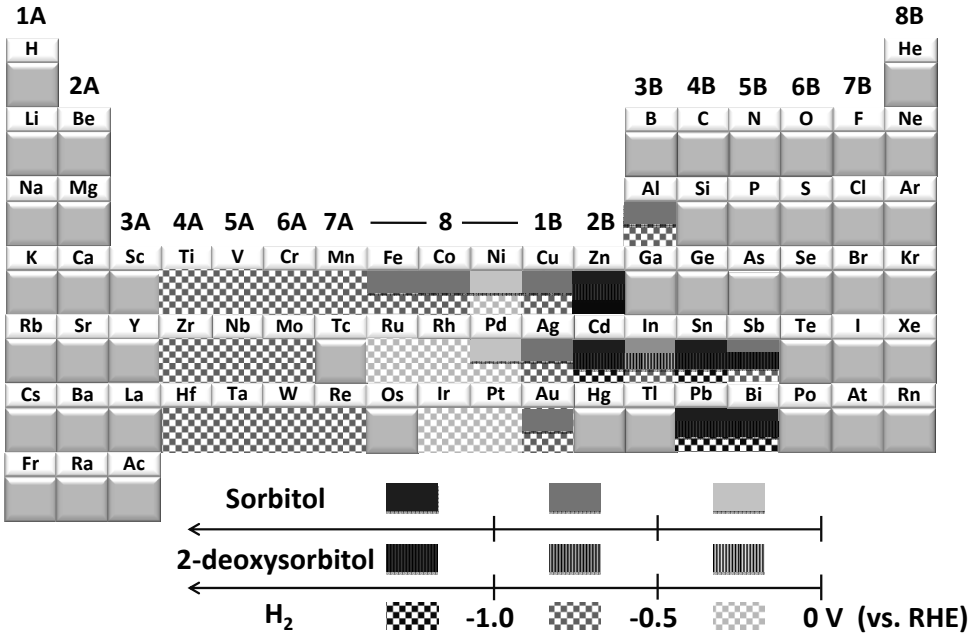

Figure 5. Periodic Table showing the trends of catalysts for hydrogen evolution and the glucose reduction of sorbitol and 2-deoxysorbitol at ambient operating conditions in 0.1 M Na_2SO_4.

7.3.4 A mechanistic view of glucose reduction

From the relationship between voltammetry and reaction product analysis under identical experimental conditions as shown in Figure 1~4, we could clearly show that the electrocatalyst plays a crucial role in glucose hydrogenation. In addition, pH changes on electrode surface during electrolysis should be considered. These aspects were also emphasized recently for the electrochemical oxidation of hydroxymethylfurfural.[39] The pH on electrode surface increases during hydrogen adsorption (Eq. 1) and especially during hydrogen evolution (Eq. 2) due to the generation of OH^-, leading to a deviation of the interfacial pH from the pH of the bulk solution (0.1 M Na_2SO_4). The rate of generated OH^- is determined by cathodic current. The effect of the high pH near the electrode surface is that the cyclic (inactive) form of glucose easily changes to the linear (electroactive) form, which is considered as a rate-determining step.[4,6,20] However, long-time electrolysis would increase the pH in the bulk solution, which generates base-catalyzed by-products, i.e. fructose and mannose as isomers of glucose, and poly-ols, i.e. mannitol, reduced from

mannose or fructose.[9,20] Unsurprisingly, we could observe a trace of fructose, an isomer of glucose at high cathodic current in all experiments, even though the collected samples ranging in pH from 7 to 10 were immediately neutralized by adding 10 mM phosphate buffer solution. To probe the effect of a high pH on glucose isomerization to fructose or mannose, we investigated the time-dependent degradation of glucose by adding 10 mM glucose in 0.1 M NaOH under O_2-free conditions, which clearly showed that ca. 5% of glucose was converted to fructose in an hour, but not to mannose. Based on this observation, we believe that the trace of fructose derives from isomerization of glucose by the increase of pH on the electrode surface during water electrolysis. Therefore the formation of 2-deoxysorbitol on *sp* metals, which Nobe et al. believed to be formed from fructose as the ketone group is in the 2-position,[4] can be generated through the base-catalyzed process of forming the 'enediol' as an intermediate species, which can subsequently be transformed to fructose as shown in Figure 6. However, we must emphasize that postulating fructose as the precursor to 2-deoxysorbitol is an assumption. Our recent work on the dehydrogenation of 2-carbon atom oxygenates showed that the C-O bond prefers to break in a C-OH group next to a C=O group.[25] If this holds for glucose as well, glucose itself would be the precursor to 2-deoxysorbitol. In addition, the absence of mannitol, an isomer of sorbitol, in the product spectra supports the model of deoxygenation from glucose since the chiral carbon (ketone-C in fructose) is hydrogenated in general into two isomeric alcohols with similar ratio (sorbitol 40% and mannitol 60%), as demonstrated by Owoby-Andely et al.[9] We also emphasize that the formation of 2-deoxysorbitol, is an electrocatalytic reaction that occurs only on *sp* metals, for reasons that remain to be understood. The existence of OH^- near electrode surface is a necessary but not sufficient condition since the hydrogenation reaction is catalyst dependent. Importantly, acidic pH (0.5 M H_2SO_4) does not lead to glucose hydrogenation even on catalysts such as Pb, Co, and Cd, which are active in neutral media. Metals such as Ti and Ru that are not active in neutral media also remain inactive in acidic media. Therefore the presence of OH^- is a necessary factor in electrocatalytic glucose hydrogenation, but bulk alkalinity is unfavorable as it generates too many side products. This explains the importance of working in unbuffered neutral media.

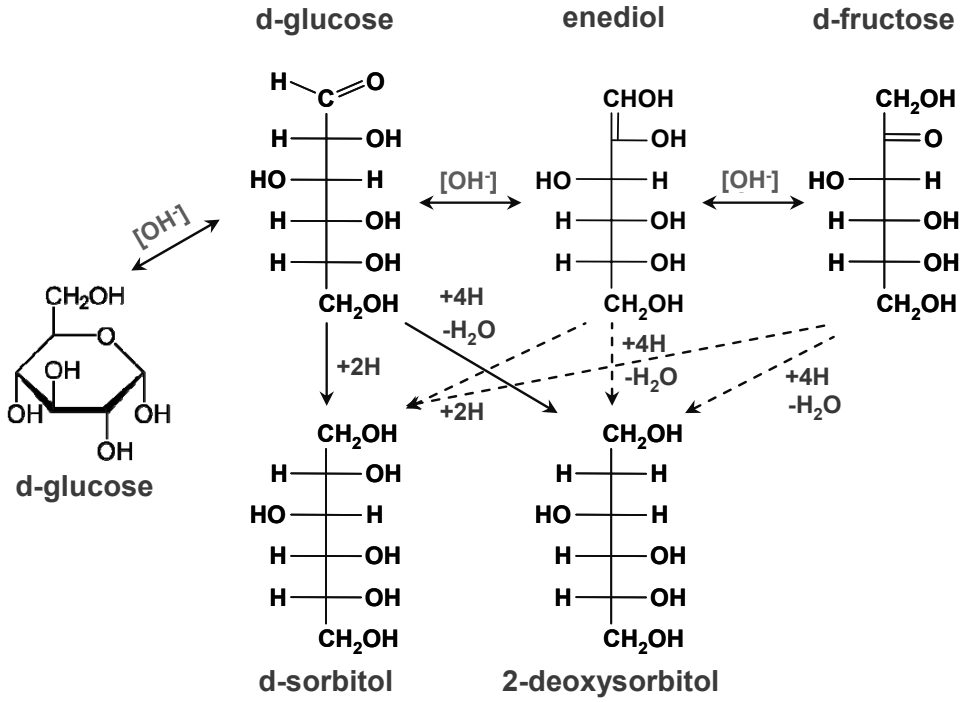

Figure 6. Suggested reaction pathways for glucose hydrogenation and deoxygenation. Solid lines/arrows are the suggested pathways, but the pathways indicated by the dashed arrows cannot be excluded.

7.4 Conclusions

This chapter has described the electochemical glucose hydrogenation to sorbitol and deoxygenation to 2-deoxysorbitol on solid monometallic electrodes in neutral solution. We studied the activity and selectivity of the catalysts for glucose hydrogenation by correlating the voltammetric scan with online product analysis using high-performance liquid chromatography (HPLC), which provides qualitative and quantitative information of sorbitol or 2-deoxysorbitol formation as a function of potential. Three groups of catalysts regarding to reaction products are distinguished from this study. Hydrogen is the only product on early transition metals (Ti, V, Cr, Mn, Zr, Nb, Mo, Hf, Ta, We, and Re) and platinum group metals (Ru, Rh, Ir, and Pt). Sorbitol and hydrogen are formed on late

transition metals (Fe, Co, Ni, Cu, Pd, Au, and Ag) and Al (*sp* metal). Sorbitol and 2-deoxysorbitol, with a high overpotential for hydrogen evolution, are formed on post-transition metals (In, Sn, Sb, Pb, and Bi) as well as on Zn and Cd (officially *d* metals). Among the late transition d metals, the lowest overpotential to form sorbitol is observed on Ni, sorbitol formation starting from -0.25 V, and Au and Cu show the highest yield of sorbitol (0.15 mM cm^{-2}) at potentials of -1.05 and -1.3 V, respectively. On poor (*sp*) metals, the formation of sorbitol is predominant, with Pb having the highest selectivity (> 87%) and high yield (< 0.7 mM cm^{-2}). Interestingly, the highest selectivity for 2-deoxysorbitol (> 90%) was observed on a Sn electrode with high overpotential (-1.5 V). Even though Pt and Ru are considered the most active catalysts for glucose hydrogenation under heterogeneous catalysis conditions (i.e. under hydrogen pressure and at higher temperature), smooth Pt and Ru electrodes do not show any hydrogenation activity under room-temperature electrochemical conditions. However on a Pt/C nanoparticle electrode with a high active surface area, the formation of sorbitol was observed from -0.21 V, albeit with low activity, suggesting that Pt does show some activity for glucose hydrogenation, either due to the specific surface sites on Pt nanoparticles or simply due to the higher catalytic surface area. From the mechanistic point of view, we believe that 2-deoxysorbitol is generated from glucose hydrogenation followed by a subsequent dehydration (or vice versa) on catalytically active post-transition metals, although we can not exclude the formation of 2-deoxysorbitol from fructose (as originally suggested by Nobe et al.[4]) since electro-generated OH^- on the catalyst surface during water electrolysis isomerise glucose to fructose *via* the endiol intermediate. Based on these observations, we conclude that the yield or selectivity of hydrogenated products is mainly catalyst dependent combined with a minimum applied potential or current and suitable local pH conditions. In combination with the ability of potential-controlled electrolysis on anode, as recently demonstrated for the cellobiose hydrolysis to glucose,[40] it may be possible to use the current work to achieve one-pot electrosynthesis of sorbitol from cellobiose or cellulose.

7.5 References

[1] G. W. Huber, S. Iborra, A. Corma, *Chem. Rev.* **2006**, *106*, 4044-4098.

[2] A. Corma, S. Iborra, A. Velty, *Chem. Rev.* **2007**, *107*, 2411-2502.

[3] P. Gallezot, P. J. Cerino, B. Blanc, G. Fleche, P. Fuertes, *J. Catal.* **1994**, *146*, 93-102.

[4] K. Park, P. N. Pintauro, M. M. Baizer, K. Nobe, *J. Electrochem. Soc.* **1985**, *132*, 1850-1855.

[5] J. C. Yu, M. M. Baizer, K. Nobe, *J. Electrochem. Soc.* **1988**, *135*, 1400-1406.

[6] A. Binkassim, C. L. Rice, A. T. Kuhn, *J. Appl. Electrochem.* **1981**, *11*, 261-267.

[7] C. L. R. Annvar Bin Kassim, Anselm T. Kuhn, *J. Chem. Soc., Faraday Trans.* **1981**, *77*, 683-695.

[8] S. G. Chen, T. Wen, J. H. P. Utley, *J. Appl. Electrochem.* **1992**, *22*, 43-47.

[9] Y. Owobi-Andely, K. Fiaty, P. Laurent, C. Bardot, *Catal. Tod*ay **2000**, *56*, 173-178.

[10] A.T.Kuhn in *Industrial Electrochemical Processes*, Elsevier, Amsterdam, 1971.

[11] H. Li, H. X. Li, J. F. Deng, *Catal. Today* **2002**, *74*, 53-63.

[12] H. X. Li, W. J. Wang, J. F. Deng, *J. Catal.* **2000**, *191*, 257-260.

[13] N. Dechamp, A. Gamez, A. Perrard, P. Gallezot, *Catal. Today* **1995**, *24*, 29-34.

[14] B. Kusserow, S. Schimpf, P. Claus, *Adv. Synth. Catal.* **2003**, *345*, A102-A102.

[15] P. Gallezot, N. Nicolaus, G. Fleche, P. Fuertes, A. Perrard, *J. Catal.* **1998**, *180*, 51-55.

[16] B. J. Arena, *Appl. Catal. A-Gen.* **1992**, *87*, 219-229.

[17] J. M. Chapuzet, A. Lasia, J. Lessard, in Electrocatalysis, ed. J. Lipkowski, P. N. Ross, Wiley-VCH, New York, **1998**, pp. 155-196.

[18] A. Fukuoka, P. L. Dhepe, *Angew. Chem. Int. Ed.* **2006**, *45*, 5161-5163.

[19] H. Kobayashi, Y. Ito, T. Komanoya, Y. Hosaka, P. L. Dhepe, K. Kasai, K. Hara, A. Fukuoka, *Green Chem.* **2011**, *13*, 326-333.

[20] P. N. Pintauro, D. K. Johnson, K. Park, M. M. Baizer, K. Nobe, *J. Appl. Electrochem.* **1984**, *14*, 209-220.

[21] Y. Kwon, M. T. M. Koper, *Anal. Chem.* **2010**, *82*, 5420-5424.

[22] A. Santasalo-Aarnio, Y. Kwon, E. Ahlberg, K. Kontturi, T. Kallio, M. T. M. Koper, *Electrochem. Commun.* **2011**, *13*, 466-469.

[23] Y. Kwon, Y. Birdja, I. Spanos, P. Rodriguez, M. T. M. Koper, *ACS Catal.* **2012**, *2*, 759-764.

[24] Y. Kwon, K. J. P. Schouten, M. T. M. Koper, *ChemCatChem* **2011**, *3*, 1176-1185.

[25] K. J. P. Schouten, Y. Kwon, C. J. M. van der Ham, Z. Qin, M. T. M. Koper, *Chem. Sci.* **2011**, *2*, 1902-1909.

[26] P. Rodriguez, Y. Kwon, M. T. M. Koper, *Nat. Chem.* **2012**, *4*, 177-182.

[27] S. C. S. Lai, M. T. M. Koper, *Faraday Discuss.* **2008**, *140*, 399-416.

[28] F. Koleli, T. Atilan, N. Palamut, A. M. Gizir, R. Aydin, C. H. Hamann, *J. Appl. Electrochem.* **2003**, *33*, 447-450.

[29] F. Koleli, D. Balun, *Appl. Catal. A-Gen.* **2004**, *274*, 237-242.

[30] B. Yu. Nogerbekov, N. N. Gudeleva, N. V. Kobets, Zhur. Prikl. Khim., **1989**, 62, 2275.

[31] E. C. H. Sykes, L. C. Fernandez-Torres, S. U. Nanayakkara, B. A. Mantooth, R. M. Nevin, P. S. Weiss, *Proc. Nat. Acad. Sci. U.S.A.* **2005**, *102*, 17907-17911.

[32] D. Teschner, J. Borsodi, A. Wootsch, Z. Revay, M. Haevecker, A. Knop-Gericke, S. D. Jackson, R. Schloegl, *Science* **2008**, *320*, 86-89.

[33] D. Teschner, Z. Revay, J. Borsodi, M. Haevecker, A. Knop-Gericke, R. Schloegl, D. Milroy, S. D. Jackson, D. Torres, P. Sautet, *Angew. Chem. Int. Ed.* **2008**, *47*, 9274-9278.

[34] A. W. Heinen, J. A. Peters, H. van Bekkum, *Carbohydr. Res.* **2000**, *328*, 449-457.

[35] K. van Gorp, E. Boerman, C. V. Cavenaghi, P. H. Berben, *Catal. Today* **1999**, *52*, 349-361.

[36] T. H. S. Ono, *Bull. Chem. Soc. Japan* **1953**, *26*, 11.

[37] M. A. Casadei, D. Pletcher, *Electrochim. Acta* **1988**, *33*, 117-120.

[38] J. T. Matsushima, W. M. Silva, A. F. Azevedo, M. R. Baldan, N. G. Ferreira, *Appl. Surf. Sci.* **2009**, *256*, 757-762.

[39] K. R. Vuyyuru, P. Strasser, *Catal. Tod.* **2012**, *195*, 144-154.

[40] Y. Kwon, S. E. F. Kleijn, K. J. P. Schouten, M. T. M. Koper, *ChemSusChem* **2012**, *5*, 1935-1943.

8

Electrocatalytic hydrogenation of 5-hydroxymethylfurfural in the absence and presence of glucose

Abstract

This chapter addresses the electrocatalytic hydrogenation of 5-hydroxymethylfurfural (HMF) to 2,5-dihydroxymethylfuran (DHMF) or other species, such as 2,5-dimethylfuran, on solid metal electrodes in neutral media, both in the absence and presence of glucose. The reaction is studied by combining voltammetry with online product analysis by high-performance liquid chromatography, which provides both qualitative and quantitative information of the reaction products as a function of electrode potential. Three groups of catalysts show different selectivity towards: (1) DHMF (Fe, Ni, Ag, Zn, Cd, and In), (2) DHMF and other products (Pd, Al, Bi, and Pb), depending on the applied potential, and (3) other products (Co, Au, Cu, Sn, and Sb) involving HMF hydrogenolysis. The rate of electrocatalytic HMF hydrogenation is not strongly catalyst dependent since all catalysts show similar onset potentials (-0.5 ± 0.1 V) in the presence of HMF. However the intrinsic property of the catalysts determines the reaction pathway towards DHMF or other products. Ag showed highest activity towards DHMF formation (max. 13.1 mM cm^{-2} with high selectivity > 85%). HMF hydrogenation is faster than glucose hydrogenation on all metals. For transition metals, the presence of glucose enhances the formation of DHMF and suppresses the hydrogenolysis of HMF. On poor metals, glucose enhances the DHMF formation on Zn, Cd, and In, however, its contribution to Bi, Pb, Sn, and Sb is limited. Remarkably, in the presence of HMF, glucose hydrogenation itself is largely suppressed or even absent. The first electron transfer step of HMF reduction is not metal dependent suggesting a non-catalytic reaction with proton transfer directly from water in the electrolyte.

The contents of this chapter have been published: Y. Kwon, E. de Jong, S. Raoufmoghaddam, M. T. M. Koper, *ChemSusChem*, **2013**, DOI: 10.1002/cssc.201300443.

8.1 Introduction

Catalytic conversion of biomass to fuels and chemicals has attracted great attention as one of the future technologies for mitigating global warming and for building up a carbon-neutral energy cycle.[1, 2] 5-hydroxymethylfurfural (HMF), one of the novel biomass-derived platform chemicals, has potential as an alternative commodity chemical for fossil fuel-based platform chemicals.[3, 4] The chemistry, production processes and potential applications of HMF have recently been reviewed.[4] HMF has been produced from fructose in water, in organic solvents (DMSO),[5] and in a biphasic system (water-MIBK)[6] and in ionic liquids[7-10] using acid catalysts (i.e. HCl, H_2SO_4),[11] solid acids (zeolite,[6] ion exchange resins[12]), and salts ($LaCl_3$, $CrCl_2$)[13, 14]. Recently, HMF was obtained in high yields not only from fructose but also from glucose via isomerization to fructose, as well as directly from cellulose.[15-17]

HMF has two functionalities (-OH, -C=O) attached to a furan ring and it can be converted into several value-added compounds through oxidation and reduction. The oxidative products of HMF are 2,5-furandicarbaldehyde (FDC) and 2,5-furandicarboxylic acid (FDCA), which are excellent candidates for monomers of biomass derived polymeric materials.[18, 19] 2-formyl-5-furancarboxylic acid (FFCA) is also an intermediate species during HMF oxidation and it can be further oxidized to FDCA, a potential replacement for the fossil fuel-based platform chemical terephthalic acid.[20] For the oxidation of HMF, Strasser et al.[21] reported 100% conversion of HMF to DFCA with 80% selectivity using Pt/C at mild temperature (50^{o}C) and pressure (10 bar O_2), in comparison the with electrochemical oxidation of HMF to FDC (18%) on a Pt electrode. The hydrogenation of the formyl group or the furan ring on HMF to 2,5-dihydroxymethylfuran (DHMF) or di-hydroxy-methyl-tetrahydrofuran (DHMTHF) has been studied using heterogeneous catalysts based on Ni, Cu, Pt, Pd, and Ru[22] or bimetallic catalysts (i.e. Ni-Pd)[23]. DHMF is used in a broad field of applications such as resins, polymers, and artificial fibers, as well as an intermediate in the synthesis of drugs.[3] DHMTHF is a useful chemical with applications as solvent,[24] monomer,[18] or as a precursor to the production of other high-value chemicals.[25] The hydrogenation of the hydroxyl group on HMF leads to the formation of 2,5-dimethylfuran (DMF), which is of particular interest due to its high energy content and potential use as a biofuel.[26] DMF can be obtained on CuRu/C[26, 27] catalysts with high yield (76-79%). Although a large number of papers related to HMF

hydrogenation has been published, the hydrogenation of HMF using electrochemical methods has not yet been explored.

Recently, we studied the electocatalytic glucose hydrogenation in neutral media on a large number of pure solid metal electrodes from across the Periodic Table and successfully demonstrated the activity and selectivity of the various catalysts by correlating the voltammetry and product analysis with online high-performance liquid chromatography (HPLC).[28] Three groups of catalysts regarding reaction products could be distinguished: 1) hydrogen formation on early transition metals (Ti, V, Cr, Mn, Zr, Nb, Mo, Hf, Ta, We, and Re) and platinum group metals (Ru, Rh, Ir, and Pt), 2) sorbitol formation on late transition metals (Fe, Co, Ni, Cu, Pd, Au, and Ag) and Al (*sp* metal), and 3) sorbitol and 2-deoxysorbitol formation on post-transition metals (In, Sn, Sb, Pb, and Bi) as well as Zn and Cd (*d* metals). As HMF is a product of subsequent glucose dehydration during acid-catalysed cellulose hydrolysis,[29] there is a need to understand the effect of the presence of glucose on the hydrogenation of HMF and vice versa.

In this chapter, we investigated the electocatalytic HMF hydrogenation to DHMF and other products (i.e. 5-methylfurfural, 2,5-dimethylfuran, 2,5-dimethyl-2,3-dihydrofuran) in the absence and the presence of glucose on a large number of pure solid metal electrodes, which are all active for glucose hydrogenation, aiming at understanding the activity and selectivity of catalysts by correlating the voltammetry and online product analysis. Reaction products are determined both quantitatively and qualitatively by using a combination of voltammetry and online high-performance liquid chromatography (HPLC).[28-35] Finally, a general mechanism for electrocatalytic hydrogenation of HMF and the effect of the presence of glucose are discussed based on the observed activity and selectivity profiles during electrolysis.

8.2 Experimental

8.2.1 Electrochemical procedures

All measurements were carried out in a conventional single compartment three-electrode glass cell, which was cleaned by employing a standard procedure[36] for removing traces of

organic and inorganic contaminants. Oxygen was removed by bubbling argon through the solution prior to the voltammetric experiments. Transition and post-transition metals (≥99.5%) used as working electrodes in the experiment were polycrystalline wires/ rods/plates, which were mechanically polished with alumina (up to 0.05 μm) and cleaned ultrasonically in pure water (MilliQ gradient A10 system, 18.2 MΩ) followed by electropolishing by cycling 3 times between -2 and 0 V (vs. RHE) in 0.1 M Na_2SO_4 solution in order to remove surface impurities and oxide before use.[28] The surface area (cm^2) of the catalysts used to calculate the current density and concentration yield of reaction products (mM cm^{-2}) was obtained based on geometric area except for Pt electrode for which we considered the electrochemically active surface area by the hydrogen desorption charge in 0.5 M H_2SO_4. In all experiments, a large gold coil was used as a counter electrode while a reversible hydrogen electrode (RHE) was employed as a reference electrode. HMF (50 mM, Sigma-Aldrich), HMF (10 mM) and Glucose (0.1 M, Merck) were dissolved into a solution of 0.1 M Na_2SO_4 (Merck, pH 7). Electrochemical cell potentials were controlled with a potentiostat/galvanostat (μ-Autolab Type III). All experiments were carried out at room temperature.

8.2.2 Fraction collection and product analysis

For the detection of intermediates and products by HPLC, samples of the electrolyte solution were collected with a small Teflon tip (inner diameter, 0.38 mm) positioned close (10 μm) to the center of the electrode surface, the tip being connected to a PEEK capillary with inner/outer diameters of 0.13/1.59 mm.[30] The tip was cleaned in a solution of 0.2 M $K_2Cr_2O_7$ and rinsed thoroughly with ultrapure water before use. The sample volume collected in each well was 60 μl on a 96-well microtiter plate (270 μl/well, Screening Devices b.v.) using an automatic fraction collector (FRC-10A, Shimadzu). The flow rate of sample collection was adjusted to 60 ml min^{-1} with a Shimadzu pump (LC-20AT). Collected samples were immediately neutralized by adding 60 μl of 10 mM phosphate buffer. After collecting samples, the microtiter plate was covered by a silicon mat to prevent the evaporation of collected samples.

Samples collected during voltammetry were analysed using a Shimadzu Prominence HPLC. The microtiter plate with the collected samples was placed in an autosampler (SIL-20A) holder, and 30 μl of sample was injected into the column. The column (Shodex SP0810) for

the analysis used pure water as the eluent. The temperature of the column was maintained at 30°C for the mixture of HMF and glucose and at 50°C for HMF, respectively, in an oven (CTO-20A). The separated compounds were detected with a refractive index detector (RID-10A). The concentrations of DHMF and other products are obtained by using a Shodex SP0810 column and the detailed compositions of other products were confirmed by an Agilent Technologies 7820A + 5975 MSD GC-MS.

8.3 Results and discussion

In order to simplify the description of the product distribution, we use the term 'DHMF' for 2,5-dihydroxymethylfuran, which is the hydrogenation product of 'C=O' in HMF, and the term 'others' for the mixture of hydrogenolysis products (i.e. 5-methylfurfural, 2,5-dimethylfuran, 2,5-dimethyl-2,3-dihydrofuran) generated through the cleavage of the '-OH' functionality in HMF as shown in Scheme 1. The lump-sum of 'others' was obtained from the HPLC analysis whereas GC-MS identified each species. The details of hydrogenation pathways will be described later in Figure 6.

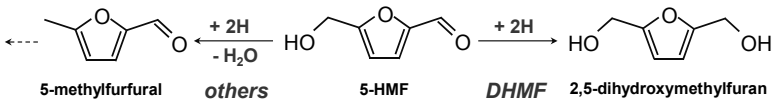

Scheme 1. HMF hydrogenation and dehydration pathways.

The metal catalysts studied are divided into three groups based on the dominant reaction products from HMF reduction in the absence of glucose; i) metals mainly forming DHMF (Fe, Ni, Ag, Zn, Cd, and In), ii) metals forming DHMF and others depending on the applied potential (Pd, Al, Bi, and Pb), and iii) metals forming mainly other products (Co, Au, Cu, Sn, and Sb). The same catalysts are compared for the reduction of a mixture of HMF and glucose. In the following sections, the term 'selectivity' is the percentage of the total of the reaction products from HMF i.e. DHMF, others, sorbitol or 2-deoxysorbitol, not taking into account hydrogen generation. The current density (mA cm^{-2}) and concentration yield of reaction products (mM cm^{-2}) to compare the catalytic activity were obtained based on geometric area of catalyst.

8.3.1 HMF reduction in the absence of glucose

Figure 1 shows the voltammograms of the HMF-free "blank" solution (dashed line) and of a solution containing 50 mM HMF (solid line) in 0.1 M Na_2SO_4 alongside the concentration profiles of the reaction products, DHMF and others, on (a) Fe, Ni, and Ag, (b) Pd and Al, and (c) Co, Au, and Cu. The cathodic current observed in the blank experiment (dashed line) is attributed to the evolution of H_2 and the solid line represents the formation of DHMF and other products from HMF reduction, as well as H_2 from hydrogen evolution reaction (HER). First of all, note that all transition metals in Figure 1 show different onset potentials for H_2 evolution in the blank scans within the potential ranges from -1 V to -0.4 V, which is consistent with our previous study.[28] For all metals, the onset potential in the presence of HMF in solution is the same or more positive compared to the blank. In the presence of HMF, the cathodic currents at high overpotentials are lower than those from blank scans, presumably due to HMF adsorption onto the electrode surface. Periodic spikes visible in the voltammograms with HMF on Cu and Ag are due to the irregularities in the pumping flow rate during fraction collection.[30] Although each metal shows a different catalytic activity, we observe certain trends in product distribution. According to the dominant reaction products, the transition metals are divided into three groups. The metals in Figure 1a show a higher activity towards DHMF formation than to other products over the entire potential range, whilst the metals in Figure 1c prefers to generate other products through hydrogenolysis of HMF over the production of DHMF. The metals in Figure 1b alternate their activity to DHMF and others depending on the applied potential.

Although Fe, Ni, and Ag show different onset potentials in the blank scans in Figure 1a, we note that in the presence of HMF, DHMF is generated from the same potential of ca. -0.4 V on each electrode. The maximum production of DHMF on these catalysts is observed at the potential of ca. -0.8 V. At higher potential H_2 evolution is dominant. On Fe, the other hydrogenolysis products are observed from -0.63 V and their concentrations increase as the cathodic potential increases. Therefore the selectivity of DHMF on Fe decreases from 100% at the onset potential to ca. 50% at -1.5 V. Ni shows the most positive onset potential in the blank and the highest current with HMF in solution. However the activity of Ni towards HMF hydrogenation is lower than that of Fe and Ag. The maximum concentration of DHMF on Ni is observed at -0.75 V whereas the other products on Ni are generated from -0.69 V and their concentrations increase gradually as the cathodic potential increases,

leading to a comparable selectivity towards DHMF and others at -1.5 V. Interestingly, the current density on Ag in the presence of HMF in solution is higher than that of blank from the onset potential until -1.3 V. The enhanced current is mainly due to the generation of DHMF since Ag shows the highest activity towards DHMF formation of all metal electrodes. The maximum concentration of DHMF on Ag is 13.1 mM cm^{-2} at -0.81 V. The selectivity of DHMF on Ag is higher than 85% at all potentials.

In Figure 1b, it is shown how Pd and Al alternate their selectivity towards DHMF and other products depending on the applied potential. Although the onset potential of each metal seems very different in the voltammetry, both electrodes generate DHMF from the same potential of -0.57 V. These electrodes show selectivity towards DHMF formation until ca. -0.9 V, below which potential the formation of other products becomes dominant.

As shown in Figure 1c, Co, Au, and Cu preferentially reduce HMF through hydrogenolysis. Cu is the most active electrode material for HMF hydrogenolysis, even though it exhibits the lowest overall reduction current. Co and Au show similar activity and selectivity to DHMF and other hydrogenolysis products.

From the above results, we conclude that the hydrogenation of HMF is not strongly catalyst dependent since all catalysts show almost identical onset potentials (-0.5 ± 0.1 V). However, the catalysts differ in their reaction pathways towards DHMF or other products. Compared to the glucose hydrogenation activity on transition metals, the maximum concentration of sorbitol was achieved on Au and Cu (ca. 0.15 mM cm^{-2} with 0.1 M glucose),[28] showing that HMF hydrogenation to DHMF and other products is at least an order of magnitude more active than glucose hydrogenation to sorbitol.

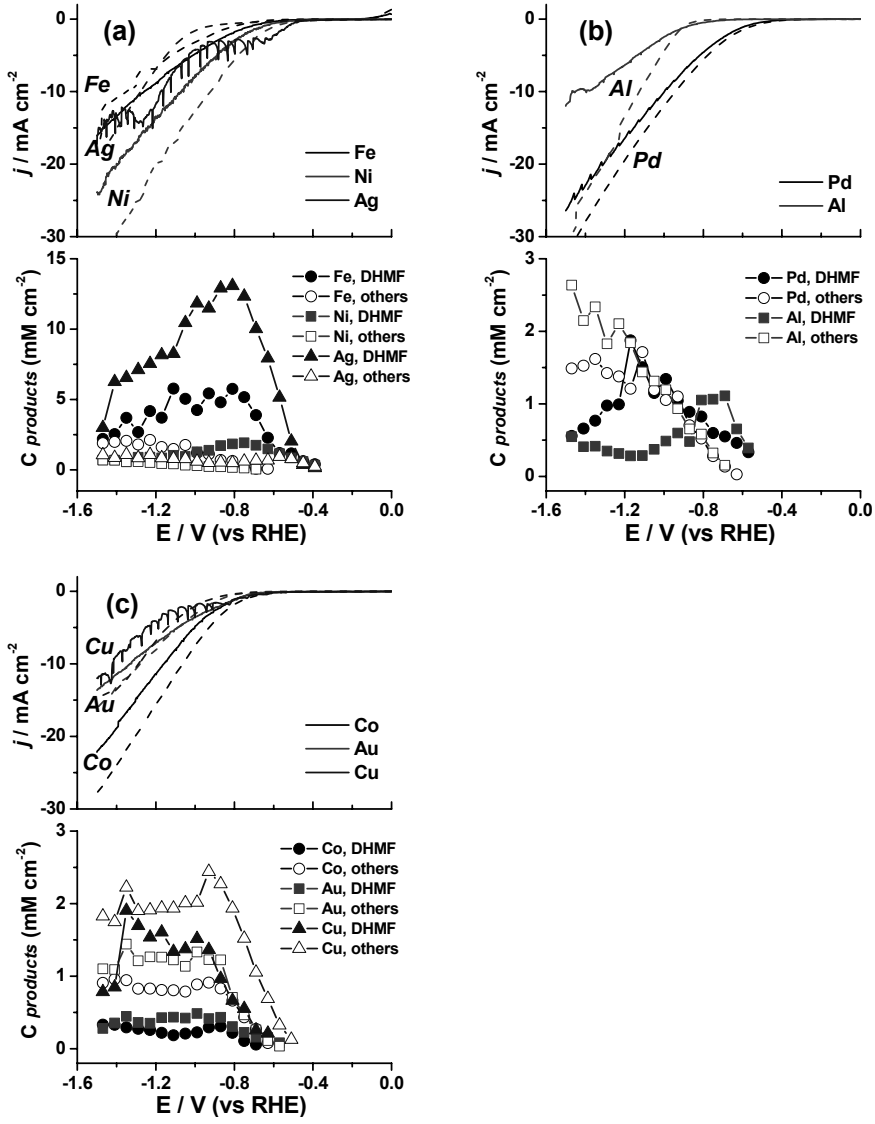

Figure 1. Electrocatalytic HMF (50 mM) reduction on Fe, Ni, and Ag, (b) Pd and Al, and (c) Co, Au, and Cu in 0.1 M Na_2SO_4. Current density profiles (upper panels) with (solid line) and without (dashed line) HMF in the solution during linear sweep voltammetry with a scan rate of 1 mV s^{-1}, and concentration profiles (lower panels) of corresponding reaction products, DHMF and others, as a function of potential.

The activity and selectivity of the post-transition *sp* metals (including Zn and Cd) are shown in Figure 2. An important difference between *sp* metals and *d* metals is the wider potential window on the *sp* metals due to their poor HER activity. Figure 2 shows the voltammograms of blank (dashed line) and of 50 mM HMF (solid line) reduction in 0.1 M Na_2SO_4 alongside the concentration profiles of the reaction products, DHMF and others, on (a) Zn, Cd, and In, (b) Bi and Pb, and (c) Sn and Sb. In general, the onset potential for hydrogen evolution in the blank scans is more negative than -1 V, which clearly differentiates the hydrogenation current of HMF from that of HER. In Figure 2a, the cathodic current with HMF on Zn, Cd and In increases from ca. -0.7 V, which is a ca. 300 mV less negative potential than that of blank. The current profile with HMF in solution is very similar to that of the Ag electrode in Figure 1a. Zn, Cd and In reduce HMF primarily to DHMF starting at ca. -0.65 V. Zn is the most active material until the production of DHMF decreases from -1.07 V, the potential at which the HER starts on Zn. Therefore we suspect that the HER interferes with the hydrogenation of 'C=O' of HMF. On Cd and In, the production of DHMF remain constant at negative potentials. On Cd, the selectivity towards DHMF appears to increases to 90% with the onset of the HER on Cd.

The voltammograms for HMF reduction on Bi and Pb in Figure 2b are similar to those in Figure 2a. DHMF and others are generated simultaneously from ca. -0.66 V. However, the selectivity towards DHMF on both electrodes is lower than those towards other hydration products before HER starts. In the potential region of the HER, the concentration of DHMF significantly increases from -1.29 V on Pb and -1.41 V on Bi, respectively. On the other hand, the formation of other products is suppressed during HER.

In Figure 2c, Sn shows a higher overpotential for HER in the blank voltammogram compared to that of Sb. However HMF reduction starts at the same potential. Both electrodes show a low activity to generate DHMF. The other products on Sn are first observed from -0.63 V, which is 120 mV earlier than that of DHMF. The concentration of DHMF is constant below -1 V and its selectivity is lower than 30%. The hydrogenolysis activity of Sn during HMF hydrogenation is consistent with the result of glucose reduction since Sn showed a 90% selectivity to 2-deoxysorbitol, also a hydrogenolysis product.[28] DHMF and other products on Sb are observed from -0.69 V. The initial selectivity of DHMF is 39%, however it gradually decreases and no DHMF is observed below -1.59 V.

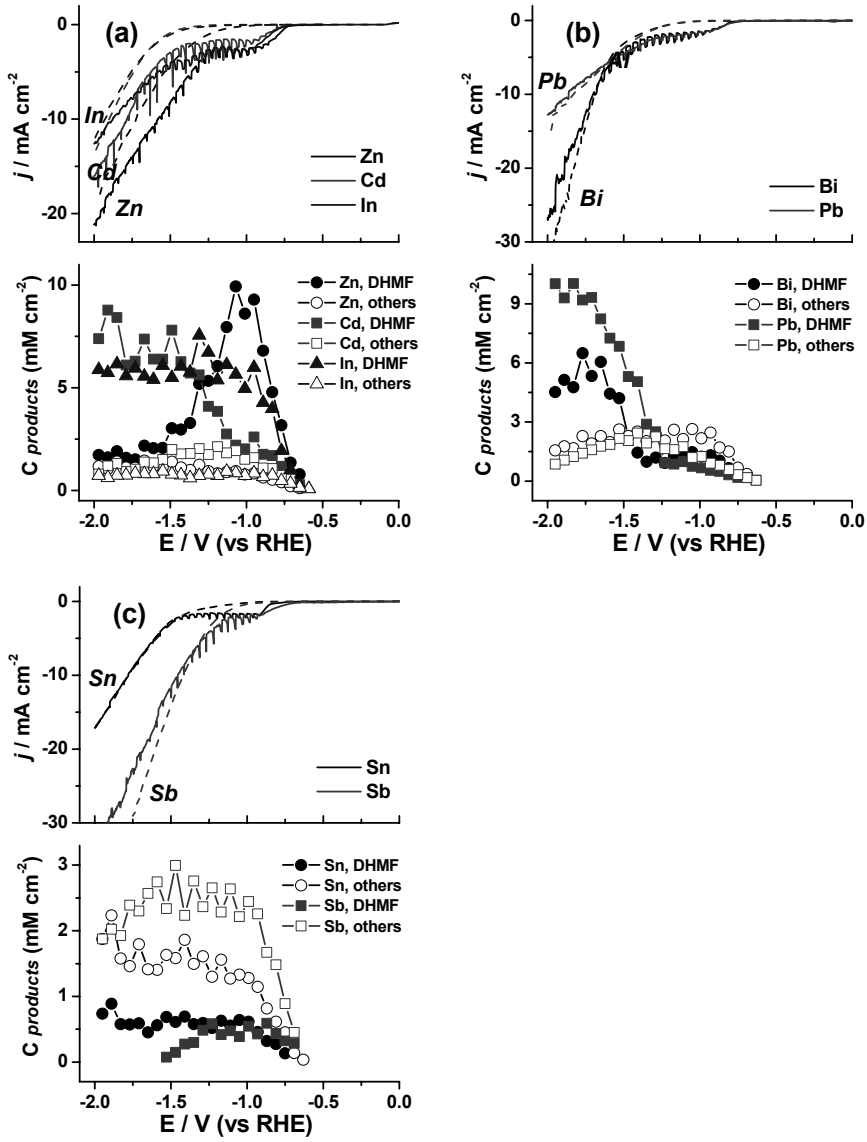

Figure 2. Electrocatalytic HMF (50 mM) reduction on Zn, Cd, and In, (b) Bi and Pb, and (c) Sn and Sb in 0.1 M Na_2SO_4. Current density profiles (upper panels) with (solid line) and without (dashed line) HMF in the solution during linear sweep voltammetry with a scan rate of 1 mV s^{-1}, and concentration profiles (lower panels) of corresponding reaction products, DHMF and others, as a function of potential.

For the poor metal electrodes, we can conclude that in agreement with the transition metals, HMF hydrogenation appears to be a non-catalytic reaction. However, there are still differences between catalysts in terms of their selectivity towards DHMF and other products. The HER on poor metals appears to influence the generation of DHMF; DHMF formation on Bi and Pb is enhanced by HER, however HER appears to suppress DHMF formation on Zn and Sb.

8.3.2 HMF reduction in the presence of glucose

Glucose and HMF are generated from acid-catalyzed cellulose hydrolysis,[29] however their reactivity during hydrogenation is quite different. From our previous work on glucose hydrogenation,[28] we demonstrated different affinities of various catalysts towards hydrogen formation (early transition and Pt group metals), sorbitol formation (late transition metals), and sorbitol and 2-deoxysorbitol formation (post-transition metals including Zn and Cd). However, from the trend of HMF hydrogenation described in the previous section, there is no clear correlation between the electronic structure of the catalysts and the product distribution. In addition, the onset potential for HMF hydrogenation seems to be more or less constant and not influenced by HER. It is of interest to study the hydrogenation of a mixture of HMF and glucose to gain insight into how they influence each other. Specifically, we selected a relatively low concentration of HMF (10 mM) compared to that of glucose (0.1 M) in order to mimic their ratio during acid-catalyzed cellulose hydrolysis. The concentration of HMF is lowered from 50 to 10 mM due to the unstability of sampling pump in a viscous solution.

3 shows the voltammograms of the blank (dashed line) and of 10 mM HMF + 0.1 M glucose (solid line) reduction in 0.1 M Na_2SO_4 alongside the concentration profiles of the reaction products on transition metals (a) Fe, Ni, and Ag, (b) Pd and Al, and (c) Co, Au, and Cu. We note that the presence of glucose in the solution does not change the general trend of current profiles compared to Figure 1, although a tenfold higher concentration of glucose (0.1 M) than that of HMF (10 mM) is added. Surprisingly, the glucose hydrogenation product, sorbitol, is not observed at any potential on any of the transition metals in Figure 3. However, the presence of glucose in solution changes the product distributions of HMF reduction. In Figure 1a, the onset potential of DHMF on Fe, Ni, and Ag is -0.39 V. However, with glucose in the solution it changes to -0.45 V on Fe, -0.21 V

on Ni, and -0.51 V on Ag, respectively. The delay of the onset potential on Fe and Ag may be explained by adsorbed glucose on the catalyst surface, but glucose accelerates HMF hydrogenation on Ni. The formation of other products generated through hydrogenolysis of HMF, is strongly suppressed at high potentials and only traces are observed on Fe and Ag. Interestingly, HER influences the product selectivity so that the concentration of DHMF decreases on Ni and Ag after hydrogen evolution starts. However, HMF reduction on Fe is less influenced by HER.

HMF reduction on Pd and Al is shown in Figure 3b. Hydrogenolysis products are dominant on these two metals, though glucose appears to enhance the DHMF production on Al. Also the onset potential for DHMF formation on Pd is 0.3 V less negative than that in Figure 1b. As a similar trend was observed on Ni in Figure 3a, we suspect that the presence of glucose enhances the hydrogenation activity on Ni and Pd, which both absorb hydrogen.[36]

Voltammograms of Co, Au, and Cu in Figure 3c are similar to those in Figure 1c, however the product distribution is different in the presence of glucose. First of all, DHMF formation on these three metals is observed from the onset potential and the formation of other products is delayed. Interestingly, the concentration of DHMF and others on Co in the presence of glucose is significantly higher than that in Figure 1c, although the concentration of HMF is 5 times lower. On Au and Cu, glucose also enhances the formation of DHMF with the suppression of other products. Suppression of DHMF formation on Cu is observed below -0.69 V when HER starts.

Similar to transition metals in Figure 3, poor metals also show different activity and selectivity in the presence of glucose. The main difference of the poor metals compared to the transition metals is that poor metals show activity towards glucose hydrogenation to generate sorbitol and 2-deoxysorbitol, also in the presence of HMF. Glucose enhances the formation DHMF on Zn, Cd, and In in Figure 4a, but the hydrogenolysis of HMF is blocked similarly to the transition metals.

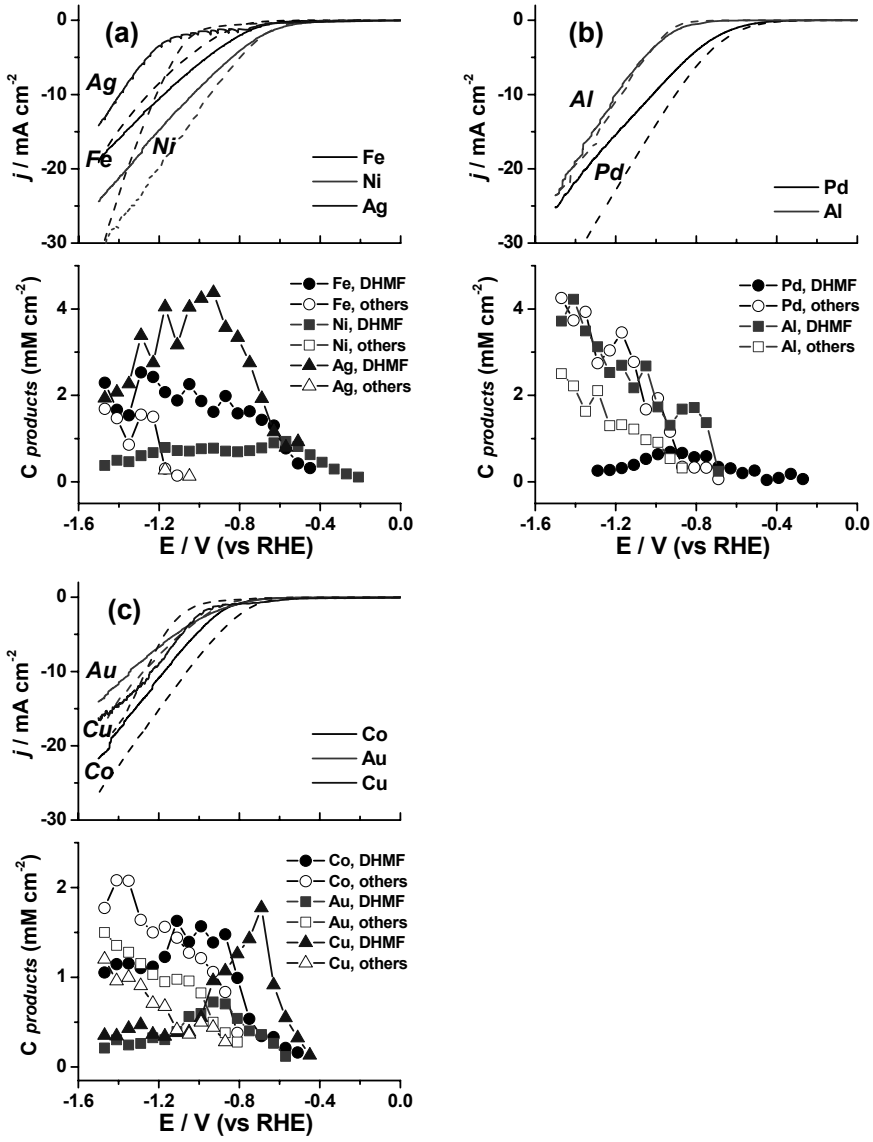

Figure 3. Electrocatalytic HMF (10 mM) + glucose (0.1 M) reduction on (a) Fe, Ni, and Ag, (b) Pd and Al, and (c) Co, Au, and Cu in 0.1 M Na_2SO_4. Current density profiles (upper panels) with (solid line) and without (dashed line) HMF + glucose in the solution during linear sweep voltammetry with a scan rate of 1 mV s^{-1}, and concentration profiles (lower panels) of corresponding reaction products, DHMF and others, as a function of potential.

The effect of glucose on HMF reduction on Pb, Sn, and Sb in Figure 4 is also rather small. Note that highest concentration of sorbitol (0.5 mM cm^{-2}) is observed on Pb, which is consistent with the activity of Pb for glucose hydrogenation to sorbitol.[28] On Sn, the selectivity of DHMF is within 15 - 40% in the whole potential range and glucose is not hydrogenated. The hydrogenolysis of HMF on Sb is accelerated in the presence of glucose especially from the potential where HER starts.

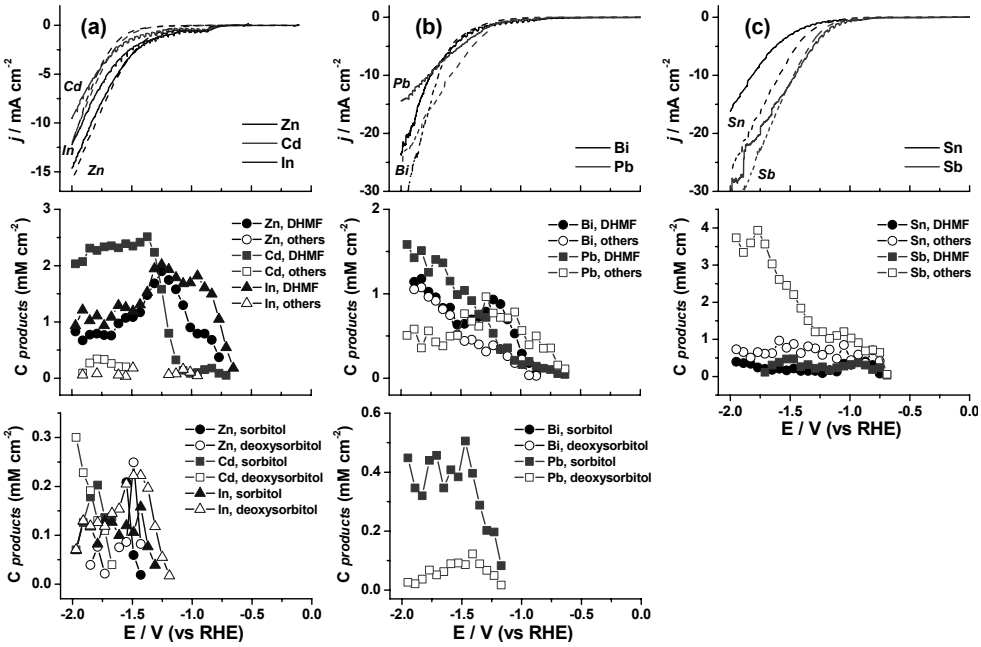

Figure 4. Electrocatalytic HMF (10 mM) + glucose (0.1 M) reduction on (a) Zn, Cd, and In, (b) Bi and Pb, and (c) Sn and Sb in 0.1 M Na_2SO_4. Current density profiles (upper panels) with (solid line) and without (dashed line) HMF + glucose in the solution during linear sweep voltammetry with a scan rate of 1 mV s^{-1}, and concentration profiles (middle and lower panels) of corresponding reaction products, DHMF and others (middle panel), sorbitol and 2-deoxysorbitol (lower panel), as a function of potential.

Based on our observations we conclude that on transition and poor metals, the presence of HMF blocks the reduction of glucose. On the other hand, glucose enhances the formation of DHMF and suppresses the hydrogenolysis of HMF on all transition metals and some (Zn,

Cd, and In) poor metals. However the influence of glucose on HMF reduction on Bi, Pb, Sn, and Sb is relatively limited.

8.3.3 A mechanistic view of HMF hydrogenation

From the relationship between voltammetry and reaction product distribution of HMF hydrogenation in the absence and the presence of glucose as shown in Figure 1-4, we conclude that the hydrogenation of HMF is always dominant and the reduction of glucose is strongly suppressed by the presence of HMF. Interestingly, the hydrogenation of HMF does not seem to be depend on the nature of the electrocatalyst, suggesting a non-catalytic reaction, based on the almost identical onset potentials (-0.5 ± 0.1 V) on all metals. This indicates that H_{ads} on metal surface is unlikely to be involved in the initial HMF hydrogenation process, which is different from general hydrogenation mechanisms of organic molecules.[37] Therefore, we assume that the initial HMF hydrogenation occurs directly by water molecules from the electrolyte:

$$HMF + 2\ H_2O + 2\ e^- \leftrightarrow DHMF + 2\ OH^- \quad (1)$$

A similar hydrogenation mechanism, not involving H_{ads}, has been suggested for the NO adsorbate reduction on Pt.[38]

As the onset potential of HMF hydrogenation is not strongly catalyst dependent, we can assume that other conductive materials can also be used as potential catalysts for HMF hydrogenation. To this end, we tested pyrolytic graphite (PG) and polycrystalline platinum for HMF reduction in 0.1 M Na_2SO_4 as shown in Figure 5. PG is normally used as a catalyst for oxygen reduction reaction (ORR) in alkaline[39] or as a stable catalyst support[40] in electrochemistry, however it does not show catalytic activity for glucose hydrogenation.[41] Polycrystalline Pt shows very limited activity towards the hydrogenation of glucose to sorbitol[28] due to its high affinity to generate hydrogen.[28] From the blank voltammograms, the HER starts from ca. -0.9 V on PG and ca. -0.3 V on Pt, respectively. The onset potential of HMF reduction on PG is ca. -0.65 V, which is a similar onset potential of HMF reduction on other metals. From ca. -0.7 V, we observe other hydrogenolysis products on PG. In contrast, DHMF is dominantly observed from ca. -0.4 V

on Pt. Therefore, these experiments confirm our hypothesis that the HMF reduction is a non-catalytic reaction.

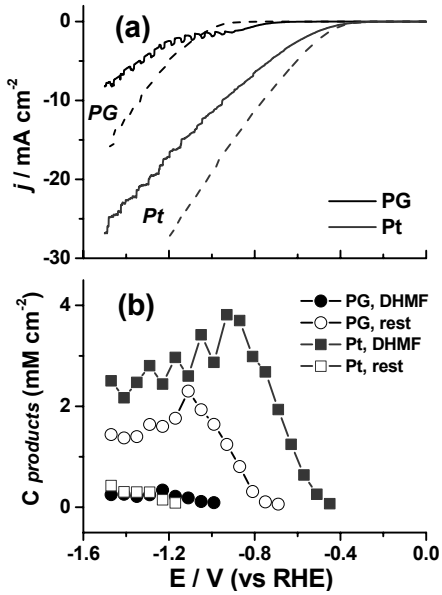

Figure 5. Electrocatalytic HMF (50 mM) reduction on pyrolytic graphite (PG) and polycrystalline Pt coil in 0.1 M Na_2SO_4. Current density profiles (a) with (solid line) and without (dashed line) HMF in the solution during linear sweep voltammetry with a scan rate of 1 mV s^{-1}, and concentration profiles (b) of corresponding reaction products, DHMF and others, as a function of potential.

The potential degradation of HMF at high pH was also investigated. 10 mM HMF was added to 0.1 M NaOH in the absence and presence of oxygen. After one hour, we could not observe any isomerization, aldol-condensation, or expected HMF oxidation products (i.e. FDA, FFCA, FDCA) under both conditions, although it is known that HMF is not stable at elevated temperature in alkaline condition.[4] As we have shown previously, high pH is essential for glucose hydrogenation since the high pH near the electrode surface mutarotates the cyclic (inactive) form of glucose to linear (electroactive) form, which is considered as a rate-determining step.[42-44] Based on this observation, we conclude that HMF is more stable than glucose at high pH at room temperature and high pH is not an essential factor for HMF hydrogenation.

In addition to the effect of pH, there is a thermodynamic reason why the hydrogenation of HMF is more favorable than that of glucose. The enthalpy change for the glucose hydrogenation to sorbitol is ca. -10 kcal mol^{-1}, as hydrogenation reactions are typically exothermic, however the hydrogenation of HMF to DHMF has an enthalpy change of ca. -20 kcal mol^{-1},[45] which may explain the preferential hydrogenation of HMF instead of glucose. Under electrochemical conditions, the identical onset potentials (-0.5 ± 0.2 V) for HMF hydrogenation should be related to the equilibrium potential of the reaction. However, the equilibrium potential of HMF hydrogenation to DHMF is ca. 0.1 V, calculated based on the Gibbs free energy changes in the gas phase at 298 K,[46] which implies that the identical onset potential for the reaction is mainly attributed to the activation energy (ca. 0.5 V), which is not or hardly influenced by catalyst. Although the hydrogenolysis of HMF is energetically neutral, it is obvious that proton and electron transfer reactions are involved in the hydrogenolysis process. Additionally, the hydrogenation of C=C bond in the furan ring of HMF is thermodynamically more favored compared to DHMF formation (i.e. ΔH = -35 kcal mol^{-1} during DHMF hydrogenation to DHMTHF[45]). Therefore, we could observe the formation of 2,5-dimethyl-2,3-dihydrofuran as one of other products during HMF electrocatalysis in Figure 6.

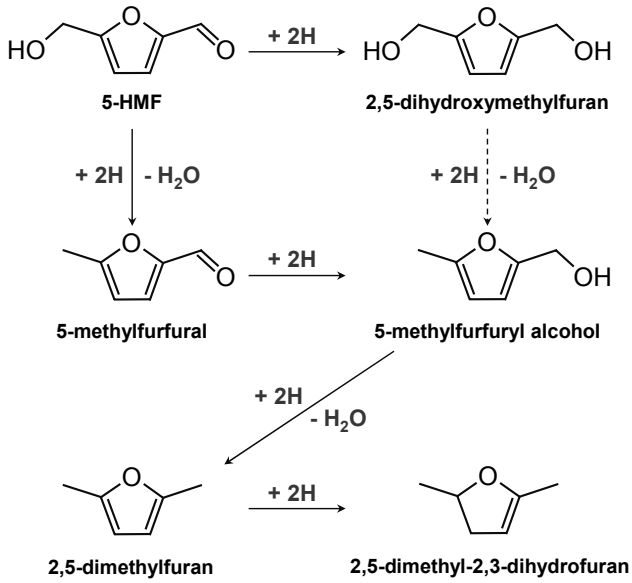

Figure 6. Schematic diagram of HMF hydrogenation pathways.

As shown in Scheme 1, the C=O group in HMF is hydrogenated to 2,5-dihydroxymethylfuran (DHMF) with 2H and 'others' are generated by hydrogenolysis of '-OH' in HMF during hydrogenation, leading first to 5-methylfurfural. To generate 2,5-dimethylfuran, the C=O moiety on 5-methylfurfural presumably first needs to be hydrogenated to 5-methylfurfuryl alcohol, although 5-methylfurfuryl alcohol is not observed from the product spectra. This indicates that the conversion rate of 5-methylfurfuryl alcohol to 2,5-dimethylfuran is extremely fast. Interestingly, DHMF is stable and not reduced to any significant extent on Ag, Cu, Pb, and Sn, highly active catalysts for HMF hydrogenation. Therefore, we conclude that 2,5-dimethylfuran derives from the hydrogenation of 5-methylfurfural through 5-methylfurfuryl alcohol, and not from DHMF. In a final step, one of the C=C bonds on 2,5-dimethylfuran is hydrogenated to 2,5-dimethyl-2,3-dihydrofuran, the most reduced reaction product observed in the GC-MS spectra. In addition to hydrogenated reaction products, we could also observe a certain amount of oxidized species (i.e. 2,5-furandicarbaldehyde) from HMF. We believe that the oxidation products are base-catalyzed reaction products, generated during electrolysis near the electrode surface. Although all the detailed concentrations of 5-methylfurfural, 2,5-dimethylfuran, and 2,5-dimethyl-2,3-dihydrofuran are not presented in Figures, the general reaction pathway shown in Figure 6 is consistent with the experimental data.

8.4 Conclusions

This chapter has studied the electrochemical 5-HMF hydrogenation in the absence and the presence of glucose on solid monometallic electrodes in neutral solution. We studied the activity and selectivity of the catalysts for HMF hydrogenation by correlating the voltammetric scan with online product analysis using HPLC, which provided qualitative and quantitative information regarding DHMF, other products from HMF hydrogenation, as well as sorbitol and 2-deoxysorbitol from the HMF and glucose mixture, as a function of potential. Three groups of catalysts regarding to reaction products from HMF hydrogenation were distinguished from this study. DHMF was mainly formed on Fe, Ni, Ag, Zn, Cd, and In. DHMF and other hydrogenolysis products were generated on Pd, Al, Bi, and Pb depending on the applied potential. Hydrogenolysis products of HMF are mainly formed on Co, Au, Cu, Sn, and Sb. The hydrogenation of HMF is not strongly catalyst dependent since all catalysts show a more or less identical onset potential (-0.5 ± 0.2 V),

mainly attributed to the activation energy which is not influenced by catalyst. However the intrinsic property of catalysts determines the reaction final product. Ag shows highest activity among all metals towards DHMF formation (with high selectivity > 85%). Some poor metals (Zn, Bi, Pb, and Sb) exhibit a change in selectivity for HMF reduction when hydrogen evolution takes place simultaneously. In the presence of glucose, the hydrogenation of HMF is always easier than glucose hydrogenation, on all metals. On transition metals, glucose enhances the formation of DHMF and suppresses the hydrogenolysis of HMF, whereas the glucose reduction itself is suppressed. On poor metals, glucose enhances the DHMF formation on Zn, Cd, and In. However, its influence on HMF reduction on Bi, Pb, Sn, and Sb is relatively limited. Since HMF can also be reduced on a graphite electrode, and the onset potential for HMF reduction is not very dependent on the nature of the electrode material, we conclude that the initial (reduction) step of HMF reduction is a non-catalytic reaction. In comparison to glucose, HMF hydrogenation does not require a high pH, such as generated close to the electrode surface during hydrogen evolution, a requirement necessary for glucose hydrogenation. As a result, the hydrogenation of glucose requires a higher overpotential than that of HMF. Finally, we note that this chapter's main aim was to scan the ability of various metals for electrochemical HMF hydrogenation by a combination of voltammetry and online HPLC. More quantitative information on efficiency and stability would require additional long-term electrolysis experiments. The current study may point towards the most interesting materials to choose for such a study.

8.5 References

[1] G. W. Huber, S. Iborra, A. Corma, *Chem. Rev*. **2006**, *106*, 4044-4098.

[2] A. Corma, S. Iborra, A. Velty, *Chem. Rev*. **2007**, *107*, 2411-2502.

[3] E.-S. Kang, D. W. Chae, B. Kim, Y. G. Kim, *J. Ind. Eng. Chem*. **2012**, *18*, 174-177.

[4] R.-J. van Putten, J. C. van der Waal, E. de Jong, C. B. Rasrendra, H. J. Heeres, J. G. de Vries, *Chem. Rev*. **2013**, *113*, 1499-1597.

[5] R. M. Musau, R. M. Munavu, *Biomass* **1987**, *13*, 67-74.

[6] C. Moreau, R. Durand, S. Razigade, J. Duhamet, P. Faugeras, P. Rivalier, P. Ros, G. Avignon, *Appl. Catal. A-Gen*. **1996**, *145*, 211-224.

[7] M. E. Zakrzewska, E. Bogel-Lukasik, R. Bogel-Lukasik, *Chem. Rev*. **2011**, *111*, 397-417.
[8] Z. Yuan, C. Xu, S. Cheng, M. Leitch, *Carbohydr. Res*. **2011**, *346*, 2019-2023.
[9] Q. Cao, X. Guo, J. Guan, X. Mu, D. Zhang, *Appl. Catal. A-Gen*. **2011**, *403*, 98-103.
[10] S. P. Simeonov, J. A. S. Coelho, C. A. M. Afonso, *ChemSusChem* **2012**, *5*, 1388-1391.
[11] F. S. Asghari, H. Yoshida, *Ind. Eng. Chem. Res*. **2006**, *45*, 2163-2173.
[12] D. Mercadier, L. Rigal, A. Gaset, J. P. Gorrichon, *J. Chem. Technol. Biotech*. **1981**, *31*, 489-496.
[13] K. Seri, Y. Inoue, H. Ishida, *B. Chem. Soc. Jpn*. **2001**, *74*, 1145-1150.
[14] H. Zhao, J. E. Holladay, H. Brown, Z. C. Zhang, *Science* **2007**, *316*, 1597-1600.
[15] A. A. Rosatella, S. P. Simeonov, R. F. M. Frade, C. A. M. Afonso, *Green Chem*. **2011**, *13*, 754-793.
[16] P. M. Grande, C. Bergs, P. D. de Maria, *ChemSusChem* **2012**, *5*, 1203-1206.
[17] S. P. Simeonov, J. A. S. Coelho, C. A. M. Afonso, *ChemSusChem* **2013**, *6*, 997-1000.
[18] C. Moreau, M. N. Belgacem, A. Gandini, *Top. Catal*. **2004**, *27*, 11-30.
[19] E. de Jong, M. A. Dam, L. Sipos, G.-J. M. Gruter, in *Biobased Monomers, Polymers, and Materials* (Ed.: P. B. Smith and R. A. Gross), *ACS Symposium Series*, **2012**, pp. 1-13.
[20] A. Gandini, *Green Chem*. **2011**, *13*, 1061-1083.
[21] K. R. Vuyyuru, P. Strasser, *Catal. Tod*. **2012**, *195*, 144-154.
[22] V. Schiavo, G. Descotes, J. Mentech, *B. Soc. Chim. Fr*. **1991**, 704-711.
[23] Y. Nakagawa, K. Tomishige, *Catal. Commun*. **2010**, *12*, 154-156.
[24] R. Alamillo, M. Tucker, M. Chia, Y. Pagan-Torres, J. Dumesic, *Green Chem*. **2012**, *14*, 1413-1419.
[25] T. Buntara, S. Noel, P. H. Phua, I. Melian-Cabrera, J. G. de Vries, H. J. Heeres, *Angew. Chem. Int. Ed*. **2011**, *50*, 7083-7087.
[26] Y. Roman-Leshkov, C. J. Barrett, Z. Y. Liu, J. A. Dumesic, *Nature* **2007**, *447*, 982-985.
[27] J. B. Binder, R. T. Raines, *J. Am. Chem. Soc*. **2009**, *131*, 1979-1985.
[28] Y. Kwon, M. T. M. Koper, *ChemSusChem* **2013**, *6*, 455-462.
[29] Y. Kwon, S. E. F. Kleijn, K. J. P. Schouten, M. T. M. Koper, *ChemSusChem* **2012**, *5*, 1935-1943.
[30] Y. Kwon, M. T. M. Koper, *Anal. Chem*. **2010**, *82*, 5420-5424.

[31] Y. Kwon, S. C. S. Lai, P. Rodriguez, M. T. M. Koper, *J. Am. Chem. Soc*. **2011**, *133*, 6914-6917.

[32] Y. Kwon, K. J. P. Schouten, M. T. M. Koper, *ChemCatChem* **2011**, *3*, 1176-1185.

[33] A. Santasalo-Aarnio, Y. Kwon, E. Ahlberg, K. Kontturi, T. Kallio, M. T. M. Koper, *Electrochem. Commun*. **2011**, *13*, 466-469.

[34] Y. Kwon, Y. Birdja, I. Spanos, P. Rodriguez, M. T. M. Koper, *ACS Catal*. **2012**, *2*, 759-764.

[35] P. Rodriguez, Y. Kwon, M. T. M. Koper, *Nat. Chem*. **2012**, *4*, 177-182.

[36] S. C. S. Lai, M. T. M. Koper, *Faraday Discuss*. **2008**, *140*, 399-416.

[37] J. M. Chapuzet, A. Lasia, J. Lessard, *Electrocatalysis*, ed. J. Lipowski, P. N. Ross, Wiley-VCH, New York, **1998**, 155– 196.

[38] A. C. A. de Vooys, G. L. Beltramo, B. van Riet, J. A. R. van Veen, M. T. M. Koper, *Electrochim. Acta* **2004**, *49*, 1307-1314.

[39] D. Qu, *Carbon* **2007**, *45*, 1296-1301.

[40] O. Brylev, M. Sarrazin, D. Belanger, L. Roue, *Appl. Catal. B-Env*. **2006**, *64*, 243-253.

[41] S. Fei, J. Chen, S. Yao, G. Deng, L. Nie, Y. Kuang, *J. Solid State Electrochem*. **2005**, *9*, 498-503.

[42] K. Park, P. N. Pintauro, M. M. Baizer, K. Nobe, *J. Electrochem. Soc*. **1985**, *132*, 1850-1855.

[43] A. Binkassim, C. L. Rice, A. T. Kuhn, *J. Appl. Electrochem*. **1981**, *11*, 261-267.

[44] P. N. Pintauro, D. K. Johnson, K. Park, M. M. Baizer, K. Nobe, *J. Appl. Electrochem*. **1984**, *14*, 209-220.

[45] H. Ed George W., Breaking the Chemical and Engineering Barriers to Lignocellulosic Biofuels: Next Generation Hydrocarbon Biorefineries, NSF, **2008**, 66-71.

[46] S. P. Verevkin, V. N. Emel'yanenko, E. N. Stepurko, R. V. Ralys, D. H. Zaitsau, A. Stark, *Ind. Eng. Chem. Res*. **2009**, *48*, 10087-10093.

9

Outlook

In the project of "Biomass electrochemistry: from cellulose to sorbitol", we were aiming at single-cell synthesis of sorbitol from cellulosic material by generating glucose as an intermediate species. This thesis has demonstrated the separate reactions of cellobiose hydrolysis to glucose by acid and hydroxyl radical on an anode (Chapter 6) and glucose hydrogenation to sorbitol on a cathode (Chapter 7) in an electrolysis cell. The glucose generated from anode can be transferred to the cathode inlet for further hydrogenation to sorbitol. Our work allows us to point out some factors that make the combination of two reactions in a cell currently still not a viable route towards cellulose valorisation.

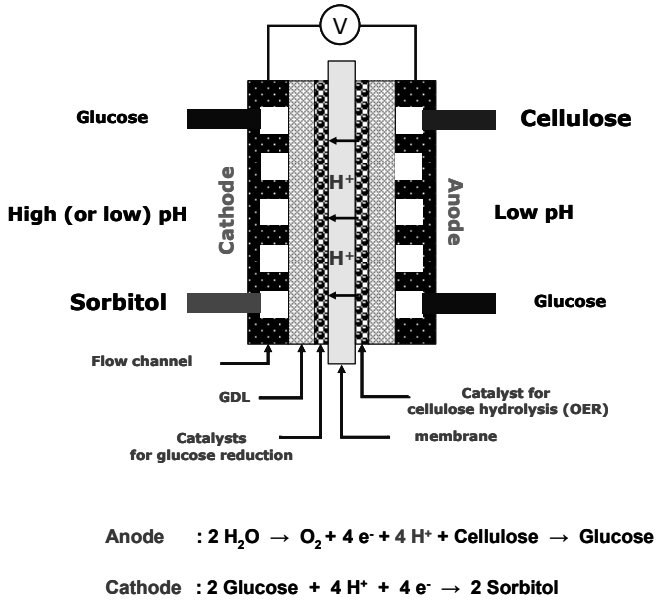

Figure 1. Schematic diagram of cellulose conversion to sorbitol in an electrolyzer.

First of all, for breaking the glycosidic bond to glucose by acid-catalyzed hydrolysis in cellulosic material, including cellobiose and cellulose, requires high temperature (around 200^{o}C), which is not easily achievable under standard electrochemical conditions. From the study of cellobiose hydrolysis by electrochemically generated acid in Chapter 6, we observed a lower selectivity towards glucose than that of acid-catalyzed hydrolysis at 80^{o}C due to the decomposition of glucose by the activated electrocatalyst or by-product formation by molecular O_2 generated during oxygen evolution reaction (OER). Therefore, an electrode with high activity for OER and low activity for glucose decomposition at high temperature is necessary for such an application. Future work should also investigate high pressures.

In contrast to acid hydrolysis, hydroxyl radical requires a lower temperature for cellobiose hydrolysis on boron-doped diamond (BDD) since the high temperature accelerates the reaction rate towards decomposition of glucose to smaller aldoses and their corresponding acids. Therefore, the application of hydroxyl radicals may be a promising technique with lower activation energy than that of the acid-catalyzed reaction, provided the hydrolyzed glucose is immediately separated from the active radical.

Compared to the cellulose hydrolysis to glucose at the anode compartment, glucose hydrogenation on a cathode is relatively well established. In Chapter 7, we could clearly show the trend of hydrogenation activity on solid metals in the Periodic Table. Especially, Pb electrode shows a high activity to form sorbitol with high selectivity (> 87%) and high yield (< 0.7 mM cm^{-2}). Therefore after optimization of cellulose hydrolysis at the anode, it should be possible to achieve one-pot electrosynthesis of sorbitol from cellobiose or cellulose.

Apart from cellulose conversion to sorbitol, this thesis includes 'glycerol oxidation' in Chapter 2 ~ 4. Since glycerol is an important biomass-related compound, both as a model poly-ol compound, and as an abundant byproduct of biodiesel, the catalytic conversion of glycerol into value-added chemicals is a topic of significant current interest in biomass research. In electrochemistry, glycerol has been considered as a potential fuel for cell cells. From a recent review of electrochemical valorization of glycerol given by Coutanceau et al. [1], glycerol is energetically more interesting reactant than water for the production of hydrogen in electrolysis cell. Furthermore, the fuelling of a fuel cell with the generated

hydrogen from glycerol electrolysis is more efficient from an energy-yield viewpoint than the direct oxidation of glycerol in a fuel cell, which brings us an idea to co-generate hydrogen and valuable chemicals (i.e. glyceraldehyde, glyceric acid, dihydroxyacetone, formic acid) depending on the applied potential in an electrolysis cell shown in Figure 2.

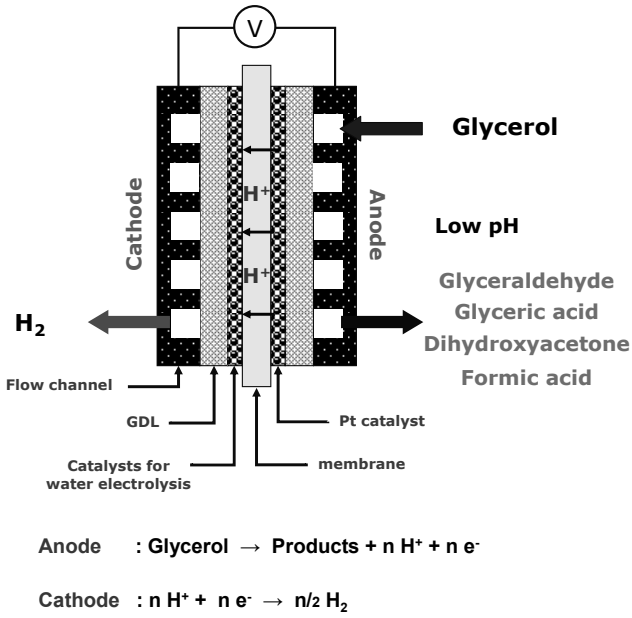

Figure 2. Schematic diagram of glycerol conversion to hydrogen and chemicals in an electrolyzer.

The selective oxidation of glycerol through the secondary alcohol oxidation pathway to generate dihydroxyacetone (DHA) was described in Chapter 4 using Bi as a modifier of the Pt catalyst. The role of Bi should be understood beyond the blocking the formation of poisoning species 'CO', which is preferentially formed from the terminal CH_2OH[2]. From an extended study of other poly-ols [C4~C6] oxidation, the role of Bi is also applicable to bigger poly-ols and changes the reaction pathway toward secondary alcohol oxidation. In addition, we found that other adatoms i.e. Sb, Pb, can also control the reaction pathway mainly dependent on the surface coverage on the Pt catalyst.

An important achievement of this thesis is online HPLC, which has enabled the detailed product analyses in the thesis. More specifically, online fraction collector (FRC) was combined with electrochemical techniques and chromatographic techniques. The application of this technique is not only limited to the study of biomass conversion, but it

includes all possible analytical methods which may be combined with electrochemistry. For instance, online sampling technique can visualize the soluble reaction products i.e. nitrite, ammonium, hydroxylamine during nitrate (or nitrite) reduction by analyzing collected samples using ion chromatography, which has not been done before. Importantly, online sampling system is also accessible to gas evolution reactions, therefore I believe that this technique will contribute to the study of global carbon and nitrogen cycles.

References

[1] M. Simoes, S. Baranton, C. Coutanceau, *ChemSusChem* **2012**, *5*, 2106-2024.

[2] P. S. Fernández, M. E. Martins, C. A. Martins, G. A. Camara, *Electrochem. Commun.* **2012**, 15, 14-17.

Summary

The primary goal of this thesis is to study the potential role of electrochemistry in finding new routes for sustainable chemicals from biomass in aqueous-phase solutions. In order to assess the potential of electrochemistry in biomass conversion, we were in need of an analysis method that is consistent with the time scale of the electrochemist's favorite technique, i.e. voltammetry. However, the combination of voltammetry especially with high-performance liquid chromatography (HPLC) has been limited due to the long analysis times in the column. To overcome the inherent time-scale differences of voltammetry and HPLC, we employed rapid sample collection while sweeping the electrode potential, using a very small micrometer-sized tip inlet system placed close to the electrode surface, with the collected sample fractions subsequently analyzed in an HPLC system. To demonstrate this method, we applied it to the glycerol ($C_3H_8O_3$) electro-oxidation on Au and Pt electrodes in alkaline media in Chapter 2, visualizing the concentration changes of glycerol and its reaction products in correspondence with the current measured in voltammetry.

The electro-oxidation mechanisms of glycerol on Au and Pt electrodes under different pH conditions are further reported in Chapter 3. Especially, glyceraldehyde and dihydroxyacetone, which are not stable in alkaline condition, are shown in product spectra by continuous injection of 'stabilizing agent' through modified sample collecting tip during sample collection. From this study, we found out that glycerol is oxidized dominantly through primary alcohol via glyceraldehyde as the first reaction product. In addition, gold only catalyzes glycerol oxidation under alkaline conditions, in contrast to platinum, which catalyzes glycerol oxidation over the entire pH range.

In order to alter the oxidation pathway of glycerol toward 'secondary alcohol', since the primary alcohol oxidation is always dominant on monometallic catalysts in Chapter 2 and 3, we introduced Bi as an adatom on Pt/C catalyst. A Pt/C electrode in a bismuth saturated solution at a carefully chosen potential is capable of oxidizing glycerol to dihydroxyacetone

with 100% selectivity. In the absence of bismuth, the primary alcohol oxidation is dominant. Using a combination of online HPLC and in situ FTIR, it is shown that Bi blocks the pathway for primary oxidation but also provides a specific Pt-Bi surface site poised for secondary alcohol oxidation.

The role of the alkaline medium and the gold electrode during alcohol oxidation is investigated in Chapter 5. Based on a comparison of the oxidation activity of a series of similar alcohols with varying pK_a on gold electrodes in alkaline solution, we find that the first deprotonation is base catalyzed, and the second deprotonation is fast but gold catalyzed. The base catalysis follows a Hammett-type correlation with pK_a, and dominates overall reactivity for a series of similar alcohols. The high oxidation activity on gold compared to platinum for some of the alcohols is related to the high resistance of gold toward the formation of poisoning surface oxides. These results indicate that base catalysis is the main driver behind the high oxidation activity of many organic fuels on fuel cell anodes in alkaline media, and not the catalyst interaction with hydroxide.

Based on fundamental understanding of the electrocatalysis of biomass derived alcohols with online HPLC in Chapters 2~5, we extended our interest to the challenging topic of cellobiose conversion to sorbitol.

For cellobiose conversion to sorbitol, cellobiose hydrolysis to glucose is first investigated in Chapter 6. Platinum and boron-doped diamond (BDD) electrodes were employed to generate acid (H^+) and hydroxyl radicals ($OH\cdot$), respectively, the results of which were compared with the hydrolysis promoted by conventional acid (H_2SO_4) and $OH\cdot$ from Fenton's reaction. Cellobiose hydrolysis follows a first-order reaction obeying Arrhenius' law over the temperature range from 25°C to 80°C with different activation energies for the acid- and radical-promoted reaction, i.e. ca. 118±8 kJ mol^{-1} and ca. 55±1 kJ mol^{-1}, respectively. The high local acidity with electrochemically generated acid (H^+) on the Pt anode increases the rate of glucose formation, however the active electrode (PtO_x) interacts with glucose and decomposes it further to smaller organic acids. The hydroxyl radical

(OH•) generated on a BDD anode first hydrolyzes the cellobiose to glucose, but rapidly attacks the aldehyde on glucose, which is further decomposed to smaller aldoses and finally formaldehyde, which is subsequently oxidized electrochemically to formic acid.

As a coupled reaction of cellobiose hydrolysis to glucose, the glucose hydrogenation to sorbitol in neutral solution on solid metal cathodes is described in Chapter 7. Three groups of catalysts in a Periodic Table regarding to reaction products clearly show their affinities toward: 1) hydrogen formation on early transition metals (Ti, V, Cr, Mn, Zr, Nb, Mo, Hf, Ta, We, and Re) and platinum group metals (Ru, Rh, Ir, and Pt), 2) sorbitol on late transition metals (Fe, Co, Ni, Cu, Pd, Au, and Ag) and Al (sp metal), and 3) sorbitol and 2-deoxysorbitol on post-transition metals (In, Sn, Sb, Pb, and Bi) as well as Zn and Cd (d metals). Ni shows the lowest overpotential for sorbitol formation from -0.25 V whereas Pb generates sorbitol with the highest yield (< 0.7 mM cm^{-2}). Different from a smooth Pt electrode, a large surface-area Pt/C electrode hydrogenates glucose to sorbitol from -0.21 V with relatively low current, which emphasizes the importance of the active sites and the surface area of the catalyst. In combination with the ability of potential-controlled electrolysis on anode (Chapter 6), it may be possible to achieve one-pot electro-synthesis of sorbitol from cellobiose or cellulose.

As 5-hydroxymethylfurfural (HMF) is a by-product of glucose dehydration during acid-catalysed cellulose hydrolysis, the effect of the presence of glucose on the hydrogenation of HMF and vice versa is investigated in Chapter 8. Three groups of catalysts show different selectivity towards: (1) 2,5-dihydroxymethylfuran (DHMF) (Fe, Ni, Ag, Zn, Cd, and In), (2) DHMF and other products such as 2,5-dimethylfuran (Pd, Al, Bi, and Pb), depending on the applied potential, and (3) other products (Co, Au, Cu, Sn, and Sb) involving HMF dehydration. The rate of electrocatalytic HMF hydrogenation is not strongly catalyst dependent since all catalysts show similar onset potentials (-0.5 ± 0.2 V) in the presence of HMF. However the intrinsic property of the catalysts determines the reaction pathway towards DHMF or other products. Ag showed highest activity towards DHMF formation (max. 13.1 mM cm^{-2} with high selectivity > 85%). HMF hydrogenation is faster than

glucose hydrogenation on all metals. For transition metals, the presence of glucose enhances the formation of DHMF and suppresses the dehydration of HMF. On poor metals, glucose enhances the DHMF formation on Zn, Cd, and In, however, its contribution to Bi, Pb, Sn, and Sb is limited. Remarkably, in the presence of HMF, glucose hydrogenation itself is largely suppressed or even absent. The first electron transfer step of HMF reduction is not metal dependent suggesting a non-catalytic reaction with proton transfer directly from water in the electrolyte.

This thesis has shown the potential of electrochemistry and electrocatalysis toward generating sustainable chemicals from biomass by combining voltammetry and chromatography. This simple and innovative approach enables the monitoring of soluble reaction products during voltammetry with chromatographic techniques, and thereby allows for new insights into the mechanisms of complex multi-step electrode reactions.

Samenvatting

Het primaire doel van dit proefschrift is het bestuderen van de potentiële rol van elektrochemie in het vinden van nieuwe processen voor duurzame chemicaliën van biomassa in waterige oplossingen. Voor het vaststellen van het potentieel van elektrochemie in biomassa conversie was een analyse techniek nodig die consistent is met de tijdschaal van de meest favoriete techniek van de elektrochemicus, namelijk voltammetrie. Echter, het combineren van voltammetrie met high-performance liquid chromatography (HPLC) lijdt onder lange analyse tijden in de kolom. Om de inherente verschillen in tijdschaal tussen voltammetrie en HPLC te verhelpen, gebruikten we een methode om snel monsters te nemen tijdens de verandering van de elektrode potentiaal met behulp van een zeer klein tip-inlaatsysteem van een micrometer ordegrootte, dat dicht bij het elektrode oppervlak wordt geplaatst. De genomen monsterfracties worden vervolgens geanalyseerd in een HPLC systeem. Deze methode werd gedemonstreerd door het toe te passen bij glycerol ($C_3H_8O_3$) elektro-oxidatie aan Au en Pt elektroden in basische oplossingen in Hoofdstuk 2, waarbij veranderingen in concentratie van glycerol en reactieproducten waar te nemen zijn, die corresponderen met de stroom gemeten middels voltammetrie.

De mechanismen van glycerol elektro-oxidatie aan Au en Pt elektroden bij verschillende pH omstandigheden worden verder onderzocht in Hoofdstuk 3. Vooral glyceraldehyde en dihydroxyaceton, die niet stabiel zijn in basisch milieu, zijn aangetoond in de product spectra door continue injectie van een ‘stabiliserende component’ via een gemodificeerde tip tijdens het nemen van monsters. Uit deze studie is gebleken dat de glycerol-oxidatie voornamelijk via de primaire alcohol plaatsvindt met glyceraldehyde als eerste reactieproduct. Verder is gebleken dat goud de glycerol oxidatie alleen onder basische omstandigeden katalyseert, in tegenstelling tot platina, waar de glycerol oxidatie plaatsvindt over het gehele pH bereik.

Om het reactiepad van de glycerol oxidatie te wijzigen naar de secundaire alcohol – de primaire alcohol oxidatie is altijd dominant aan mono-metallische katalysatoren in Hoofdstuk 2 en 3 – is Bi als adatom aangebracht op een Pt/C katalysator. Een Pt/C elektrode in een verzadigde bismuth oplossing bij een zorgvuldig uitgekozen potentiaal is in staat om glycerol te oxideren tot dihydroxyaceton met een selectiviteit van 100%. In afwezigheid van bismuth is de primaire alcohol oxidatie dominant. Door de combinatie van online HPLC en in situ FTIR, is aangetoond dat Bi niet alleen het reactiepad voor de primaire oxidatie blokkeert, maar ook zorgt voor een specifiek Pt-Bi oppervlak geschikt voor de secundaire alcohol oxidatie.

De rol van het basische milieu en de goud elektrode tijdens alcohol oxidatie is bestudeerd in Hoofdstuk 5. Een vergelijking van de oxidatie activiteit van een groep gelijksoortige alcoholen met variërende pK_a aan goud elektroden in een basische oplossing, resulteert in het inzicht waarbij de eerste deprotonering wordt gekatalyseerd door de base en de tweede deprotonering snel plaatsvindt en wordt gekatalyseerd door goud. De katalyse door de base is gebaseerd op een Hammett-type correlatie met pKa en domineert de 'overall-reactiviteit' van een groep gelijksoortige alcoholen. De hoge oxidatie activiteit aan goud vergeleken met platina is voor sommige van de alcoholen gerelateerd aan de hoge weerstand van goud om oppervlakteoxides te vormen. Deze resultaten geven aan dat base-katalyse de drijvende kracht is achter de hoge oxidatie activiteit van vele organische brandstoffen aan de anodes van brandstofcellen in alkalische media en niet de interactie tussen katalysator met het hydroxide.

Met het fundamenteel inzicht in de elektrokatalyse van alcoholen, afgeleid van biomassa, verkregen met behulp van online HPLC in de Hoofdstukken 2~5, zijn wij vervolgens geïnteresseerd in het uitdagende gebied van cellobiose omzetting in sorbitol.

Voor de omzetting van cellobiose in sorbitol, is eerst de hydrolyse van cellobiose tot glucose onderzocht in Hoofdstuk 6. Platina en boron-gedoteerd diamant (BDD) elektroden zijn gebruikt voor het maken van respectievelijk zuur (H^+) en hydroxyl-radicalen (OH•). De

resultaten hiervan zijn vergeleken met de hydrolyse door een vaak gebruikt zuur (H_2SO_4) en OH• van de Fenton's reactie. Cellobiose hydrolyse volgt een eerste-orde reactie volgens de wet van Arrhenius in een temperatuurbereik van 25^{o}C to 80^{o}C met verschillende activeringsenergieën voor de zuur- en radicaal-gekatalyseerde reactie van respectievelijk ca. 118±8 kJ mol^{-1} en ca. 55±1 kJ mol^{-1}. De hoge lokale zuurgraad van het elektrochemisch gegenereerde zuur (H^+) aan de Pt anode versnelt de vorming van glucose, terwijl de actieve elektrode (PtO_x) reageert met glucose waardoor deze wordt ontleed tot kleinere organische zuren. Het hydroxyl radicaal (OH•), gevormd aan eenBDD anode, hydrolyseert eerst cellobiose tot glucose, maar werkt al gauw in op de aldehyde van glucose, welke verder wordt ontleed tot kleinere aldosen en uiteindelijk tot formaldehyde die op zijn beurt elektrochemisch geoxideerd wordt tot mierenzuur.

Analoog aan de gekoppelde reactie van cellobiose hydrolyse tot glucose, wordt de glucose hydrogenering tot sorbitol in een neutrale oplossing aan vaste metaal-kathoden bestudeerd in Hoofdstuk 7. Drie groepen van katalysatoren in het Periodiek Systeem vertonen overeenkomsten op basis van de reactieproducten: 1) vorming van waterstof aan de 'vroege' transitiemetalen (Ti, V, Cr, Mn, Zr, Nb, Mo, Hf, Ta, We en Re) en platina groep metalen (Ru, Rh, Ir en Pt), 2) sorbitol aan de 'late' transitie metalen (Fe, Co, Ni, Cu, Pd, Au en Ag) en Al (sp metaal) en 3) sorbitol en 2-deoxysorbitol aan de post-transitie metalen (In, Sn, Sb, Pb en Bi) en verder Zn en Cd (d metalen). Ni vertoont de laagste overpotentiaal voor de vorming van sorbitol van -0.25 V, terwijl Pb sorbitol produceert met de hoogste opbrengt (< 0.7 mM cm^{-2}). In tegenstelling tot een Pt elektrode, hydrogeneert een Pt/C elektrode met een groot oppervlak glucose tot sorbitol van -0.21 V met een relatief kleine stroom. Dit benadrukt de belangrijke rol van actieve sites en de grootte van het oppervlak van de katalysator. In combinatie met de optie tot potentiaal gecontroleerde elektrolyse aan de anode (Hoofdstuk 6), is het maken van 1-pot elektro-synthese van sorbitol van cellobiose of cellulose mogelijk.

Omdat 5-hydroxymethylfurfural (HMF) een bijproduct is van de dehydratatie van glucose tijdens zuur-gekatalyseerde hydrolyse van cellulose, is het effect van de aanwezigheid van

glucose op de hydrogenering van HMF en visa versa bestudeerd in hoofdstuk 8. Drie groepen katalysatoren vertonen elk een selectiviteit naar verschillende producten: (1) 2,5-dihydroxymethylfuran (DHMF) (Fe, Ni, Ag, Zn, Cd en In), (2) DHMF en andere producten zoals 2,5-dimethylfuran (Pd, Al, Bi en Pb), afhankelijk van de aangebrachte potentiaal en (3) andere producten (Co, Au, Cu, Sn en Sb) gerelateerd aan de dehydratatie van HMF. De snelheid van de elektrokatalytishe HMF hydrogenering is niet sterk afhankelijk van de katalysator, aangezien alle katalysatoren een overeenkomstige beginpotentiaal vertonen (-0.5 ± 0.2 V) in aanwezigheid van HMF. Daarentegen bepaalt de intrinsieke eigenschap van katalysatoren het reactiepad richting DHMF en andere producten. Ag vertoont de hoogste activiteit voor de vorming van DHMF (max. 13.1 mM cm^{-2} met een hoge selectiviteit > 85%). HMF hydrogenering is sneller dan glucose hydrogenering aan alle metalen. De aanwezigheid van glucose verhoogt de vorming van DHMF en onderdrukt de dehydratatie van HMF aan overgangsmetalen. Aan p-block metalen verhoogt glucose de vorming van DHMF aan Zn, Cd en In, terwijl haar bijdrage aan Bi, Pb, Sn en Sb gelimiteerd is. Opmerkelijk is het feit dat in aanwezigheid van HMF, glucose hydrogenering zelf onderdrukt wordt of zelfs geheel afwezig is. De eerste elektron overdracht stap van HMF reductie is niet metaal afhankelijk, wat wijst op een niet-katalytische reactie met proton overdracht direct vanuit water in het elektroliet.

In dit proefschrift wordt aangetoond dat elektrochemie en elektrokatalyse potentie hebben voor de vorming van duurzame chemicaliën van biomassa door het combineren van voltammetrie en chromatografie. Deze simpele en innovatieve benadering maakt de controle van oplosbare reactieproducten tijdens voltammetrie met chromatografische technieken mogelijk en dit leidt vervolgens tot nieuwe inzichten in de mechanismen van complexe meerstaps elektrodereacties.

List of Publications

This thesis is based on the following publications:

Chapter 2

Y. Kwon and M. T. M. Koper, Combining Voltammetry with HPLC: Application to Electro-Oxidation of Glycerol, *Anal. Chem.* **82** (2010) 5420-5424.

Chapter 3

Y. Kwon, K.-J. P. Schouten, and M. T. M. Koper, Mechanism of the catalytic oxidation of glycerol on polycrystalline platinum and gold electrodes, *ChemCatChem*, **3** (2011) 1176-1185.

Chapter 4

Y. Kwon, Y. Birdja, I. Spanos, P. Rodriguez, and M. T. M. Koper, Highly selective electro-oxidation of glycerol to dihydroxyacetone on platinum in the presence of bismuth, *ACS Catal.*, **2** (2012) 759–764.

Chapter 5

Y. Kwon, S. C. S. Lai, P. Rodriguez, and M. T. M. Koper, Electrocatalytic oxidation of alcohols on gold in alkaline media: base or gold catalysis?, *J. Am. Chem. Soc.*, **133** (2011) 6914–6917.

Chapter 6

Y. Kwon, S. E. F. Kleijn, K. J. P. Schouten, and M. T. M. Koper, Cellobiose Hydrolysis and Decomposition by Electrochemical Generation of Acid and Hydroxyl Radicals, *ChemSusChem*, **5** (2012) 1935-1943.

Chapter 7

Y. Kwon and M. T. M. Koper, Electrocatalytic hydrogenation and deoxygenation of glucose on solid metal electrodes, *ChemSusChem*, **6** (2013) 455-462.

Chapter 8

Y. Kwon, E. de Jong, S. Raoufmoghaddam, and M. T. M. Koper, Electrocatalytic hydrogenation of 5-hydroxymethylfurfural in the absence and presence of glucose, *ChemSusChem*, 2013, DOI: 10.1002/cssc.201300443.

In addition, the author has contributed to the following articles:

- Y. Kwon, S. J. Raaijman, and M. T. M. Koper, Role of peroxide in the catalytic activity of gold for oxidation reactions in aqueous media: an electrochemical study, 2013, submitted.

- H. Li, F. Calle-Vallejo, M. J. Kolb, Y. Kwon, Y. Li, and M. T. M. Koper, Why the (100) terrace breaks and makes bonds: oxidation of dimethylether on platinum single-crystal electrodes, 2013, submitted.

- J. Yang, Y. Kwon, M. Duca, and M. T.M. Koper, Combining voltammetry and ion chromatography: application to the selective reduction of nitrate on Pt and PtSn electrodes, 2013, submitted.

- R. Kortlever, K. H. Tan, Y. Kwon, and M. T. M. Koper, Electrochemical CO_2 reduction on copper in weakly alkaline media, *J. Solid State Electrochem.*, **7** (2013) 1843-1849.

- P. Rodriguez, Y. Kwon, and M. T. M. Koper, The promoting effect of adsorbed carbon monoxide on the oxidation of alcohols on a gold catalyst, *Nature Chem*., **4** (2012) 177-182. (**Front Cover of Issue**)

- K. J. P. Schouten, Y. Kwon, C. J. M. van der Ham, Z. Qin, and M. T. M. Koper, A new mechanism for the selectivity to C_1 and C_2 species in the electrochemical reduction of carbon dioxide on copper electrodes, *Chem. Sci.*, **2** (2011) 1902-1909. (**Inside Cover of Issue**)

- A. Santasalo-Aarnio, Y. Kwon, E. Ahlberg, K. Kontturi, T. Kallio, and M. T. M. Koper, Comparison of methanol, ethanol and iso-propanol oxidation on Pt and Pd electrodes in alkaline media studied by HPLC, *Electrochem. Commun.* **13** (2011) 466-469.

In magazine

- Y. Kwon and M. T. M. Koper, Product detection in electrochemical cells: combining cyclic voltammetry and HPLC by employing fraction collection, *Shimadzu News* **3** (2010) 20-21.

Other publications

- Y. Kwon, H. J. Lee, and J. Lee, Autonomous interfacial creation of nanostructured lead oxide, *Nanoscale*, **3** (2011) 4984-4988. (**Front Cover of Issue**)

- Y. Kwon and J. Lee, Formic Acid from Carbon Dioxide on Nanolayered Electrocatalyst, *Electrocatal.* **1** (2010) 108-115.

- H. Jeon, J. Joo, Y. Kwon, S. Uhm, and J. Lee, Morphological features of electrodeposited Pt nanoparticles and its application as anode catalysts in polymer electrolyte formic acid fuel cells, *J. Power Sources* **195** (2010) 5929-5923.

- J. Y. Joo, J. K. Lee, Y. Kwon, C. R. Jung, E. S. Lee, J. H. Jang, H. J. Lee, S. Uhm, and J. Lee, Enhancement of CO Tolerance on Electrodeposited Pt Anode for Micro-PEM Fuel Cells, *Fuel Cells* **10**(6) (2010) 926-931.

- J. Lee, Y. Kwon, R. L. Machunda, and H. J. Lee, Electrocatalytic Recycling of CO_2 and Small Organic Molecules, *Chem. Asian J.* **4** (2009) 1516-1523.

- Y. Kwon, J. K. Lee, D. Ji, and J. Lee, Electrochemical characteristics of home-made bipolar plate and its relationship with fuel cell performance, *J. Korean Electrochem. Soc.* **12**(1) (2009) 68-74. (Korean)

- S. Uhm, H. J. Lee, Y. Kwon, and J. Lee, A Stable and Cost-Effective Anode Catalyst Structure for Formic Acid Fuel Cells, *Angew. Chem. Int. Ed.* **47** (2008) 10163-10166.

- Y. Kwon, S. Uhm, and J. Lee, Development of a Direct Formic Acid Fuel Cell Anode by Multi-Layered Bismuth Modification, *Korean Chem. Eng. Res.* **46** (2008) 697-700. (Korean)

- S. Uhm, Y. Kwon, S. T. Chung, and J. Lee, Highly effective anode structure in a direct formic acid fuel cell, *Electrochim. Acta* **53** (2008) 5162-5168.

Curriculum Vitae

Youngkook was born in Gimcheon, a city in North Gyeongsang Province in South Korea in 1979. After high school, he moved to Seoul to study Environmental Engineering at Kwangwoon University (1998-2005, including military service for 26 months) and finished his bachelor study with the research topic of "*Arsenic Removal from Mine Tailings*". Before starting master course, he worked in companies to learn business and economics especially in sales and accounting departments until 2007. For his master's degree, he studied electrochemistry in the department of environmental science and engineering at GIST (Gwangju Institute of Science and Technology) under the supervision of Prof. Dr. Jaeyoung Lee with the research topic of "*Electrocatalytic Recycling of CO_2 and Small Organic Molecules*" 1) developing a stable and cost-effective anode catalyst for formic acid fuel cells, and 2) CO_2 reduction to formic acid on Pb electrode.

In September 2009, Youngkook started his PhD work in Leiden University (the Netherlands) under the supervision of Prof. Dr. Marc T. M. Koper with the project title of "*Biomass Electrochemistry: from cellulose to sorbitol*" sponsored by the CatchBio Smart Mix Program, to find out new electrochemistry-based routes of catalysis for sustainable chemicals from biomass. The results of this work are presented in this thesis. Parts of his work have been presented at several international conferences.